STRESS IN THE CARTILAGE OF THE HUMAN HIP JOINT

by

THOMAS MACIROWSKI

SUBMITTED IN PARTIAL FULFILLMENT
OF THE REQUIREMENTS FOR THE
DEGREES OF

BACHELOR OF SCIENCE

and

MASTER OF SCIENCE

and

DOCTOR OF SCIENCE

at the

MASSACHUSETTS INSTITUTE OF TECHNOLOGY

February 1983

Signature of Author. ....
Department of Mechanical Engineering, February 1983

Certified by ....
Thesis Supervisor

Accepted by ....
Departmental Chairman

STRESS IN THE CARTILAGE OF THE HUMAN HIP JOINT

by

Thomas Macirowski

Submitted to the Department of Mechanical Engineering on February 15, 1983 in partial fulfillment of the requirements for the Degrees of Bachelor of Science, Master of Science, and Doctor of Science.

ABSTRACT

To understand the possible role of the mechanical factors which determine tissue deformation and fluid flow in normal synovial joints in the pathogenesis of osteoarthritis, the state of stress in the cartilage *in situ* in the human hip joint is described. In particular, the nature of the interarticular boundary condition and its implications for the function of the synovial joint are discussed.

The geometry and the poroelastic constitutive properties of normal adult articular cartilage in the human hip joint have been measured experimentally. The time response of both the surface stress distribution and the surface displacement of the cartilage in the acetabulum of the human hip joint when loaded by instrumented endoprostheses has been measured. Modelling of the human hip joint, incorporating the measurements described has been used to predict the surface boundary conditions governing interarticular fluid flow, i.e. the the local and global resistance to fluid flow in the interarticular space. Fluid flow toward and parallel to the space are included. The result is the first experimentally determined estimate of the time dependent resistance to fluid flow in the interarticular space and its effects on the solid stress and fluid pressure in the cartilage.

The ratio of the resistance to fluid flow in the interarticular space to the resistance to flow in the cartilage layer increases under static load from about one to twenty. The flow in the interarticular space relative to that in the layer decreases in about the same proportion. It appears that for good interarticular sealing to occur the interarticular space needs to be much smaller than the unloaded shape of the cartilage surface.

The fluid pressure typically supports ninety percent of the load, even after twenty minutes; correspondingly the stress in the solid matrix remains small. This has important implications for the load bearing and lubrication functions of articular cartilage.

Thesis Supervisor: Robert W. Mann
Title: Whitaker Professor of Biomedical Engineering
Department of Mechanical Engineering

To Chris,

My sine qua non

ACKNOWLEDGMENTS

First, I would like to thank Professor Robert W. Mann, my advisor, for the opportunities he gave me. I have benefited greatly from his experience, insight, guidance, and support. Most of all, he provided us with a wonderful environment to learn and grow in.

Slobodan Tepic, my friend and collaborator, contributed his magnificant skills, insight, and patience unselfishly. Our projects have always been done jointly, and I only wish this thesis could have been so also.

Doctor William H. Harris has provided this project with all his clinical and medical expertise. I am grateful for his time, effort, and enthusiasm.

Professors Klaus-Jurgen Bathe and Michael P. Cleary were responsible not only for teaching me the fundamentals of mechanics but also the physical insight necessary to apply them in a sensible way. Their readiness to offer advice and criticism is most appeciated.

Paul Rushfeldt, who began the <u>in vitro</u> experimental program, left an enormous amount of working hardware and software, without which none of the experiments would have been possible. John Dent, who introduced me to this project, did an excellent job of tackling the difficult subject of cartilage mechanics in a clear and practical way. The roots of this work trully come from Paul's and John's investigations and discoveries.

I thank Dave Palmer for his technical and other contributions to this project. The hip simulator he designed and built has performed admirably.

Ralph Burgess has always been able and willing to lend a helping hand with the electronics and general trouble-shooting.

Dr. Charles McCutchen, who pioneered the concept of interarticular fluid flow, has provoked many interesting discussions.

Erik Antonsson was always willing to share his talents, particularly in times of distress. The laboratory's computers haver run as well.

Brad Hunter provided much needed electronic and computing help in the early days and has continued as a friend.

Dr. Joe Halcomb and Dr. Andy Hodge were always helpful on clinical and other matters. Their willingness to contribute in an engineering environment is appreciated.

Maureen Hayes kept our financial and other bueracratic affairs in order and was always willing to lend a sympathetic ear.

Lucille Blake typed too many abstracts and proposals on too short deadlines without complaint.

Steve Madreperla, Bob Fijan, and Tim Harrigan contributed their respective talents to the project in general.

Cary Abul-Haj was a friend and confidant through it all.

The Department of Mechanical Engineering Staff made MIT a socialble place to work.

I thank my parents-in-law Richard and Mary Torbinski, who treated me the best way they knew -- like a son, and my parents who only wanted me to do my best.

Finally, I am indebted to Christina. Her love and devotion are unequaled and her advice has always been insightful. I couldn't have done it without her.

This work was conducted in the Eric P. and Evelyn E. Newman Laboratory for Biomechanics and Human Rehabilitation in the Department of Mechanical Engineering at the Massachusetts Institute of Technology, and was supported by: The Kroc Foundation, The Office of the Provost at MIT, and the Whitaker Professorship of Biomedical Engineering. The National Institutes of Health Grant Number 5-R01-AM16116 supported earlier phases of the study.

TABLE OF CONTENTS

LIST OF FIGURES

CHAPTER 1

INTRODUCTION

Synovial or diarthroidal joints provide mobility to the human skeleton. Healthy joints perform extremely well, carrying loads that can reach three to five times body weight in the lower extremities during normal walking, at velocities ranging down to near zero, with a coefficient of friction as low as 0.01, over a life-time of several million cycles per year. Unfortunately, the biological bearing material in synovial joints, articular cartilage, is not indestructible. The most widespread joint affliction is a degenerative disease known as osteoarthritis. Its incidence and severity generally increase with age; over 16 million Americans are affected seriously enough to require medical treatment [1]. In fact, the almost ubitquitous occurence of this type of joint failure has been the major motivation for the study of the mechanics of the synovial joints and articular cartilage. Despite extensive biological and epidemiological research the etiology of osteoarthritis is unknown [106].

Both the inherent load-bearing function of diarthroidal joints and the morphology of the lesions that characterize osteoarthritis suggest that mechanical factors are important in the etiology and subsequent development of the disease. The changes in osteoarthritic cartilage, most notably fraying and splitting at the surface, occur in localized areas and vary in severity at different locations in the affected joint [45].

The research hypothesis we advance here assumes that local mechanical factors which determine tissue deformation and fluid flow in normal synovial joints also play an important role in the pathogenesis of osteoarthritis. The goal of this work is to explicate the importance of these mechanical factors for the behavior of the cartilage in the synovial joint and their possible role in its failure in osteoarthritis.

The determination of the state of stress in cartilage in synovial joints and its relation to mechanical factors such as joint load magnitude, direction, and frequency and the geometry and mechanical properties of the cartilage layers, along with information on the strength of the tissue, is essential to support the hypothesis that under certain physiological conditions and circumstances mechanical failure of the tissue is likely or even inevitable. The goal of this thesis is to develop a model to estimate stress in the cartilage layer of the human hip joint.

Chapter 2 contains background information on synovial joint mechanics. Chapter 3 develops some simple theoretical models for the compression of cartilage under various conditions. Chapter 4 describes the experimental techniques and the results of measurements of the geometry of the cartilage layer and the stress on the surface of the cartilage in the intact acetabulum. Chapter 5 incorporates the experimental results and theoretical analysis in a model of the cartilage layer. Finally Chapter 6 contains the conclusions and recommendations for future research.

CHAPTER 2

BACKGROUND

2.1 THE SYNOVIAL JOINT

The bones of the skeleton are connected at articulations or joints. In the movable joints or diarthroses the parts of the bones (usually the ends) forming the joint are covered by articular cartilage, which forms the joint surface, and enclosed in a capsule formed of ligaments. The capsule is lined with a synovial membrane, hence a common synonym, synovial joint. The membrane secretes a thick, viscous, transparent fluid -- synovial fluid.

2.1.1 Cartilage

The articular cartilage is of the hyaline variety, as distinguished from fibro-cartilage. The tissue consists of a sparse distribution of cells (chondrocytes) immersed in an extracellular matrix. The matrix is mostly water, typically 70 to 80 percent by weight. The remainder is a meshwork of collagen fibers and a nonfibrous filler known as proteoglycans (PG). The proteoglycans are composed of chains of charged disaccharides known as glycosaminoglycans (GAG) attached to a protein core. The PG molecules have a high affinity for water, tending to expand their volume in solution. The swelling of the PG's is resisted by the collagen fiber mesh. In cartilage the intrinsic equilibrium volume of the PG gel is greater than the actual physiological equilibrium; i.e. the swelling PG's are restrained by the collagen network, which in turn is tensioned by the PG's [90]. This "tensioning" appears to be a molecular scale or fiber level phenomenon since its effects influence wave propagation in the ultrasonic (5-20 MHz) range (see section 4.2).

Morphologically, the composition of cartilage is neither homogeneous nor isotropic. The cartilage layer is classified into four descriptive zones, distinguished by the morphology of the collagen fibers and the cells (Figure 2-1). The most superficial few microns appear to be formed from a layer of fine fibers known as the lamina splendons (LS) [70] that covers the articular cartilage. In order of increasing distance from the cartilage surface the layers are:

1. The superficial (tangential) zone in which the collagen fibers are oriented primarily parallel to the surface. Locally there is a preferred orientation which varies with joint type and location. The cells are generally oval shaped with long axes also parallel to the surface. This layer has the greatest collagen and water content [101].

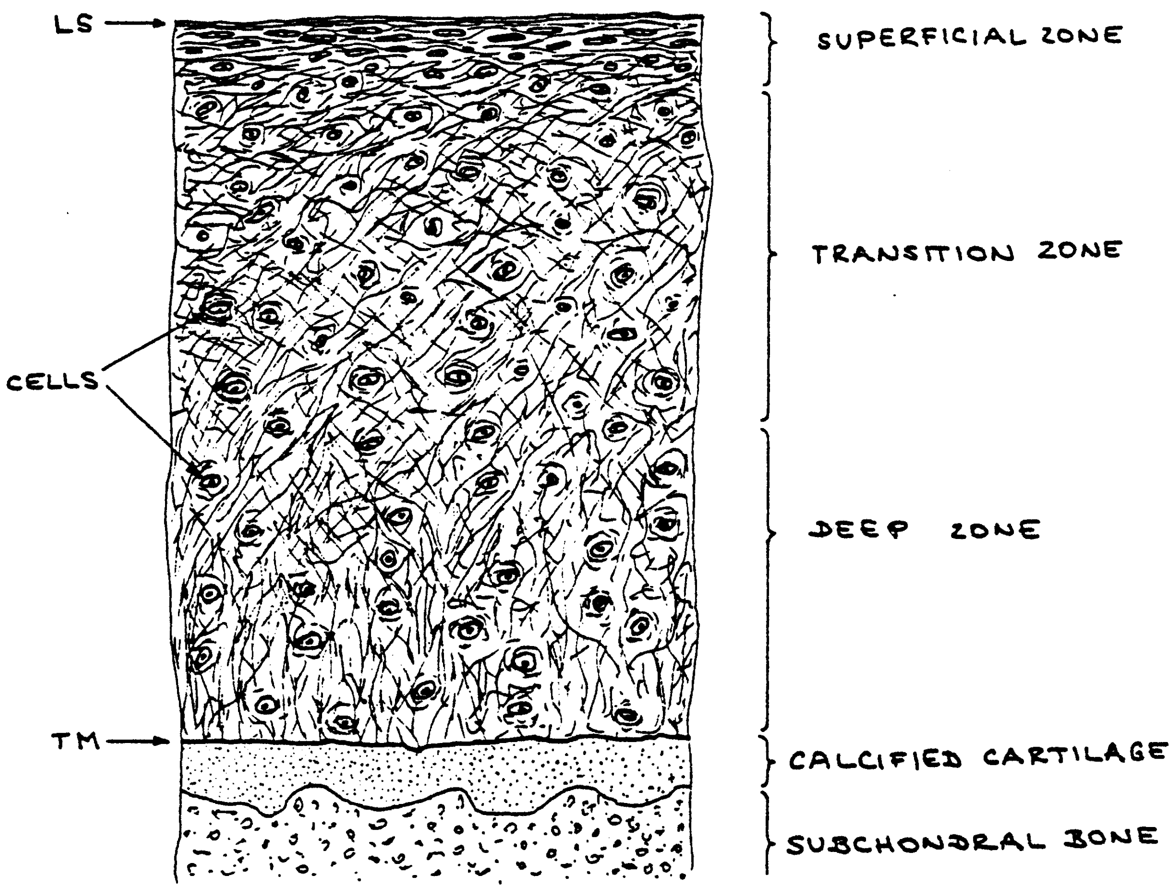

Figure 2-1. Cross-Section of an Articular Cartilage Layer

2. The transitional zone in which the fibers are arranged obliquely in a more random network.

3. The deep zone in which the fibers are predominately radial to the surface. The cells are large and round.

4. The calcified zone in which there are few cells and the matrix contains many salt crystals. It is divided from the deep zone by the "tidemark" (TM), a blue line visible in hematoxyline stained preparations. In older tissue multiple tidemarks are often visible [115].

The cells or chondrocytes seem to lack DNA synthesis and meiotic activity. However, cell division and synthesis has been observed near clefts and defects in arthritic cartilage and the cells do divide in culture. The cells are metabolically active and the effects of external influences (such as injury [82], pressure [107], and temperature [81]) are currently the subject of intense research. The cartilage is devoid of nerves, lymphs, and vascularization. This implies that information, nutrients, and wastes must be exchanged through the matrix via the synovial fluid.

2.1.2 Function

Synovial joints and articular cartilage often last a lifetime under a wide range of demanding conditions. There are two basic functional requirements for synovial joints;

load carriage and articulation. The joint surfaces provide smooth kinematic constraint during articulation while transferring load across the bones of the joint. The loads that act across the joints have two components; those that result from the gravitational and inertial forces acting on the limbs and the forces of the muscles acting across the joint. In many cases, including the weight-bearing lower extremities, the muscle forces provide the major contribution. Since this thesis is concerned with the human hip joint it is instructive to consider its functional requirements in more detail.

The ball and socket geometry of the hip joint (Figures 2-2 & 2-3) reflects the functional demands for mobility; the movements of the hip (Figure 2-4) consist of flexion/extension in the anterior-posterior plane, adduction/abduction in the medial-lateral plane, and rotation along the long axis of the femur. The muscle forces across the hip must provide both stabilty and motion to the joint. Even the simplest cases of equilibrium when standing on one leg or during the stance phase of walking require large muscle forces. The moment arm of the abductor muscles is relatively small (relative to the distance from the center of mass) so the muscle force must be comparatively large to balance the torque generated by the weight of the body. Typically the net load across the joint is estimated to be two to three times body weight during

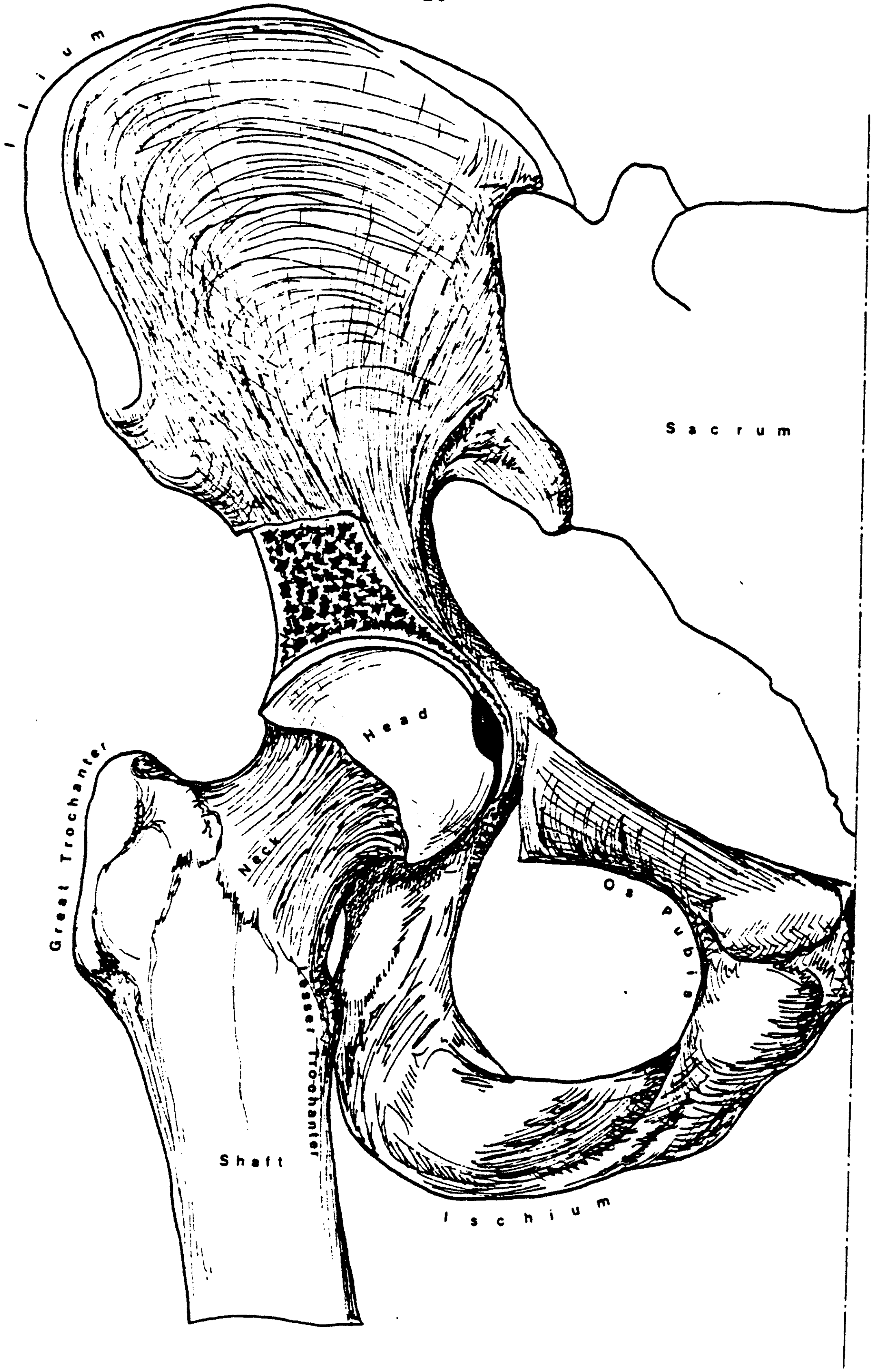

Figure 2-2. Frontal View of the Hip Joint

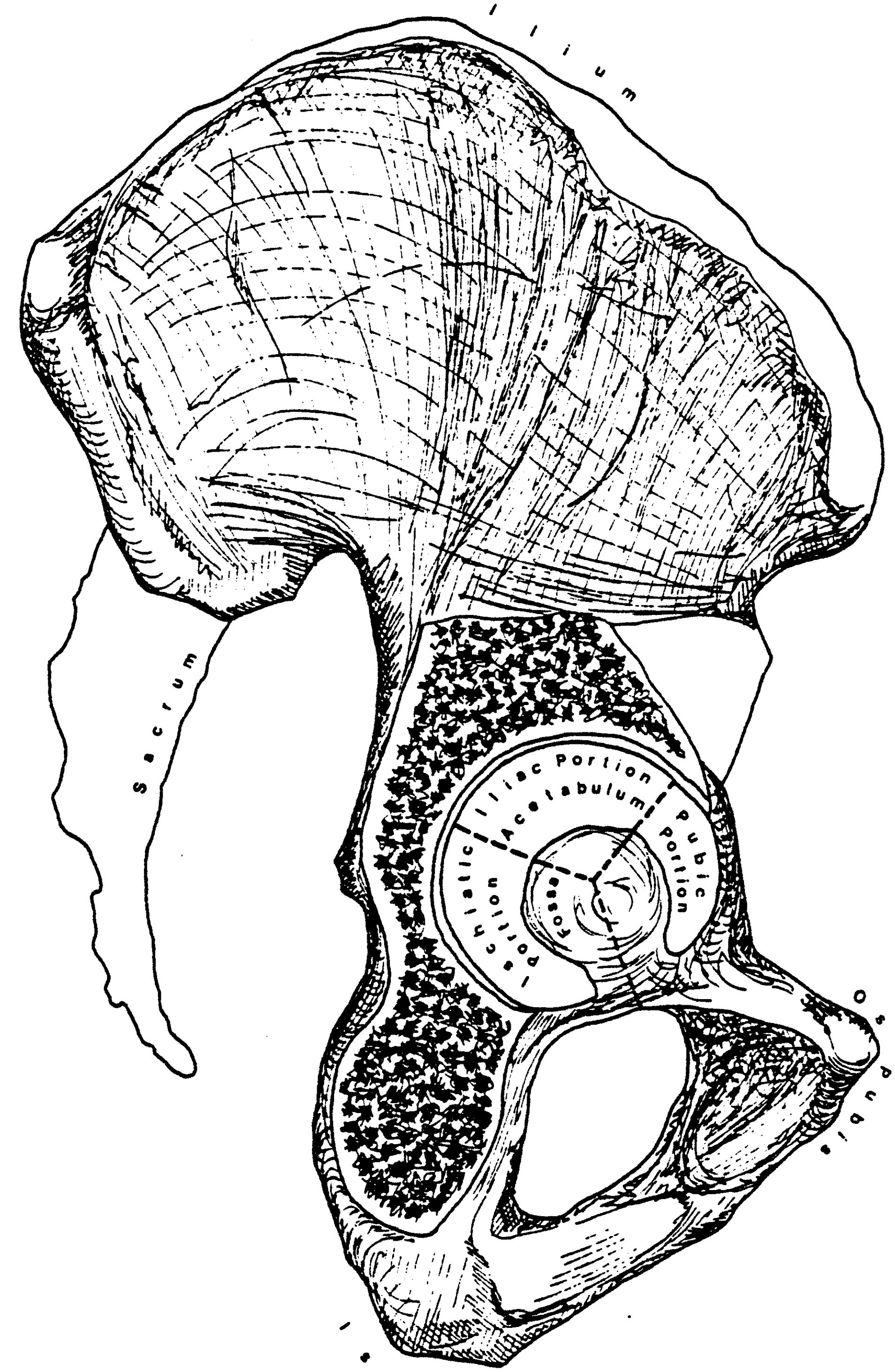

Figure 2-3. Side View of the Hip Joint

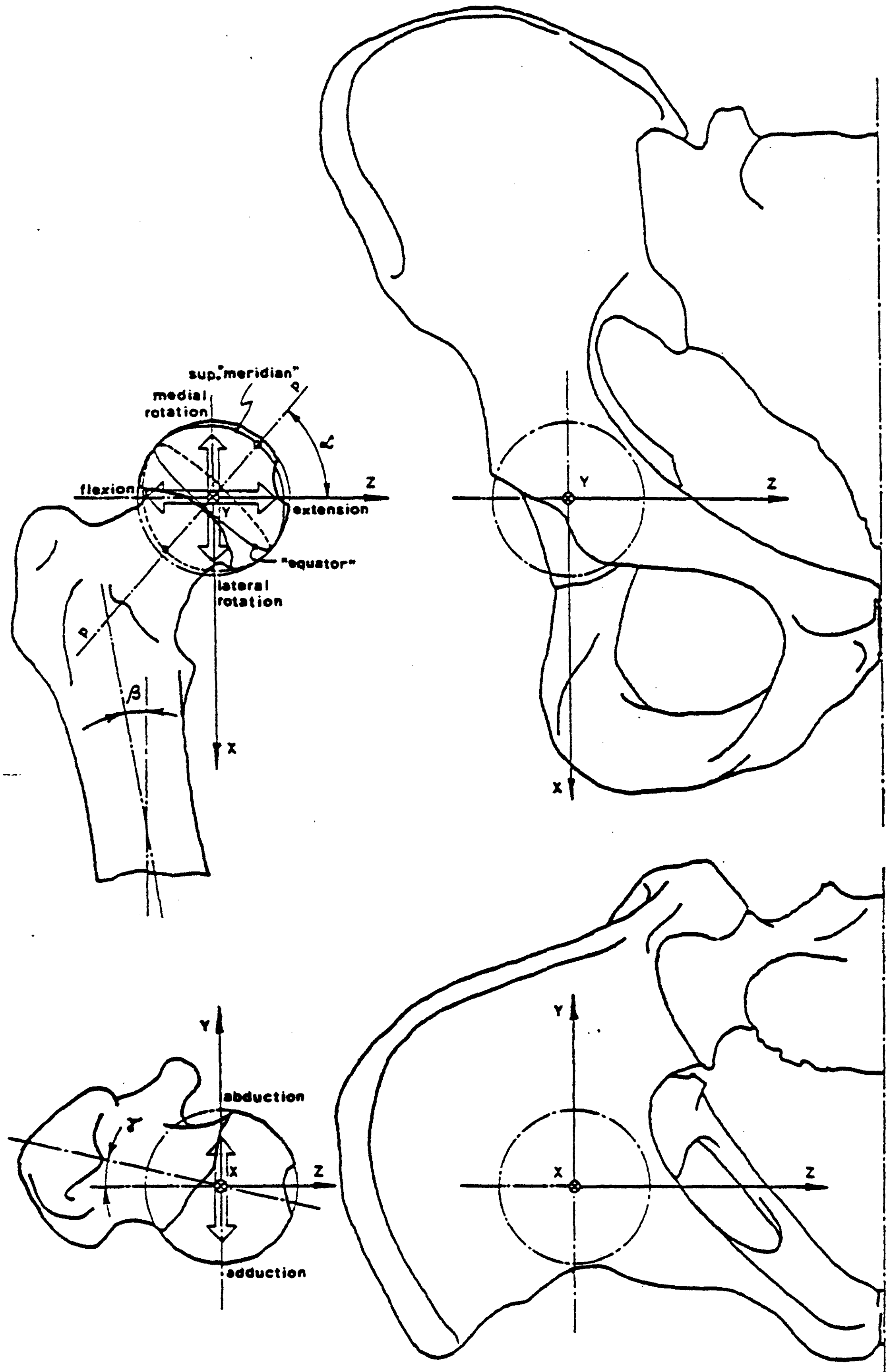

Figure 2-4. Axes of Motion at the Hip Joint

walking and seven to ten times body weight during running and jumping [32],[109]. It is important to note that in most cases the muscle forces represent an estimate based on the force required to generate a measured kinematic motion; higher muscle forces which produce the same net torques about the joint are possible if the muscles are co-contracting.

These loads must be supported by the cartilage layers of the acetabulum and the femoral head. In the adult hip joint the total cartilage area in the acetabulum is typically 1000 mm . During normal walking a load of twice body weight or 750 N dictates an average stress of 1.5 MPa on the cartilage; however we have found the maximum stress is much higher. The hip joint will routinely experience this load during one million walking cycles each year. The performance of healthy synovial joints under these conditons is astonishingly good. The friction coefficient of whole hip joints has been measured in the range of 0.005 to 0.024 [24]. This is better than Teflon against Teflon (0.04). Many joints seem to perform well for a lifetime; unfortunately many do not. The frequency of failure of synovial joints can be very high, especially in older people.

2.2 OSTEOARTHRITIS

The most common disease of the joints (and the major cause for their failure) is a disease known as osteoarthritis. Despite its suffix it is a non-inflammatory disease characterized by degeneration of the articular cartilage (hence a less used name -- degenerative joint disease). Rheumatoid arthritis, in contrast, attacks the synovial membranes.

Osteoarthritis is widespread, increasing in incidence with age [1]. Although not an inevitable consequence of aging, it is the most common cause of work disability [129]. If for no other reason than its omnipresence, it has been a major subject for medical research.

2.2.1 Description

Disintegration of the articular cartilage is the most common feature of osteoarthritis. Early in the course of the disease the cartilage becomes soft and fraying of the surface (fibrillation) appears. Meanwhile the chondrocytes increase their metabolic rate, both with respect to the rate of synthesis of proteoglycans and collagen [87], along with cell division and proliferation near splits and mechanically damaged cartilage. As the disease progresses the cartilage often becomes thinner, leading in some cases to total loss of the cartilage, exposing the bone (eburnation). As the bone becomes exposed it undergoes dramatic changes via active remodelling; including formation of bone cysts and new bone (osteophytes) and thickening of the trabeculae. Joint pain after activity is the classical symptom of incipient osteoarthritis; later in the course of the disease joint function may be further impaired by the remodelling of the bone and joint surfaces.

2.2.2 Classification

Osteoarthritis is classified by the (lack of) evidence of etiological factors in the disease. "Secondary" arthritis results from changes in the joint previous to the onset of the disease, such as gross anatomical abnormalities or other disease (such as rheumatoid arthritis). The majority of cases (58 percent by one estimate [134]) do not have a known cause: these are the so-called idiopathic or primary cases. A pervasive problem in identifying first causes is that the progressive changes associated with the disease have obliterated any primary changes. Mild deformaties (such as seen after a slipped epiphysis or Legg-Perthes disease) have been identified in a majority (79 percent) of cases in a particular study of "idiopathic" osteoarthritis [134]. Evidence that such changes lead directly to mechanical damage of the cartilage (perhaps through excessive stress) is still lacking. The association of mechanical factors with the initiation and development of osteoarthritis is the primary hypothesis of this research.

2.2.3 Pathogenesis

Although the mechanical role of cartilage in synovial joints is inescapable, the exact influence of mechanical factors such as geometry and stress on the functioning synovial joint is obscure. This is the first step toward establishing a relationship between the mechanics of the joint and its failure in osteoarthritis. This thesis attempts to relate the state of stress in the cartilage to the loads and boundary conditions imposed during daily activity. Once the way cartilage functions in a normal synovial is understood, the role of mechanical factors in the pathogenesis of osteoarthritis can be addressed. Further work on the strength of cartilage, for example, might be suggested by predictions of the details of the effects of the abnormalities that presumably can lead to osteoarthritis.

2.3 PREVIOUS WORK

Biomechanical studies of synovial joints have focussed primarily on two topics: lubrication and the mechanics of articular cartilage. Cartilage is a complex material and its role in the function of synovial joints is poorly understood and the subject of much research and intense debate. The most common cause of the confusion has been the misapplication of traditional engineering models to cartilage as a material and/or the synovial joint as a system. A brief history of the relevant research in this field is given here to orient the reader with respect to the work described in this thesis.

2.3.1 Lubrication

Joint lubrication studies have been of two different categories. (1) *In vitro* whole joint studies have measured an average coeffìcent of friction for human and animal joints under various conditions. The quoted values (for the human hip joint) have ranged from 0.003 [78] to 0.05 [149]. Even the highest values are much better than almost all types of man-made bearings and comparable to fluid-film hydrodynamic bearings. (2) Experiments on small cartilage specimens against an artificial surface have been used to allow more precise calculation of the loaded contact area and geometry and to achieve steady-state rather than oscillatory sliding. McCutchen [94] performed the first experiments of this type with small bovine cartilage plugs sliding on glass. The most significant result was that the friction began low (0.002 to 0.02) and rose with time (up to 0.2) as the cartilage consolidated. If the cartilage was separated from the glass for a few seconds and then replaced, the friction was reduced but quickly rose when the load was reapplied (Figure 2-5). A more recent set of experiments using cartilage samples in a rotating geometry demonstrated that the friction and deformation under dynamic loading is much less than under static loading.

Various lubrication theories from traditional engineering have been "adapted" to explain the phenomenally low friction coeeficient of cartilage. In fact, virtually <u>every</u> lubrication regime has been proposed for cartilage. The list includes [135]:

1. Hydrodynamic Lubrication (MacConaill [79]). This mechanism depends upon the maintenance of a thick, wedge-shaped film of synovial fluid between the joint surfaces. This is unlikely given the reciprocating motion of a synovial joint.

2. Boundary Lubrication (Charnley [24]). A thin layer of molecules, presumably from the synovial fluid, attaches to the cartilage surfaces and provides the low friction. Charnley suggested this could account for the near independence of the friction with sliding speed.

3. Elastohydrodynamic (Dintenfass [36]). An extension of 1., compliance of the bearing surfaces and the change in lubricant viscosity are included in order to enhance the maintenance of a layer of fluid separating the surfaces.

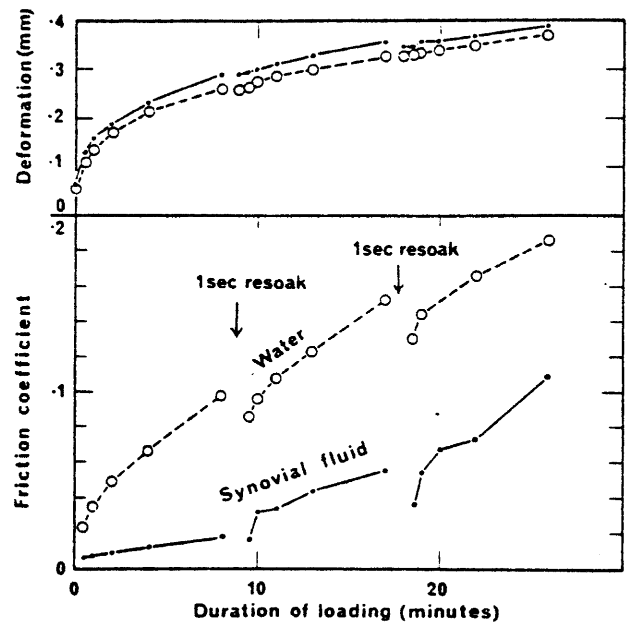

Figure 2-5. Friction and Deformation versus Time for Cartilage on Glass

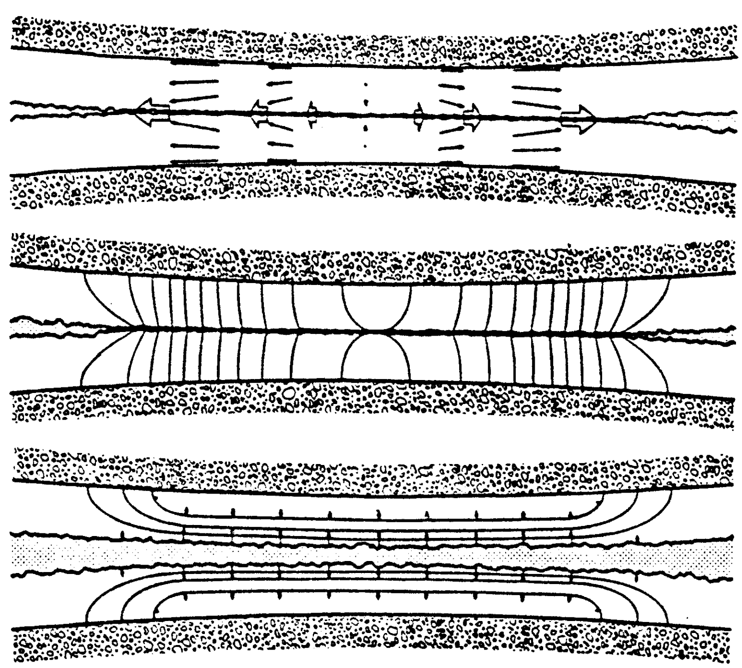

Figure 2-6. Weeping Lubrication

4. Boosted Lubrication (Walker, et al. [150]). If the large molecules of the synovial fluid are unable to enter the small (6 nm) pores of the cartilage then a concentrated hyaluronate would be left on the surface to lubricate. The most obvious problem with this theory [96] is that it requires fluid to flow from the squeeze film into the cartilage layers.

5. Weeping Lubrication (McCutchen [94]). This proposes a type of self-pressurized hydrostatic bearing, where most of the load is supported (in a nearly frictionless manner) by the slow seepage of fluid, supplied from compression of the cartilage layers, into the space between the layers (Figure 2-6). Solid-solid contact of the asperities is the source of the friction (which is well-lubricated by the synovial fluid if the solid stress is less than 0.45 MPa [98]) and of the local seal to prevent the pressurized fluid from quickly flowing out of the interarticular space. He noted that actual rate of seepage would depend on the microstructure of the cartilage surface [93].

The question of whether a squeeze film can prevent the opposing surface of cartilage from making contact has been analyzed in much detail by Piotrowski [111]. He included the effects of shear-thinning of the synovial fluid. Dent [34] applied these equations to a hypothetical bearing 13 mm in radius, with an applied load of 700 N. The film thickness was predicted to reach 2 um in 0.2 s. This is the order of the tertiary roughness of the cartilage surface, hence the shear-thinning of synovial fluid can not prevent contact under conditions simulating heel-strike during the stance phase of walking.

2.3.2 Cartilage Properties

Most previous experimental investigations of the properties of cartilage have been limited to the measurement of the time-dependent behavior of isolated cartilage specimens, usually small plugs for compression tests or thin strips for tensile tests. The major problem with most of these tests has been inattention to the exact state of stress in the sample; the results are therefore at best simply descriptive. Since the goal of most biomechanical studies of cartilage is ultimately the prediction of the state of stress in the cartilage under physiological conditions it is important to perform the tests with some specific constitutive model in mind. In addition such a model should be capable of predicting the stress in the cartilage if the loading and boundary conditions are known.

2.3.2.1 Compression -

For example, the time-dependent response of cartilage when it is loaded by an indentor while it is still attached to the underlying bone has been measured by many investigators (e.g. [65]). The incomplete recovery of the cartilage after the load was removed led to the discovery that the "creep" behavior observed was due primarily to the expression of the interstitial water. These tests have been frequently used to quantify the "topographical variation of the resistance of cartilage to indentation" [65] and relate this "creep modulus" to the chemical constituents of cartilage (the GAG and collagen contents) [64]. The so-called "2 second creep modulus" was determined from the equations relating the depth of indentation on rubber sheets to the applied loads and indentor geometries. The compressive stiffnesses measured in this way was found to correlate to a large extent with the GAG content but not with the collagen content. A similar result was obtained by Freeman [43]; in addition the GAG content was found to be lower in fibrillated tissue (and the strains higher). Finally the creep modulus correlated inversely with the permeability [67], which also has been shown to be inversely proportional to the GAG content [91]. None of the above experiments found any correlation of the stiffness with age.

The equilibrium compressive stiffness of a cartilage plug loaded by a porous loader in compression was measured by McCutchen [94]. The stiffness was quite linear for strains less than about 40 percent. The stiffness for cartilage soaked in tap water was nearly twice that measured in NaCl solution. This was the first illustration of the Donnan contribution of the charged GAG's to the stiffness of the cartilage. The salt neutralizes many of these charges.

2.3.2.2 Tension -

In an analagous manner the response of cartilage to tensile stress has also been measured and compared with age, pathological appearance, and various biochemical contents. The most extensive tests have been performed on 200 um dumbbell shaped cartilage specimens excised from the femoral condyles of human knee joints [66]. The specimens were aligned with the long axis either parallel or perpendicular to the "pin prick" or "split line" patterns. These are elongated cleavage lines that are visible when the point of a round pin is inserted into the cartilage surface. The lines tend to follow the dominant orientation of the nearby surface collagen fibers [101]. This pattern varies from joint to joint but is consistent for any one type of joint.

The specimens were loaded in tension at a rate of 5 mm/min. The tensile stiffness and fracture strength were strongly related to the collagen fiber orientation and collagen content. Those loaded parallel to the predominant oreintation of the collagen fibers had a higher stiffness and fracture strength than those loaded perpendicular to the fiber direction. The stiffness decreases with age and the depth from the surface. The tensile properties of stiffness and strength depend strongly on the collagen content and slightly on the proteoglycan content. Treatment of the cartilage with proteolytic enzymes to degrade the PG's lowers the tensile stiffness at low stress values, especially in the deep zone of the cartilage and perpendicular to the fiber direction. The fracture strength was not affected. Treatment of the cartilage with collagenase lowers both the tensile stiffness and the fracture strength.

2.3.2.3 Fatigue -

The fatigue strength of cartilage is of particular interest since one of the hypotheses for failure is that surface fibrillation is the result of fatigue. The tensile fatigue strength of similar specimens from 30 femoral heads was measured by Weightman [153]. The results indicate that cartilage exhibits typical fatigue behavior (i.e. the stress and number of cycles to cause failure are inversely related). The fatigue resistance varied considerably from one femoral head to another and decreases with age. Periodic compressive loads by an indentor on the surface of a femoral head also produced damage that appeared similar to fibrillation. Again the major problem with these results is how to relate the tensile stresses and strains to cartilage *in vivo*.

2.3.2.4 Permeability -

Since the time response of cartilage to loading is dependent on the flow of the interstitial water, the permeability of cartilage is also an important material parameter. The permeability for flow perpendicular to the surfaces decreases with the depth of the cartilage and the tangential permeability is the same as the typical premeability in the middle zone [91]. Cartilage appears to exhibit a non-linear dependence on the compressive strain; presumably the "pores" become smaller.

2.3.3 Synovial Joint Modelling

McCutchen [98] has reviewed the previous attempts to analyze the fluid flow in the cartilage layers. He has pointed out many errors in describing the real physical problem and the mathematical analysis.

Two published models are relevant to this work. McCutchen [97] has described the fluid flow when the opposing skeletons of cartilage touch. He assumed there is a conductive path for fluid flow due to the channels between contact, which determines the flow and pressure in the cartilage. He estimated skeletal stress is least when tangential fluid flow in the cartilage layers is about the same as in the gap.

Kenyon [68] calculated the amount of flow between the surfaces and the pressure in the fluid film as a function of the resistance to flow in the gap. He points out that even if the surface resistance is high, the gap flow is not necessarily prevented, although the solid stress is minimal.

CHAPTER 3

THEORETICAL ANALYSIS

3.1 POROELASTICITY

The physical structure of cartilage (Section 2.1.1) and its response to load (Section 2.3.2) are similar to many materials known as porous media. Any material so characterized (including cartilage) is comprised of a solid matrix (in this case the collagen fibers, proteoglycans, and cells) which contains pores saturated with some interstitial fluid (the water). Most of the research on porous media has been motivated by and applied to geological materials following the classical work of Biot [11]. More recently the application of the theory of mixtures of interacting continua has become a popular approach to the study of porous media [116] and of articular catilage [103]. In spite of the notoriety afforded the so-called "biphasic theory" (I suppose because a binary <u>mixture</u> is analyzed) the results thus far have provided no additional insight over the Biot formulation.

A more serious problem with any porous medium model of cartilage may be the characterization of the collagen network and the proteoglycan gel as one equivalent single network. While the networks are structurely coupled and appear to move together, this characterization ignores the complex interaction of the elastic and osmotic forces which make up the single equivalent force which balances an externally supplied load. In fact, we (and others [92]) have exploited this unique coupling of the components of the matrix stress to osmotically load the cartilage. In terms of analysis of the response of cartilage to loading discussed herein the concept of a single equivalent solid matrix proves useful and adequate.

3.1.1 Compressible Constituents

The simplest approach [116] to the formulation of the governing equations for the response of a porous medium is to define total stresses and pore pressure as the state variables. It is assumed these are related to the strains in the solid matrix and the mass per unit volume of the pore fluid. Rice and Cleary have shown that for linear isotropic materials (with arbitrary constituent compressibility) these relations can be given in terms of four elastic constants as:

$$2G\epsilon_{ij} = \sigma_{ij} - \frac{\nu}{1+\nu}\sigma_{kk}\delta_{ij} + \zeta_\epsilon \frac{(1-2\nu)}{(1+\nu)} p\,\delta_{ij} \tag{1}$$

$$m - m_o = \frac{\rho_o \zeta_\epsilon (1-2\nu)}{2G(1+\nu)}\left[\sigma_{kk} + \frac{3}{B}p\right] \tag{2}$$

Where:

$$\zeta_\epsilon = \frac{3(\nu_u - \nu)}{B(1-2\nu)(1+\nu_u)}$$

Fluid mass flow q_i is assumed to be governed by D'Arcy's law:

$$q_i = -\rho_o \frac{K}{\mu}\frac{\partial p}{\partial x_i} \tag{3}$$

It is conventional to define an 'effective stress' $\langle\sigma_{ij}\rangle$ as the portion of the stress which is directly related to the strain in the matrix via the conventional elasticity equations.

$$2G\epsilon_{ij} = \langle\sigma_{ij}\rangle - \frac{\nu}{1+\nu}\langle\sigma_{KK}\rangle\delta_{ij} \tag{4a}$$

$$\langle\sigma_{ij}\rangle \equiv \sigma_{ij} + \zeta_{\epsilon} p \delta_{ij} \tag{4b}$$

Equilibrium of the forces and mass conservation lead to:

$$\frac{\partial\sigma_{i}}{\partial X_j} = 0 \qquad \sigma_{ij} = \sigma_{ji} \tag{5}$$

$$\frac{\partial q_i}{\partial X_i} + \frac{\partial m}{\partial t} = 0 \tag{6}$$

Finally, they observe that the usual form of a diffusion equation can be obtained in terms of the stress and pore pressure:

$$C\nabla^2\left(\sigma_{KK} + \frac{3}{B}p\right) = \frac{\partial}{\partial t}\left(\sigma_{KK} + \frac{3}{B}p\right) \tag{7}$$

where the diffussivity is given by:

$$C = \frac{K}{\mu}\left[\frac{2G(1-\nu)}{(1-2\nu)}\right]\left[\frac{B^2(1+\nu_u)^2(1-2\nu)}{9(1-\nu_u)(\nu_u-\nu)}\right] \tag{8}$$

Comparison with Equation 2 shows the fluid mass always satisfies a diffusion equation. Note that the first term in brackets is the drained uniaxial modulus.

3.1.2 Incompressible Constituents

The classical Biot formulation for incompressible constituents can be easily obtained from these equations. The change in mass content is simply volumetric strain (since the pore pressure does not affect the solid matrix) and the effective or matrix stress is the total stress minus the pore pressure. In terms of the elastic parameters the undrained Poisson's ratio $\nu_u = 1/2$ and $\eta_E = 1$. Equations 1, 2, and 4b become:

$$2G\epsilon_{ij} = \sigma_{ij} - \frac{\nu}{1+\nu}\sigma_{KK}\delta_{ij} + \frac{1-2\nu}{1+\nu}p\delta_{ij} \qquad (9)$$

$$m - m_o = \frac{\rho_o(1-2\nu)}{2G(1+\nu)}\left[\sigma_{KK} + 3p\right] \qquad (10)$$

$$\langle\sigma_{ij}\rangle \equiv \sigma_{ij} + p\delta_{ij} \qquad (11)$$

The constituents of cartilage are usually assumed to be incompressible. Cartilage is 70 to 80 percent water, which has a bulk modulus (2.2 Gpa) 100 times greater than the maximum pressures measured in the hip joint. The remaining solids (collagen fibers, proteoglycan gel, and a probably insignificant number of cells) are also composed of molecules typically considered incompressible [91]. The pore pressures induced in typical plug experiments on cartilage are usually less than 0.2 MPa in order to keep the solid matrix strains in the elastic range. The frequency response of cartilage was measured herein in order to check this assumption (Section 3.2.3).

3.2 ONE DIMENSIONAL CONSOLIDATION

There are very few analytical solutions to the equations of Section 3.1. Simplifying assumptions are usually made about the state of strain (such as plane or uniaxial strain) and the direction of fluid flow. Some simple cases are considered here for two reasons. The first is their applicability to experiments on isolated cartilage plugs. The second is to illustrate the importance of the boundary conditions for fluid flow and their effect on the stress in the cartilage. In all cases the cartilage consolidation (displacement of the solid matrix) is assumed to be limited to the direction of load application. For the plug experiments this implies the plugs are tightly confined so lateral bulging of the plug is not possible. In application to the cartilage layer in the intact synovial joint this translates into the radial displacement of the cartilage layer is uniform or at least that shear is small. This is discussed later in Section 5.1.1.

3.2.1 Vertical Flow

Cartilage plugs are often tested in lateral confined compression. The specimens are put in a closely fitting (usually cylindrical chamber) and loading in compression via a very permeable loader Figure 3-1). A preload is usually applied to assure the plugs fit tightly. A constant compressive load is applied and the time response of the thickness of the specimen is measured.

Since the problem is one dimensional the only non-zero variables are the pressure p(z,t) and the z displacement w(z,t). The effective stress in the load direction $\langle \sigma_{zz} \rangle$ is directly related to the strain ε_{zz} via single elastic constant $\bar{E}$ the uniaxial strain modulus. If the material is isotropic this is simply:

$$\bar{E} = \frac{2G(1-\nu)}{(1-2\nu)} \tag{12}$$

If not $\bar{E}$ can be derived simply from the elastic constants (see [34] for an example of a transversely isotropic material). Equation 10 gives the change in fluid mass content which is directly proportional to the strain. Also, since the total stress is constant the diffusion equation (7) simply becomes, in terms of the fluid pressure:

$$\frac{K}{\mu}\bar{E}\frac{\partial^2 P}{\partial x^2} = \frac{\partial P}{\partial t} \tag{13}$$

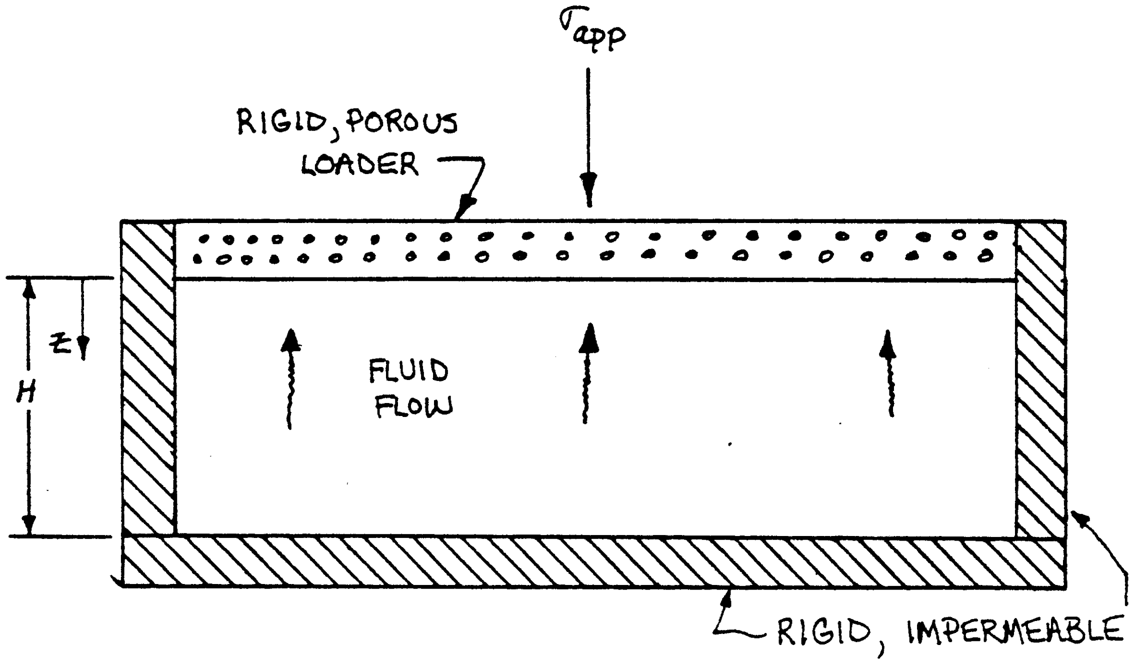

Figure 3-1. Vertical Flow Model Geometry

The boundary and initial condtions are:

$$P(0,t) = 0 \tag{14a}$$

$$\frac{\partial P}{\partial z}(H,t) = 0 \tag{14b}$$

$$P(z,0) = \sigma_{app} \tag{14c}$$

The solution is given by:

$$P = 2\sigma_{app} \sum_{N=1}^{\infty} \frac{1}{\lambda_N} \exp\left(-\lambda_N^2 \frac{K}{\mu} E t / H^2\right) \sin\left(\lambda_N z / H\right) \tag{15}$$

where τ the fundamental time constant and λ_n the eigenvalues are:

$$\tau = \frac{4H^2}{\pi^2 \frac{K}{\mu} E} \tag{16a}$$

$$\lambda_N = \left(\frac{2N-1}{2}\right)\pi \tag{16b}$$

The surface displacement is related to pressure by:

$$\omega(0,t) = \frac{H}{E}\left(\sigma_{app} - P(H,t)\right) \tag{17}$$

It is unlikely that cartilage in a synovial joint under load has zero flux or a free draining surface. Resistance to flow at the surface is analyzed here by modifying the boundary condition Equation 14b to be: [34]

$$P(0,t) = R_d \frac{\partial P}{\partial z} \tag{14b'}$$

where Rd is an effective resistance at the surface of the cartilage layer. This is called a convective boundary condition from the analogy to heat flow. The solution is then[34]

$$\omega(0,t) = \frac{H}{E}\sigma_{app}\left(\hat{R}\sum_{N=1}^{\infty} b_N \tan^2\left[\lambda_N\left(1 - \exp(\lambda_N^2 t/\tau)\right)\right]\right) \tag{18}$$

where:

$$\lambda_N \tan\lambda_N = (\hat{R})^{-1} \qquad \hat{R} = Rd/H \tag{19a}$$

$$b_N = \frac{2\hat{R}\tan^2\lambda_N}{1 + \sin\lambda_N\cos\lambda_N + \tan^2\lambda_N + (1+\hat{R}\sin\lambda_N)} \tag{19b}$$

The results (Figure 3-2) depend on the surface resistance. If Rd is large the layer consolidation is dominated by the surface resistance and the consolidation is nearly constant.

3.2.2 Lateral Flow

This model assumes the cartilage is loaded by a flat, rigid, impermeable loader [34]. The specimen is also a disk of thickness h and radius a, confined at the lateral edges by very porous walls (Figure 3-3). If the cartilage is attached to bone and h << a then bulging is negligible and lateral confinement is not necessary. Since there is no flow toward the loader the only non-zero variables are p(r,t) and w(r,t). Mass conservation (Equation 6) can be written as:

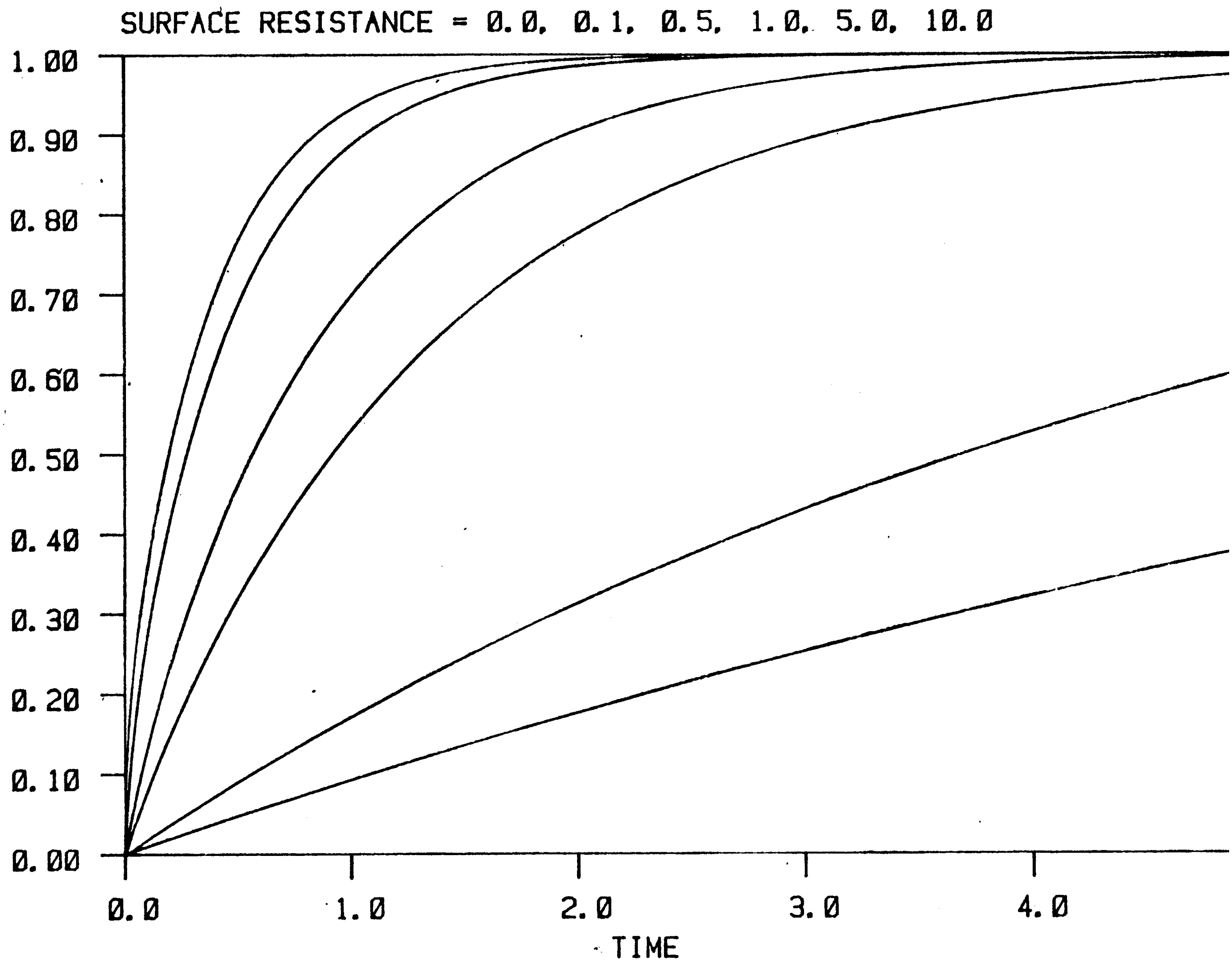

Figure 3-2. Consolidation versus Time for Vertical Flow

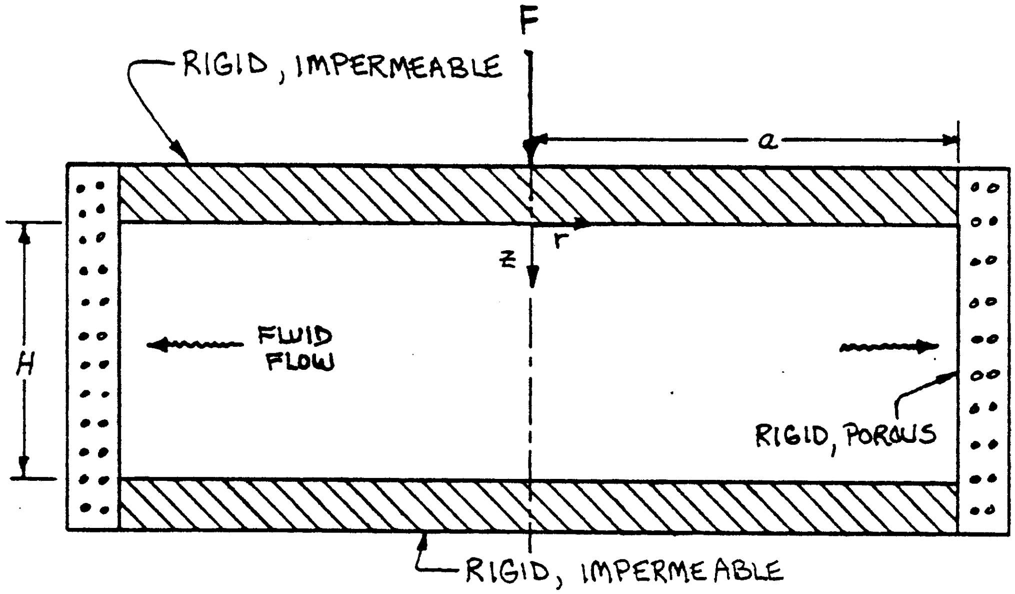

Figure 3-3. Lateral Flow Model Geometry

$$\frac{K}{\mu}\frac{1}{r}\frac{\partial}{\partial r}\left(\frac{r\partial P}{\partial r}\right)=\dot{\epsilon} \tag{20}$$

Integrating using the boundary condtions:

$$\frac{\partial P}{\partial r}(0,t)=0 \tag{21a}$$

$$P(a,t)=0 \tag{21b}$$

$$P(r,t)=\frac{\dot{\epsilon}}{4K/\mu}(a^2-r^2) \tag{22}$$

Vertical equilibrium requires:

$$-F=2\pi\int_0^a\left[\frac{\dot{\epsilon}}{4K/\mu}(a^2-r^2)+\bar{E}\epsilon\right]r\,dr \tag{23}$$

This can be integrated as:

$$\tau_R\dot{\epsilon}+\epsilon=\frac{-F}{\pi a^2\bar{E}} \tag{24}$$

where τ_R the radial time constant is:

$$\tau_R=\frac{a^2}{8\frac{K}{\mu}\bar{E}} \tag{25}$$

The solution to Equation 21 assuming zero initial strain is:

$$\epsilon(t)=\frac{-F}{\pi a^2\bar{E}}\left[1-\exp(t/\tau_R)\right] \tag{26a}$$

$$P(r,t)=\frac{2F}{\pi a^2\bar{E}}\left[1-(r/a)^2\right]\exp(-t/\tau_R) \tag{26b}$$

3.3 FREQUENCY RESPONSE

Recently the response of a cartilage plug to a sinusoidal varying load was measured by Lee, et al. [72]. The response of a plug of cartilage with the boundary conditions of Section 3.2.1 was derived by Lee and confirmed by Tepic [139] using a lumped model. The results for compressible constituents are derived here.

For uniaxial strain the effective vertical stress $\langle \sigma_{zz} \rangle$ is related to the total effective stress $\langle \sigma_{KK} \rangle$ since $\epsilon_{xx} = \epsilon_{yy} = 0$.

$$\langle \sigma_{zz} \rangle = \frac{1-\nu}{1+\nu} \langle \sigma_{KK} \rangle \tag{27}$$

Vertical equlibrium requires:

$$\frac{\partial \sigma_{zz}}{\partial z} = \frac{\partial}{\partial z}\left(\frac{2G(1-\nu)}{1-2\nu} \epsilon_{zz} - \zeta_E P \right) \tag{28}$$

The equation for mass conservartion can be rewritten as:

$$\frac{K}{\mu} \frac{\partial^2 P}{\partial z^2} = \frac{\zeta_E (1-2\nu)}{2G(1+\nu)} \frac{\partial}{\partial t} \left(\sigma_{KK} + \frac{3}{B} P \right) \tag{29}$$

Finally, in terms of surface displacement and fluid pressure the equations of motion are:

$$\frac{2G(1-\nu)}{(1-2\nu)} \frac{\partial^2 \omega}{\partial z^2} - \zeta_E \frac{\partial}{\partial t}\left(\sigma_{KK} + \frac{3}{B} P \right) \tag{30}$$

$$\frac{K}{\mu} \frac{\partial^2 P}{\partial z^2} = \frac{\partial}{\partial t}\left[\zeta_E \frac{\partial \omega}{\partial z} + \frac{3\zeta_E (1-2\nu)}{2G(1+\nu)} \left(\frac{1}{B} - \zeta_E \right) P \right] \tag{31}$$

This is the same form as Equations 2.6 and 2.7 in Wijesinghe and Kingsbury [156]. The phase shift (Figure 3-4) is:

$$\tan\theta = \frac{\sinh\sqrt{\tau\omega} + \sin\sqrt{\tau\omega}}{\sinh\sqrt{\tau\omega} + \sin\sqrt{\tau\omega} + \frac{\bar{E}_0}{\bar{E}_\infty - \bar{E}_0}\sqrt{\tau\omega}\left(\cosh\sqrt{\tau\omega} + \cos\sqrt{\tau\omega}\right)} \tag{32}$$

where the time constant is:

$$\tau = \frac{2\zeta_E^2 H^2}{\frac{K}{\mu}\bar{E}_0} \qquad \bar{E}_\infty = \frac{2G(1-\nu_u)}{(1-2\nu_u)} \tag{33}$$

Where $\bar{E}_0$ is drained and $\bar{E}_\infty$ is undrained, the phase shift will be 45 degrees only if:

$$1 \ll \tau\omega \ll \left(\frac{\bar{E}_\infty}{\bar{E}_0}\right)^2 \tag{34}$$

3.4 INTERARTICULAR RESISTANCE

The fluid pressure and solid stress in the cartilage clearly depend on the resistance to fluid flow at the loaded surface of the cartilage. This concept of surface resistance to fluid flow was first introduced by Dent [34] and Kenyon [68] in reference to the boundary condition at the loaded surface of compressed cartilage specimens, but it is equally applicable to the interarticular resistance to flow in whole *in situ* synovial joints. They noted the resistance will depend on the thickness of the fluid film, the cartilage roughness, and the effective length of the fluid flow paths. It is likely to vary with time, as the cartilage surface compresses under load and the average gap height decreases. This can happen at many different height (and length) scales ranging from the physical roughness of

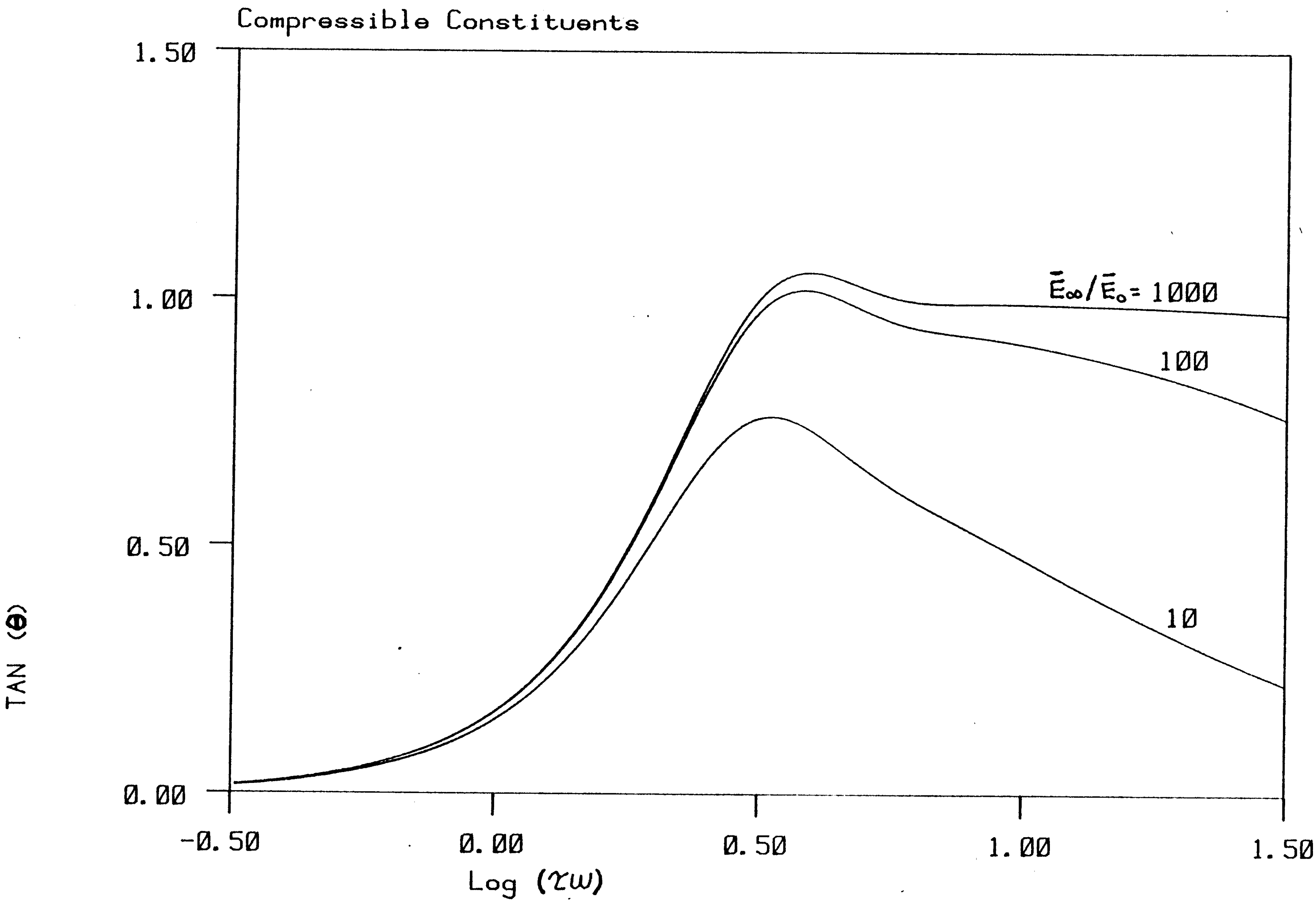

Figure 3-4. Phase Shift for Compressible Constituents

the cartilage surface (0.5 to 2.0 μm [126]) to the global deviations from sphericity measured by Rushfeldt [121] and Tepic [138] (RMS $\approxeq$ 75 um).

The resistance to interarticular flow is important for both functions of articular cartilage -- load support and low friction. These are in fact more intimately related than casual observation suggests. As the cartilage consolidates fluid must flow out of the cartilage, either into and then through the interarticular space or laterally through the layer itself. The stress supported by the solid matrix is directly related to the strain in the matrix by the drained uniaxial strain modulus, typically about 1 MPa. In vitro experiments by Rushfeldt [121] and myself [80], performed by loading human acetabula with 2250 N for 30 minutes, have demonstrated that the maximum total compression is less than 30 percent. Since cartilage should be nearly in equilibrium this corresponds to a stress in the solid matrix of 0.3 MPa (= 1 MPa). The total measured stress on the surface is typically 7 to 10 MPa over this time period indicating the fluid pressure is supporting the difference, i.e. more than 95 percent of the total stress. The resistance to fluid flow between the layers must be high enough to support this pressure across the radius of contact (about 15 to 20 mm). The lubrication quality of the cartilage depends only upon supporting this relatively small solid stress component at the locations where solid-solid contact occurs.

A simple model (Figure 3-5) illustrates the relation between interarticular resistance and the relative magnitudes of lateral flow and film flow and of solid and fluid stress. A layer of cartilage of thickness h and radius L is consolidating with fluid flow both laterally in the layer and toward the film. The conductance to fluid flow in the gap is Σ and the cartilage permeability is K/μ. The average fluid pressures are $\bar{P}_l$ in the layer (near the bone say) and $\bar{P}_g$ in the gap. The total vertical flow Q_v, lateral flow in the layer Q_l, and gap flow are:

$$Q_v = (\pi L^2)\frac{K}{\mu}\left(\frac{(\bar{P}_l - \bar{P}_g)}{h}\right) \tag{35}$$

$$Q_l = (2\pi L h)\frac{K}{\mu}\left(\frac{\bar{P}_g + \bar{P}_l}{2L}\right) \tag{36}$$

$$Q_g = (2\pi L)\,\Sigma\,(\bar{P}_g/L) \tag{37}$$

The gap flow must come from the vertical flow so $Q_g = Q_v$ and the ratios of flows and pressures are:

$$Q_l/Q_g = \left(\frac{h}{L}\right)^2 (R+1) \tag{38}$$

$$\bar{P}_g/\bar{P}_l = R/(R+2) \tag{39}$$

where R is defined as

$$R \equiv \frac{L^2 K/\mu}{h\Sigma} \tag{40}$$

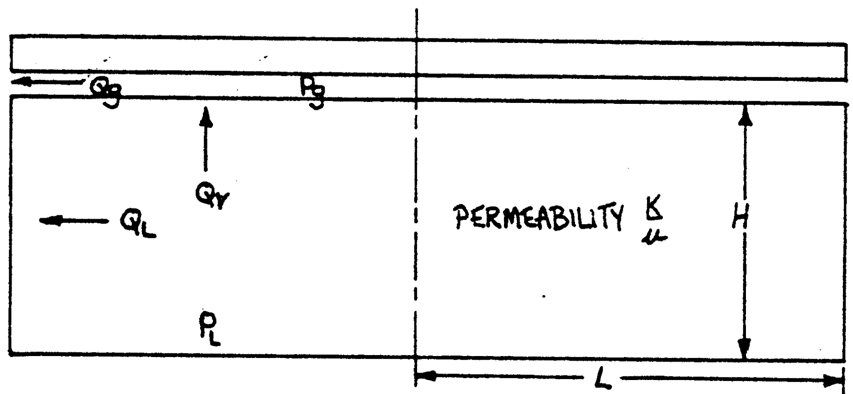

Figure 3-5. Surface Flow Model

Note this is just the ratio of the macroscopic resistance to flow in the gap (over length L) to flow in the layer (over length h).

$$R = \frac{L^2 K/\mu}{h\Sigma} = \left[\frac{K/\mu\, h/h^2}{\Sigma/L^2}\right] \tag{41}$$

Experimental estimates for the resistance to flow are described in Chapter 5.

CHAPTER 4

EXPERIMENTAL TECHNIQUE AND RESULTS

4.1 EQUIPMENT

The equipment used to perform the experiments described in this thesis is part of the *in vitro* hip joint testing facility, located in the Eric P. and Evelyn E. Newman Laboratory for Biomechanics and Human Rehabilitation at MIT. This unique facility, Figure 4-1, was designed for the *in vitro* measurement of the pressure distribution on and the geometry of the cartilage layer in the human acetabulum by Paul Rushfeldt [121] and David Palmer [122]. The instrumentation for the measurement of geometry and acoustic impedance of the cartilage covering the femoral head was added by Slobodan Tepic [138]. Tepic and I automated the measuring technique by adding the capability for recording snd off-line processing of the ultrasonic signals.

The major components of the facility are:

1. A three degree of freedom, hydraulically powered, servo-controlled hip simulator which is used to replicate physiological motions and loads across human hip joints.

2. Instrumented femoral head prostheses, which are used to load the cartilage in the acetabulum and measure either the stress on the surface of the cartilage or its thickness under load.

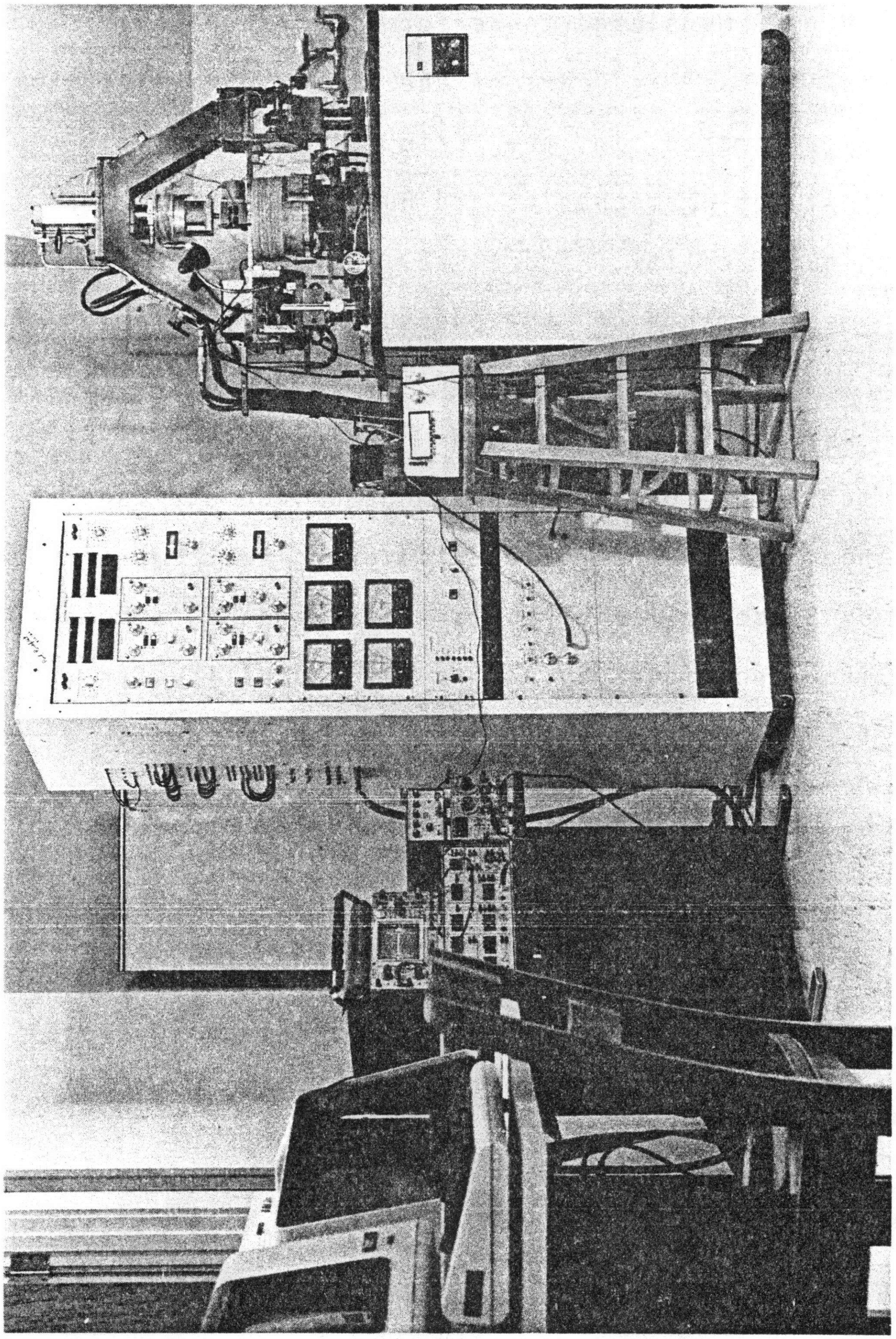

Figure 4-1. In Vitro Facility

3. A control console which provides the interfaces for manual and/or computer control of the hip simulator.

4. A two degree of freedom, stepper motor driven scanning system which is used to ultrasonically measure the geometry of the components of human hip joints. The ultrasonic equipment is computer interfaced via a waveform recorder.

5. A DEC PDP 11/60 computer and interfaces which are used for control and data acquisition during the experiments and subsequent analysis and plotting.

The laboratory resources include an additional multi-user DEC PDP 11/60 computer for data reduction and color graphics display with DECnet connections to the *in vitro* 11/60 and the Joint Computer Facility (of the Departments of Mechanical, Civil, Aero and Astro, and Ocean Engineering) DEC VAX 11/782.

4.1.1 Hip Simulator

The hip simulator has three independent hydraulic actuators that simulate load, flexion, and rotation of the hip joint. The simulator can apply compressive loads up to 4500 N over a dynamic bandwidth of 15 Hz while a combined load and torque cell provides measurement and feedback signals. The load actuator position is measured with a DCDT over the full 50 mm stroke; the center 2.5 mm range of stroke is instrumented with a second DCDT to measure the deformation of the cartilage. The loading frame can be positioned up and down with an electric motor drive to adjust for specimen size and mounting.

A rotary actuator attached to the load cell provides the capability for rotation around the load axis over a range of 280 degrees. Rotation position is measured with a precision potentiometer which is geared to the rotary actuator.

The loading frame can be rotated about a fixed axis to simulate flexion and extension while the load is applied. Although the loading frame has a large moment of inertia, a large rotation actuator can achieve 140 degrees of flexion at 10 Hz, adequate to simulate walking and other physiological movements. The flexion angle is also measured with a precision potentiometer.

The specimens, immersed in a temperature controlled saline bath, are mounted on a rotary base. A mounting device provides adjustment of the specimen orientation relative to the simulator axes.

4.1.2 Instrumented Prostheses

A specially instrumented femoral head prosthesis is used to apply load to the acetabulum and measure the pressure distribution over the surface of the cartilage. The design was developed by Carlson [18] to measure the pressure distribution over the cartilage in the hip joint in a consenting human needing a femoral head prosthesis. It utilizes fourteen pressure tranducers which are an integral part of the wall of the prosthesis (Figure 4-2). Fourteen diaphragms (3 mm diameter and 0.25 mm thick are machined into the hemisphere. A small pin rests on the center of the diaphram and transmits the small deflection of the diaphram under external pressure (sensitivity is 4 um / 7 MPa) to a single-crystal silicon beam with four strain gauges diffused onto its surface. A Wheatstone bridge produces an electrical output proportional to the pressure applied to the external surface of the prosthesis.

The pressure transducers are located in pairs at every ten degrees of latitude measured from the location through which the resultant load vector passes. By rotating the prosthesis 180 degrees about the load axis in 10 degree steps the pressure transducers sweep the full range of the longitude. A special apparatus rotates one transducer from its location at 10 degrees latitude into the pole under the load vector.

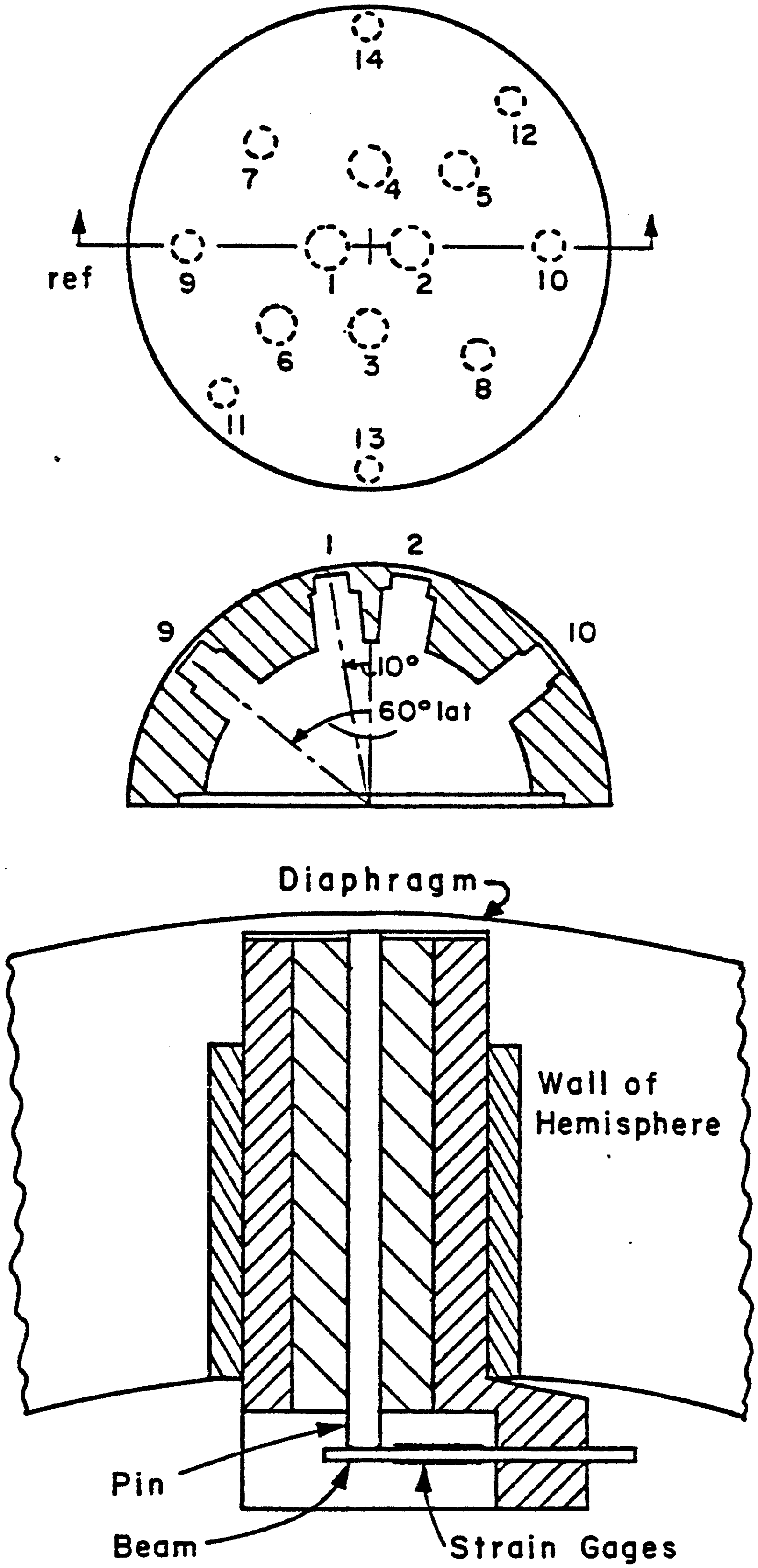

Figure 4-2. Instrumented Prosthesis

A second prosthesis has an ultrasonic transducer mounted flush with the surface (Figure 4-3). This transducer is used to measured the distance from the ball to the cartilage to calcified-cartilage interface when a load is applied to the joint. The transducer can be positioned at the pole or 30 degrees latitude.

4.1.3 Control Console

The console contains the feedback control circuits for the hydraulic actuators, displays of the values of load, stroke, torque, flexion, and rotation, and limit meters that activate an interlock system to shut off the hydraulic power if any parameter exceeds a preset limit. The input control signals to the simulator can be set internally by a set of potentiometers on the console , or externally from a connection to the computer or a signal generator. The bridge outputs from the pressure transducers are time-multiplexed onto a single signal and the simulator state signals are amplified for output to the computer or display on an oscilloscope.

A "menu box" is connected via the console to the digital input and output registers of the computer. It is used to send digital instructions to the computer or prompt the experimenter for input during an experiment.

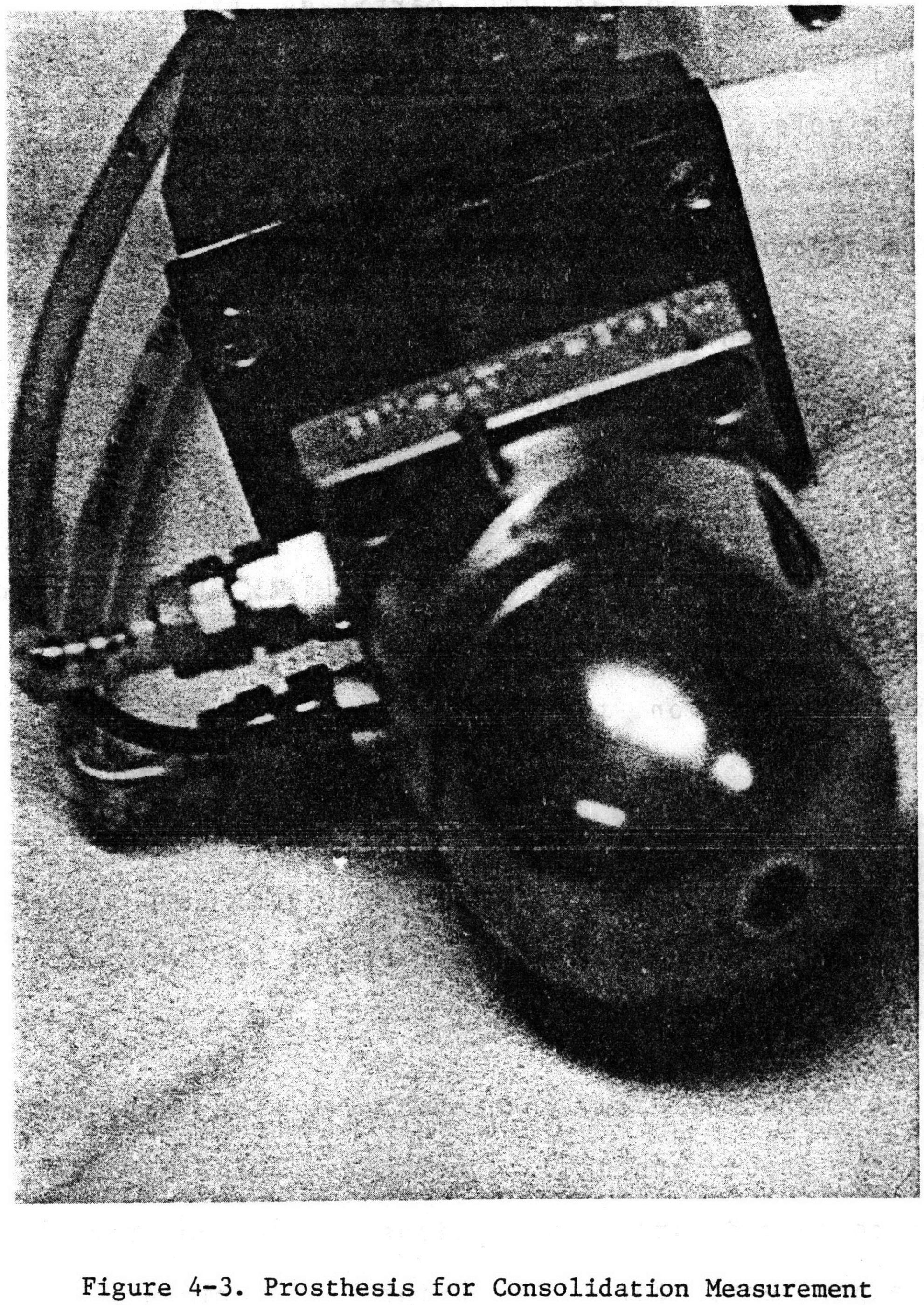

Figure 4-3. Prosthesis for Consolidation Measurement

4.1.4 Ultrasonic Apparatus

The scanning motions for the ultrasonic measurement are provided by two stepper motors. The first (longitude) is rotation of the base on which the specimen is mounted. The second (latitude) is rotation of the arm which carries the ultrasonic transducer, either around the femoral head or inside the acetabulum. The carrier for the femoral head scanner has an additional degree of freedom, capable of moving the transducer about its focal point anywhere within a solid angle of eight degrees, driven open loop by a DC motor. A controller converts an external pulse train from the computer into the signals required to drive the motors. Additional digital circuitry counts the number of pulses sent to each motor and calculates and displays on LED's the position of each axis in degrees. Manual control of the scanners is also possible.

The ultrasonic signals are generated and amplified by a Panametrics PR 52 pulser/receiver (Figure 4-4). The signals are sampled for 20.48 μs at 100 MHz and digitized with 8 bit resolution by a Biomation 8100 waveform recorder. The sampling is initiated by a signal from the computer and synchronized with the pulser/receiver by a Tektronix FG 501 function generator; in this way averaging of the signals to improve the SNR is facilitated. An analog reconstruction of the signal stored in the waveform recorder is displayed on a

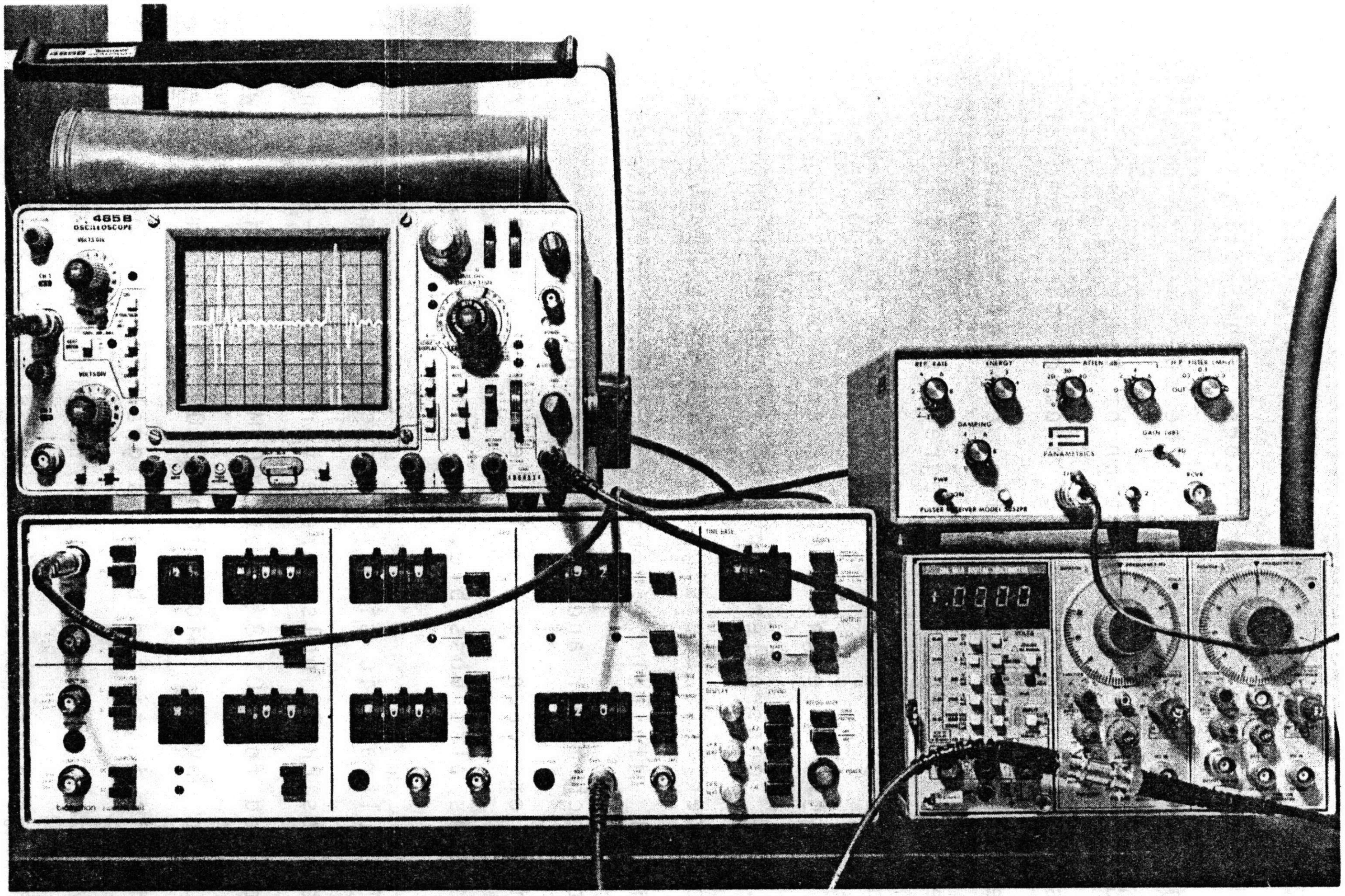

Figure 4-4. Ultrasonic Apparatus

Tektronix 465B oscilloscope; the data can also be transferred to the computer where it is averaged and stored on disk for processing.

4.1.5 Computer Interfaces

There are two interfaces from the PDP 11/60 to the *in vitro* equipment. The first is a DEC Lab Peripherals System (LPS) which includes 16 digital inputs and 16 digital outputs, 8 analog input channels which are multiplexed through a 12 bit A/D converter, 2 programmable relays, and 2 D/A outputs. The analog signals are used to monitor the hip simulator states and generate the control signals. The digital channels provide various control functions for the simulator, waveform recorder, and stepper controller.

The second interface is a DECkit 11-D, a high speed interface for Direct Memory Access (DMA) transfers between the PDP-11 memory and an external device; in this case the Biomation waveform recorder. Once data taking is initiated by the 11/60 and completed by Biomation the data is transferred into the computer memory without intervention by the processor, which is free to begin averaging the data with the previous samples, for example. The high speed of the data transfer ($\sim$0.5 million 8-bit samples per second) enables sampling averaging of about 250 records/second.

4.2 GEOMETRY

The specimens used in these studies were obtained at autopsy at the Massachusetts General Hospital by Dr. William H. Harris and his associates. Kirschner wires are inserted into the pelvis and femur perpendicular to the sagittal and frontal planes of the body. These wires are later used as reference axes when mounting the joint components for the geometry and pressure measurements.

The intact joint with capsule is removed, usually as a hemipelvic section. The joint is x-rayed to calculate the size of the acetabulum. Rushfeldt [121],[124] has demonstrated the fit of the prosthesis in the acetabulum has a strong affect on the pressure distributions. Since the natural joint components fit very closely [138] only acetabulae which fit the prosthesis size (49 mm) are selected for the pressure studies. Nearly any size can be accomodated for the geometry measurements. The joints are stored in plastic bags at -20 C. We have compared the pressure distributions for one acetabulum which was studied immediately after autopsy with data taken after freezing for both 12 hours and 18 months and then thawing. There was little change in the pressure distribution.

The specimens are thawed in room temperature saline. The capsule is opened and removed. The diameter of the femoral head is measured with calipers and recorded. Clinical evaluation of the condition of the cartilage is performed by Dr. Harris or one of his associates. After drawings and photographs are made, India ink is swabbed is onto the cartilage and rinsed off using saline solution, as described by Meachim [100]. Slight fibrillation of the cartilage surface, one of the early signs of osteoarthritis, is made more easily visible by this technique. Another set of photographs is taken if there is any discernible fault in the cartilage condition.

The femoral head is mounted on a base plate as shown in Figure 4-5 using polymethyl methacrylate cement. The lateral-medial axis is positioned vertical and upward and the superior-inferior axis is horizontal and to the right. The base plate is mounted on the rotary table in the circulating saline bath controlled at body temperature of 37 C.

The corresponding acetabulum is mounted in a similar orientation (Figure 4-6). Since the joint will later be loaded by the instrumented prosthesis care is taken to mount the acetabulum in an orientation and manner that will be stable and secure. The following procedure has proven the

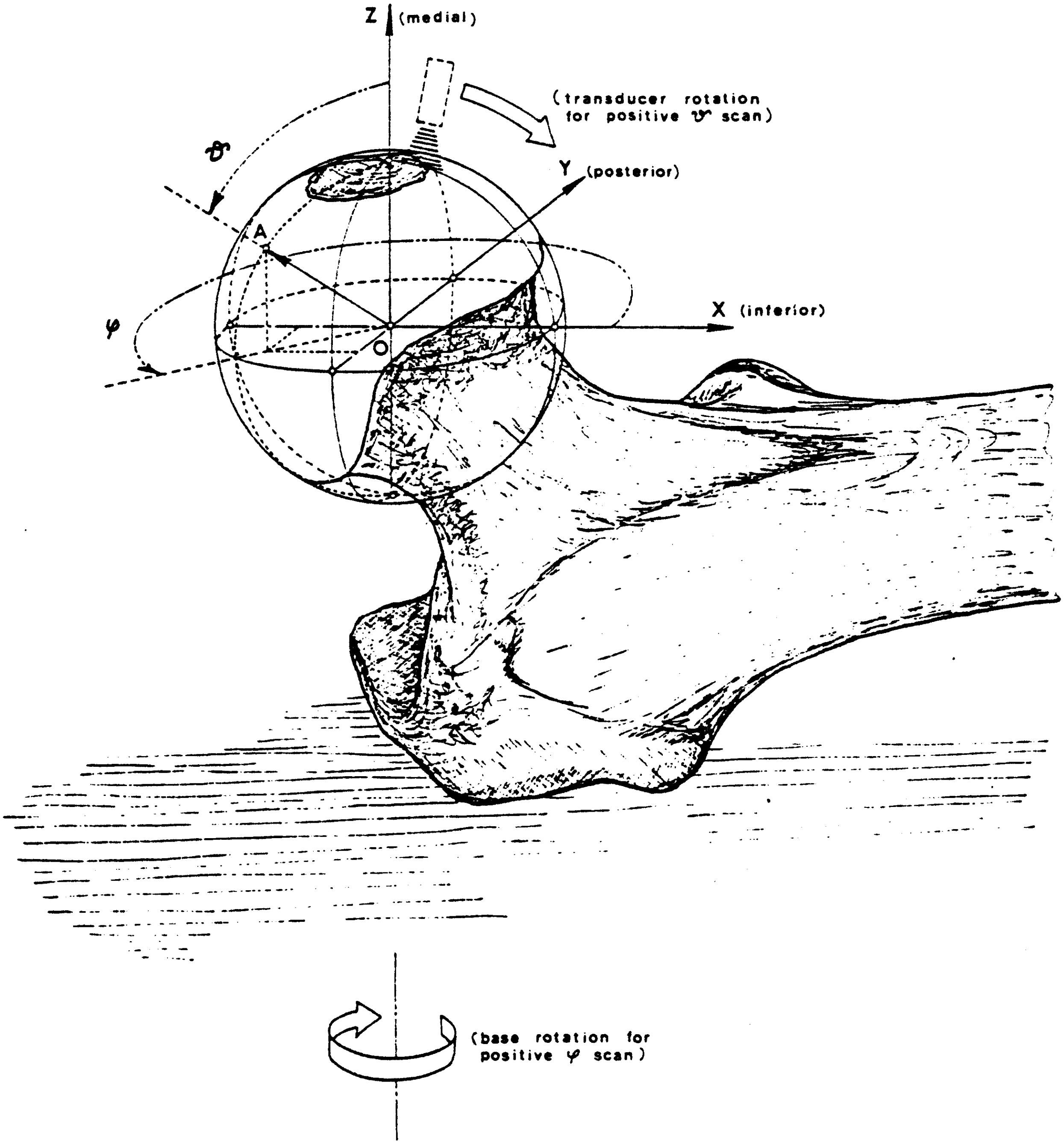

Figure 4-5. Femoral Head Mounting

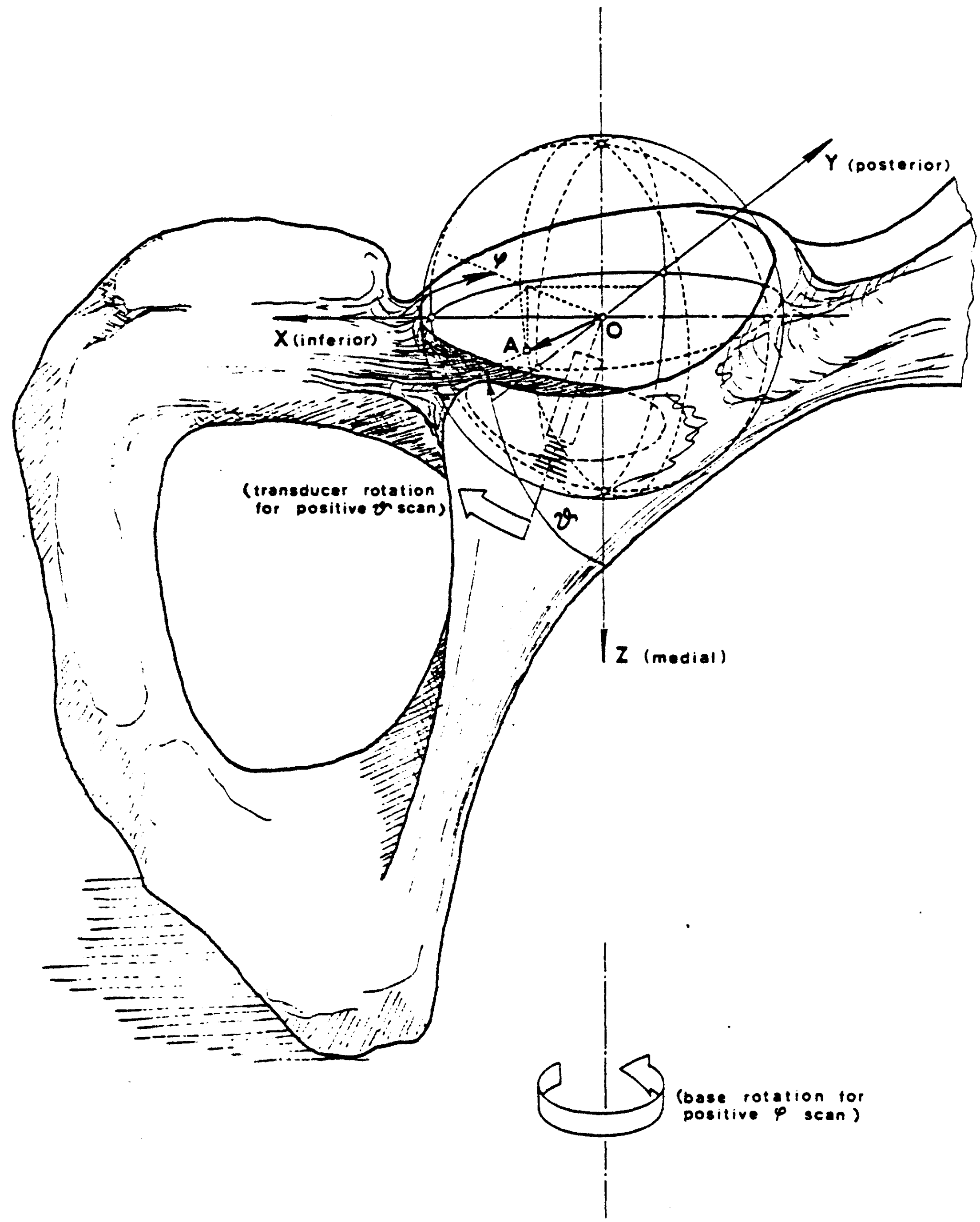

Figure 4-6. Acetabulum Mounting

most reliable. The joint is prepared for mounting by making two cuts in the pelvis, using the Kirschner wires as a guide. A transverse cut is made 50 mm above the superior edge of the acetabulum and a sagittal cut is made just medial of the acetabulum. The acetabulum is mounted on an L-shaped aluminum base using methylmethacrylate cement. The acetabulum is positioned with the medial cut in the horizontal plane for the geometry measurements and the superior cut in the horizontal plane for the pressure measurements.

The joint is first centered relative to the scanning axes approximately by eye and then accurately by monitoring the position and amplitude of the ultrasonic reflections as the joint and scanning arm are rotated back and forth. It is important to get the joint properly centered since the amplitude of the ultrasonic reflections is decreased greatly if the incidence of the ultrasonic wave axis is not normal to the cartilage.

The cartilage boundaries are inputted manually to computer storage at 20 equidistant points of the base rotation. The scanning arm is manually advanced until the ultrasonic reflections from the surface become indistinct. This position of the arm is input to the computer and stored for use later during plotting and to define the limits for the automatic scanning of the cartilage geometry. The automatic scanning locations are at even 9 degree intervals of base rotation (longitude) and the roots of the Legendre polynomial of degree 40 (about every 4.5 degrees) for the scanning arm (longitude).

The scanner is positioned automatically under computer control at every location within the cartilage boundaries. The ultrasonic reflections are sampled at 100 MHz by the waveform recorder and transferred to the computer, where 128 records 1024 samples long (10.24 μs) at each location are averaged and stored on disk. Complete scanning of a femoral head produces about 700 data locations in less than one hour. There are about 350 data locations on the acetabulum cartilage which is much smaller in area.

The recorded ultrasonic signal is analyzed off-line using a correlated receiver technique. The cross correlation of a standard reflection from a steel ball with the reflections from the cartilage is calculated for each location using Fourier transforms. The maxima of the correlation are identified as the travel times to the cartilage surface and cartilage to calcified cartilage interface. The travel times are reduced to a set of radii which describe each surface, using the speed of sound in saline (1533 m/s @ 37 C) and in cartilage (1760 ± 90 m/s) and the calibration measurements from the steel ball.

The cartilage surfaces are described in two ways. The first is by fitting a least squared error sphere to each and calculating the deviations at each location. Spherical harmonic series are also fitted to the data [138], providing a smooth function closely approximating the shape of each interface. Contour plots of constant deviation from sphericity (Figures 4-7 & 4-8) and the thickness of the cartilage (Figure 4-9) are generated from the series representations.

4.3 SWELLING

The swelling experiments described here are used to estimate the diffusivity of the cartilage and the uniaxial strain equilibrium modulus. The method exploits the unique osmotic-mechanical coupling of the cartilage. As has been noted by Maroudas [92], the osmotic pressure of the proteoglycans (based on the extrafibrillar water) supports the entire applied pressure when cartilage is compressed from the physiological equilibrium position (since the stresses in the collagen fibers are zero). Conversely, by varying the osmotic pressure of the solution bathing the cartilage, compression can be effected. It is important to note that this is not exactly the same as varying the local charge on the proteoglycans by varying the salt concentration of the bath since in the latter case the diffusion of salt ions through the cartilage introduces a

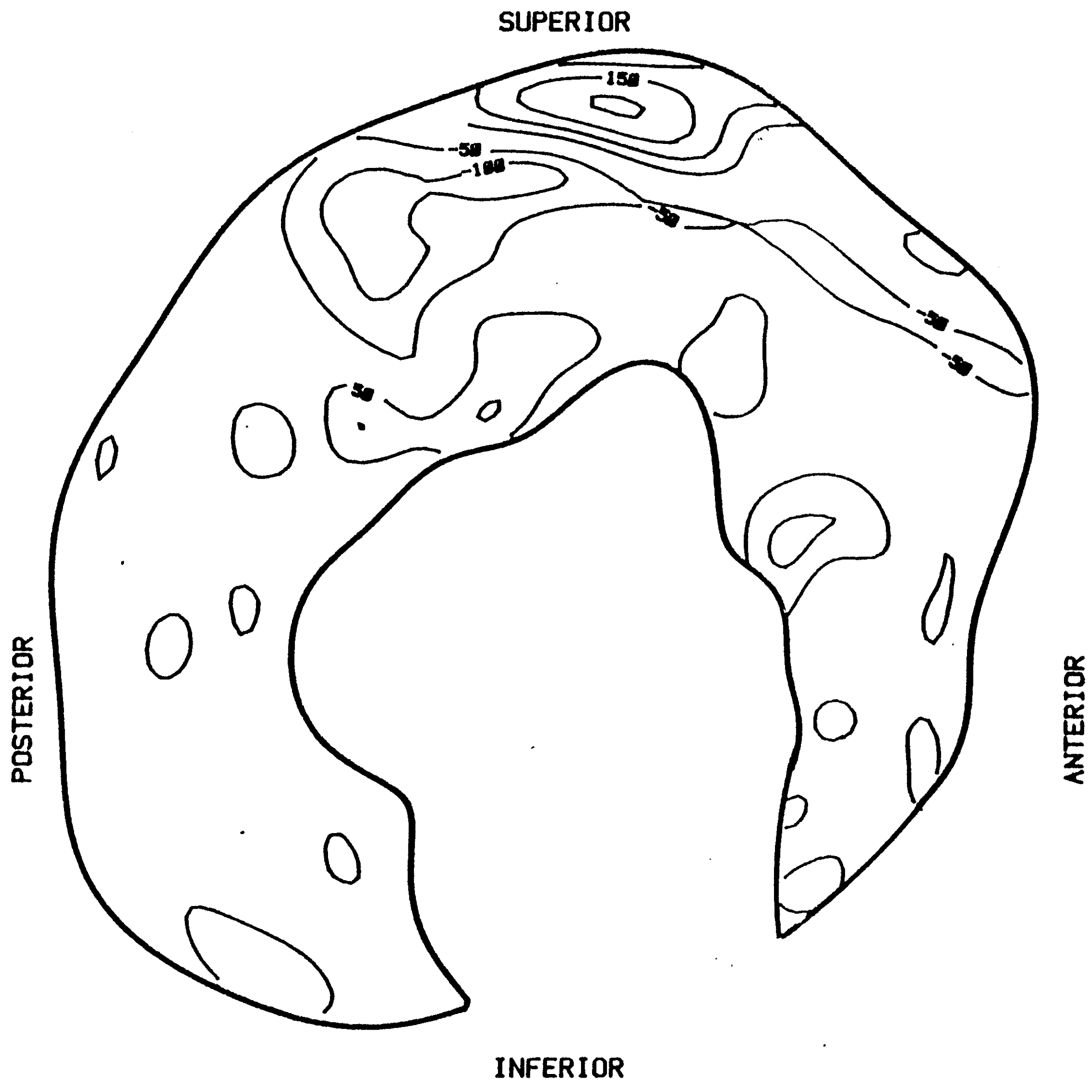

Figure 4-7. Cartilage Surface Deviations from Sphericity [um]

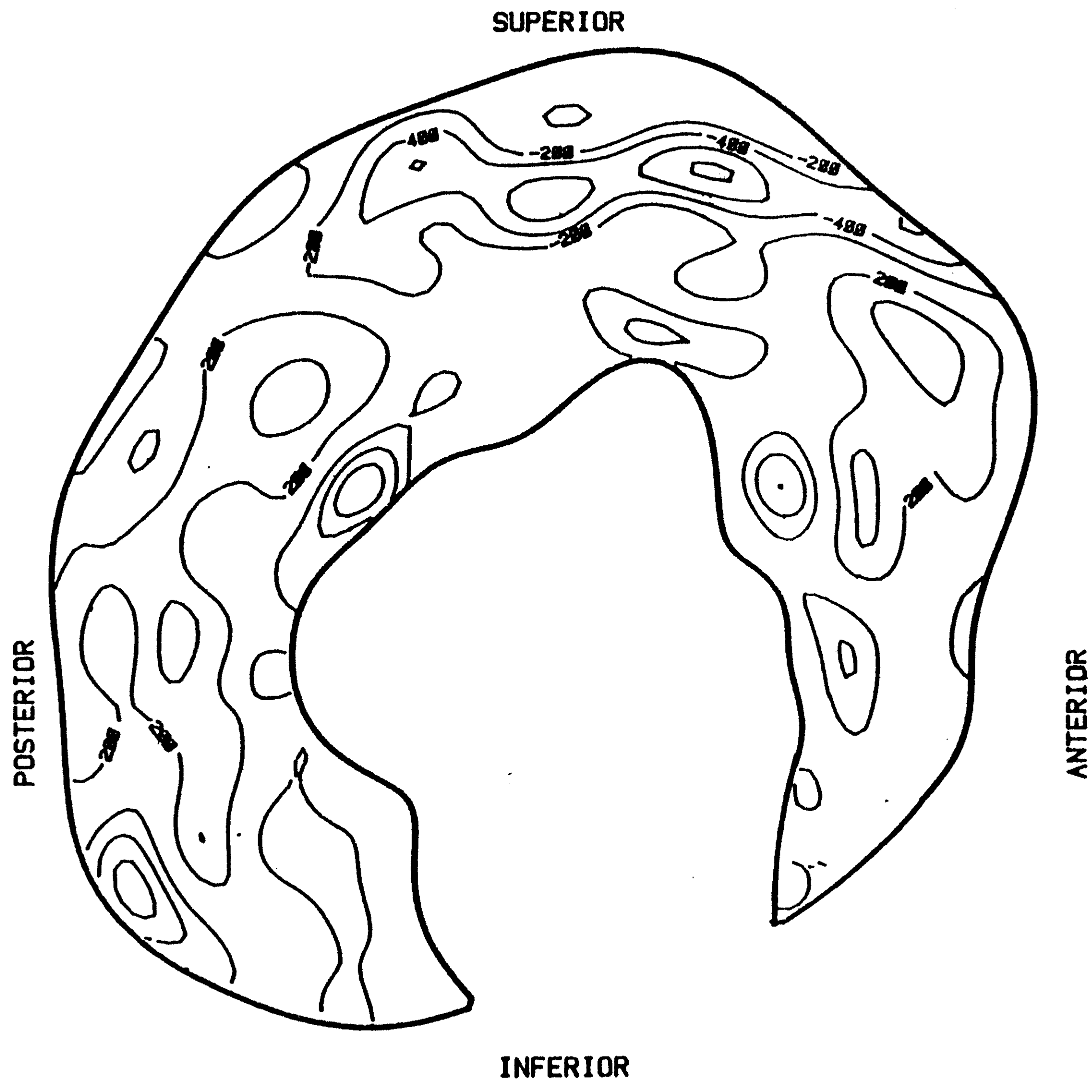

Figure 4-8. Cartilage to Calcified-Cartilage Interface Deviations from Sphericity [um]

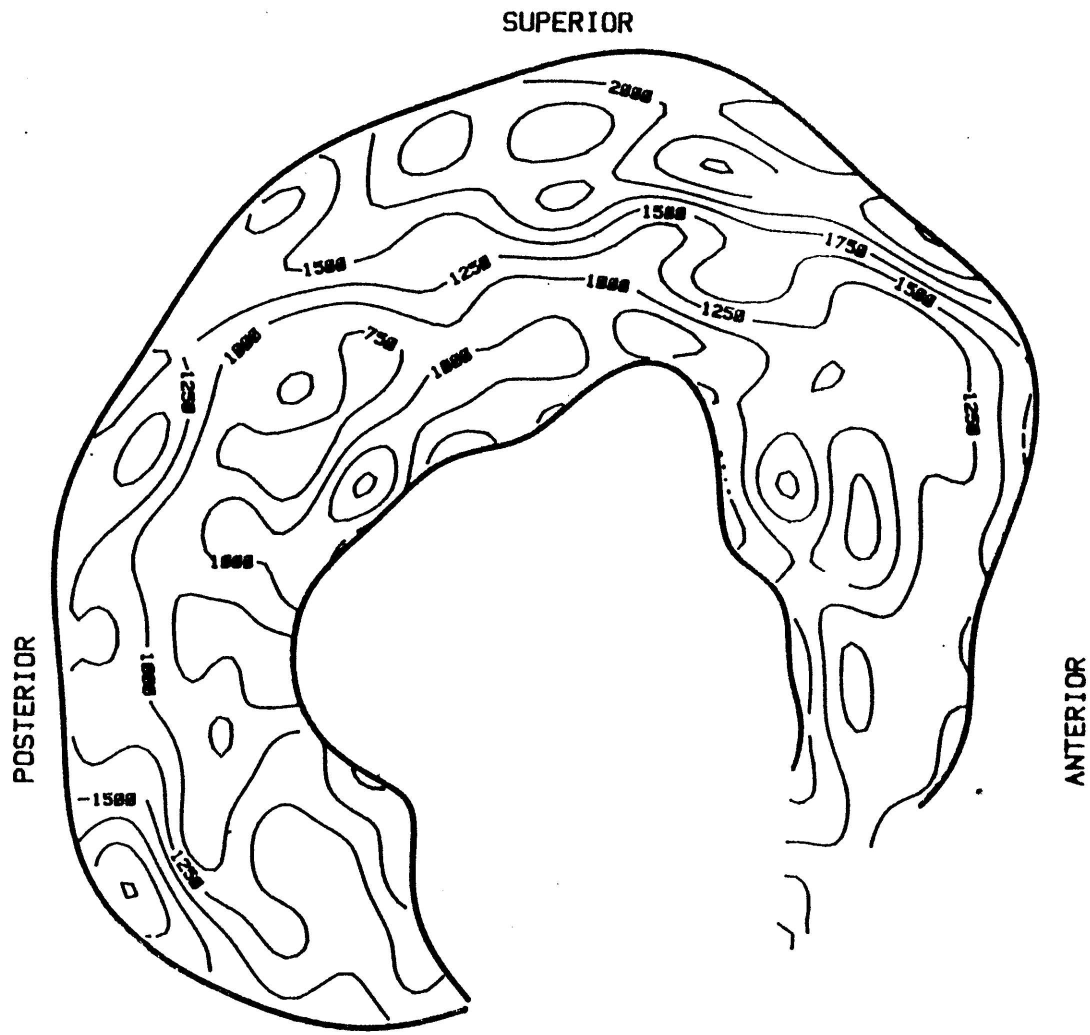

Figure 4-9. Cartilage Thickness [um]

complicating coupled diffusion problem. In fact our initial attempts to measure the time response of cartilage when changes in the equilibrium potential of the proteoglycans were induced by varying the salt concentrations of the bath were complicated by the nearly equal diffusivitites of the water and salt [53],[91].

Our next set of experiments relied on varying the osmotic potential of the PG gel by exposing the cartilage to humid air [139]. For free convection in air the time constant associated with the drying was about two orders of magnitude longer than the layer time constant. The layer is therefore in quasi-equilibrium throughout the dehydration. The layer was then resubmerged in the saline bath and the surface displacement measured using the same ultrasonic techniques and equipment as for the static geometry measurements.

There were two problems with this method. First, since the dehydration would continue well past the ten to fifteen percent compression desired to give adequate displacement while keeping nonlinear (permeability) effects to a minimum some control over the dehydration was required. This was hard to judge accurately since the dehydration rate depended on the orientation of the surface and other external influences and the amount of dehydration could not be measured without re-introducing the bathing solution.

An alternative method has been developed which uses solutions of polyethylene glycol (PEG 20,000) to osmotically load the cartilage. The concentration of the PEG determines the osmotic pressure and can be determined from thermodynamic considerations. The method is similar to and motivated by the experiments of Maroudas [92] on cartilage slices. There are two major attractions to this method. First, the equilibrium displacement can be precisely controlled via the applied pressure and second, the equlibrium modulus can be measured by varying the generated osmotic pressures.

PEG solutions are prepared by dissolving 100 to 250 g of PEG in 1 l of 0.15 M NaCl. The corresponding osmotic pressures are 0.1 to 0.6 MPa. The PEG solutions are inserted in sacs of Spectrapor 2 dialysis tubing (MW cutoff 12-14000), taking care the sacs are not fully filled. The saline bath level is lowered and a PEG sac is positioned in the acetabulum, totally covering the cartilage. After 2 to 3 hours the sac is removed (initial experiments for longer times produced no additional compression of the cartilage) and the saline bath is restored. The time response of the surface displacement and the amplitude of the reflection from the cartilage surface is measured. A set of locations at one longitude are scanned during one swelling cycle.

The surface displacement response at one location (the osmotic pressure was 0.5 MPa) is shown in Figure 4-10. Near physiological equilibrium the response is significantly different from that predicted by a simple diffusion equation; i.e. it is not well described by a single time constant (Figure 4-11). The collagen fibers appear to limit the expansion of the proteoglycan gel near equilibrium, the difference in the osmotic pressure of the proteoglycans and the tissue swelling pressure being the tensile stress in the tissue (Maroudas found typical values of 0.2 MPa). Consequently the unrestrained equilibrium volume of the gel (which the layer is moving toward prior to reaching physiological equilibrium)is greater than the _in situ_ volume of cartilage. The equilibrium volume was estimated by finding the equilibrium volume of the gel that gave the best linear fit to the log of the surface displacement relative to the gel equilibrium (Figure 4-12). The estimated equilibrium volume was 32 percent greater than the physiological equilibrium volume and the time constant was 2400 s.

A second set of experiments on the cartilage at the same location is shown in Figure 4-13. The applied osmotic pressure was 0.4 MPa and the calculated gel volume (Figure 4-14) was 29 percent greater than physiological equilibrium and the time constant was 2300 s. Refering to Equation 16 in Chapter 3, the permeability at this location

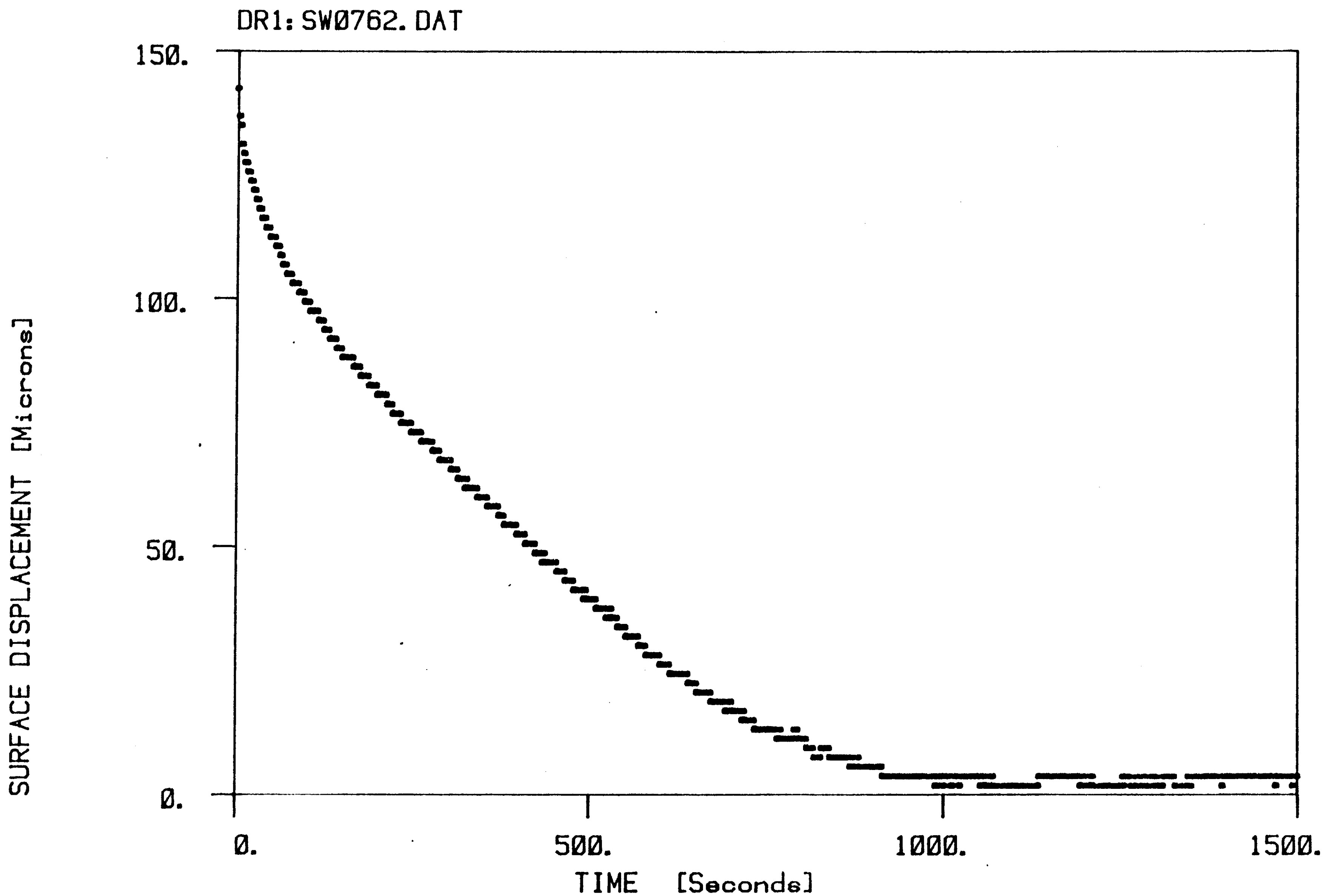

Figure 4-10. Swelling Surface Displacement

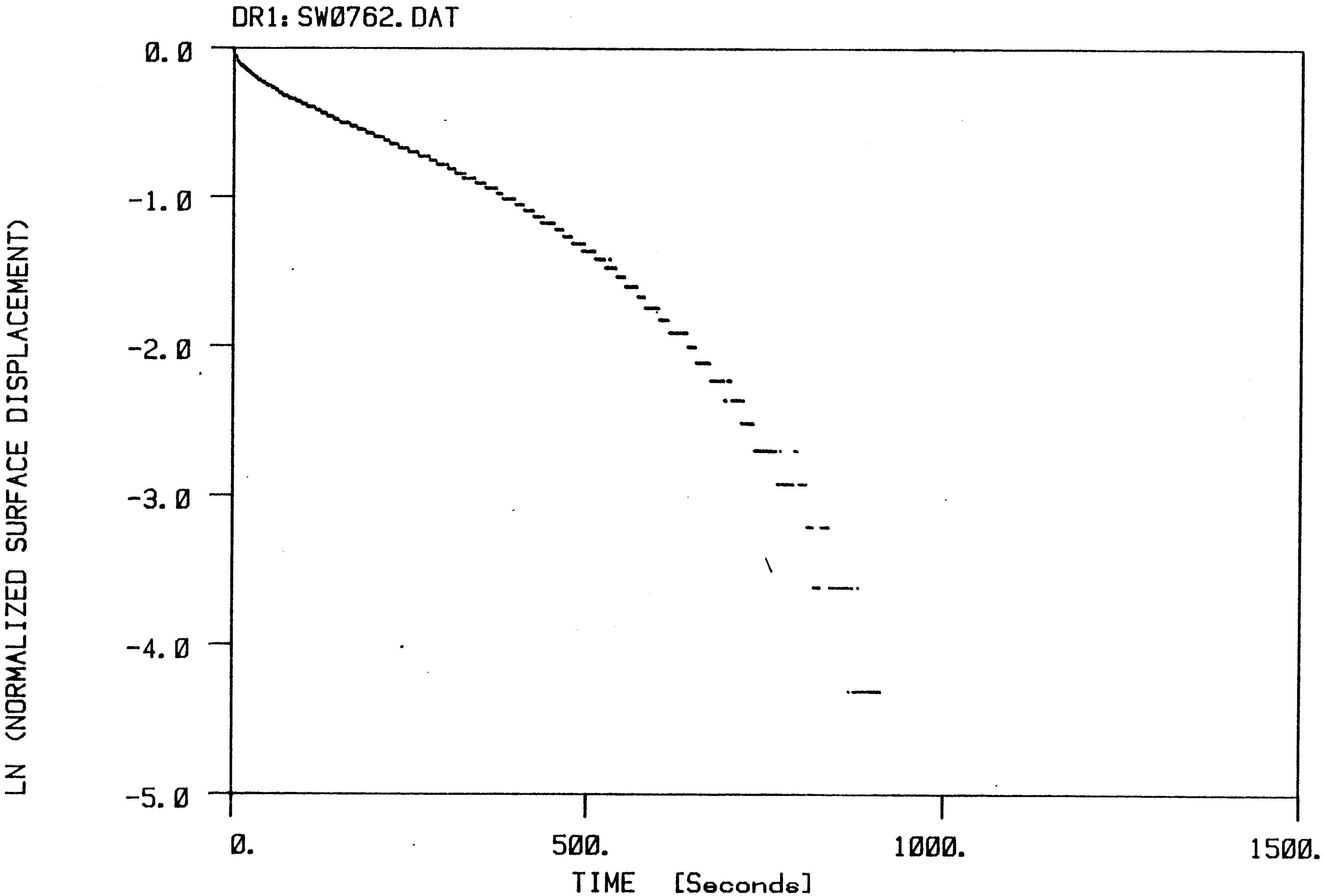

Figure 4-11. Log Surface Displacement

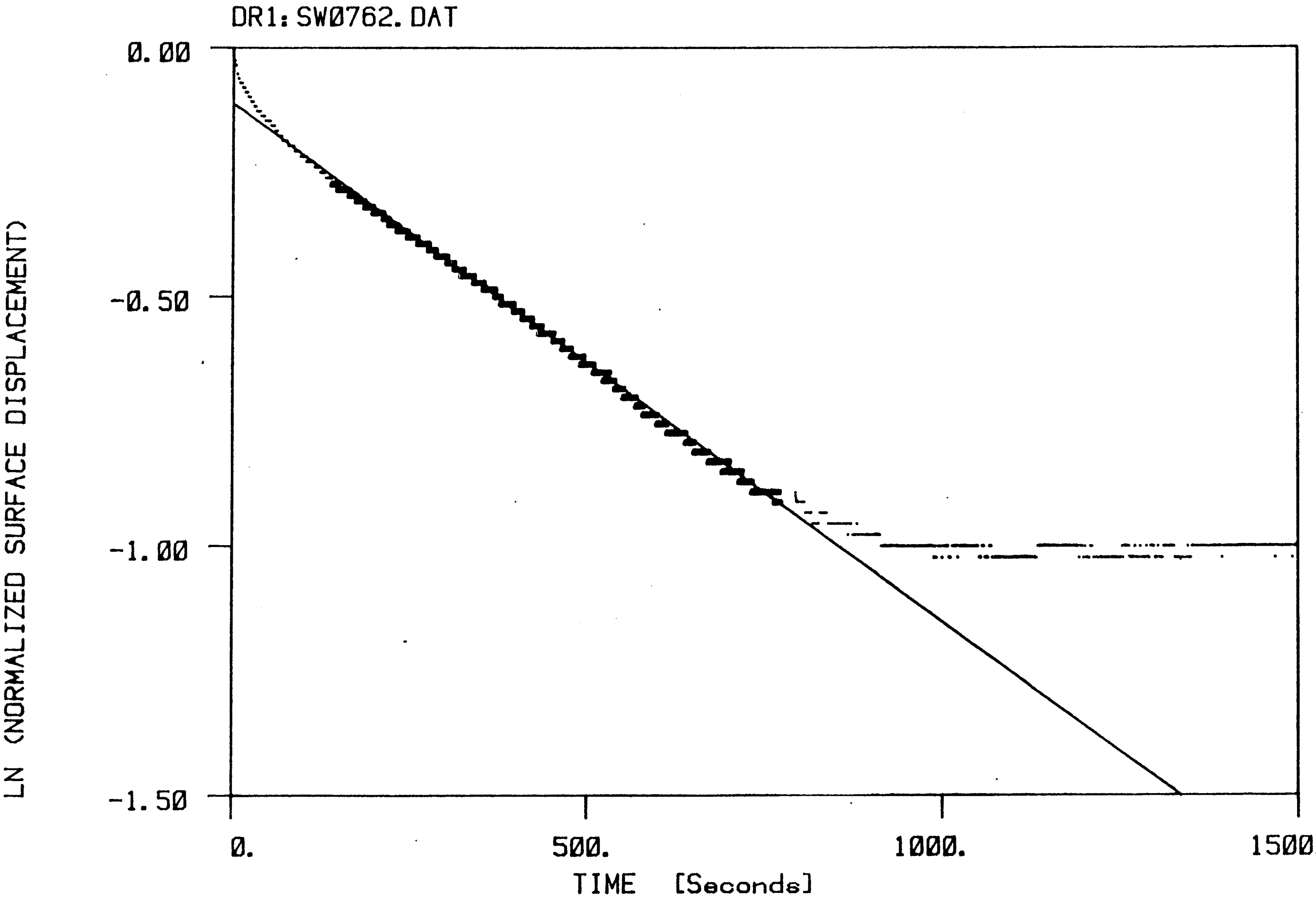

Figure 4-12. Best Linear Fit

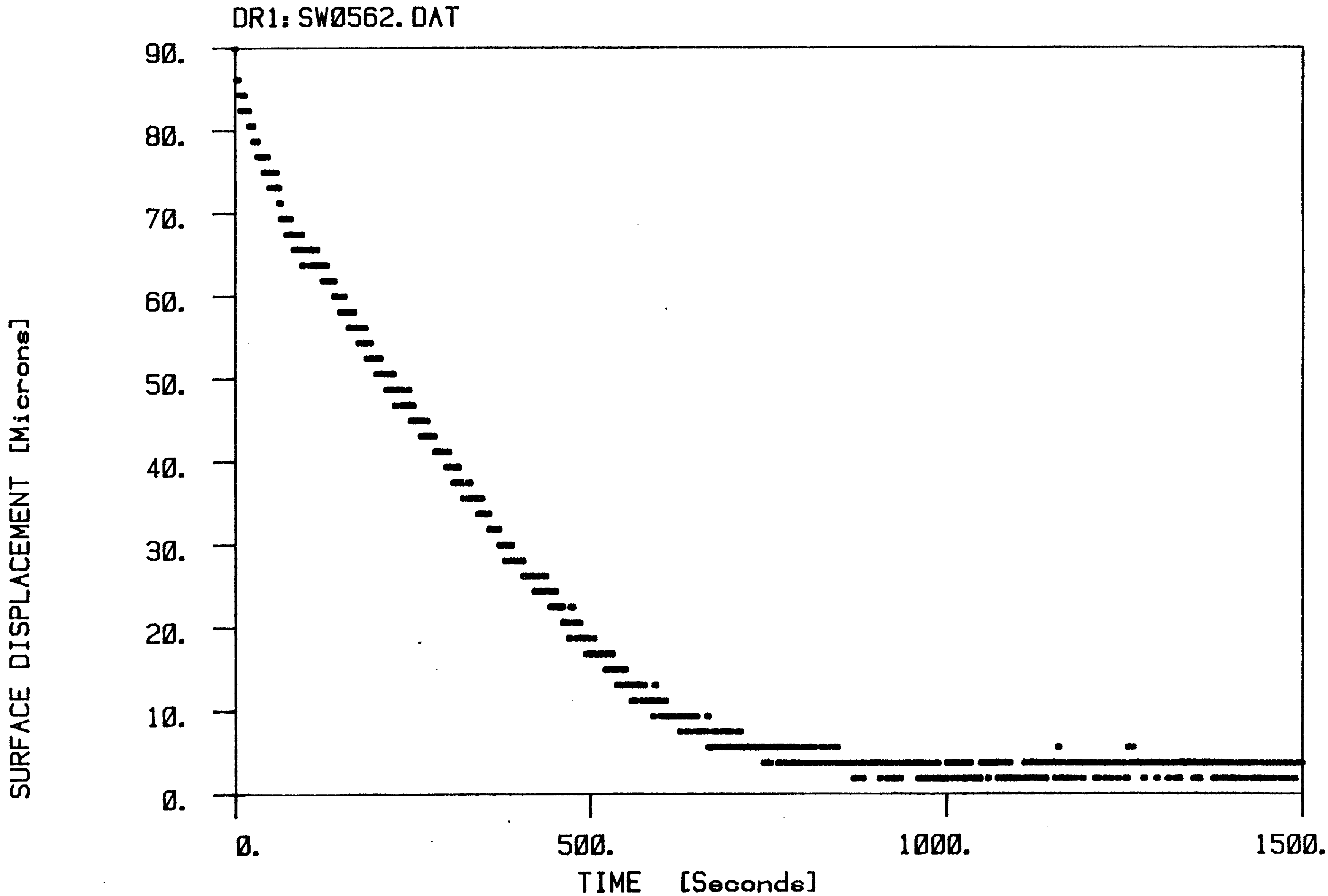

Figure 4-13. Swelling Surface Displacement

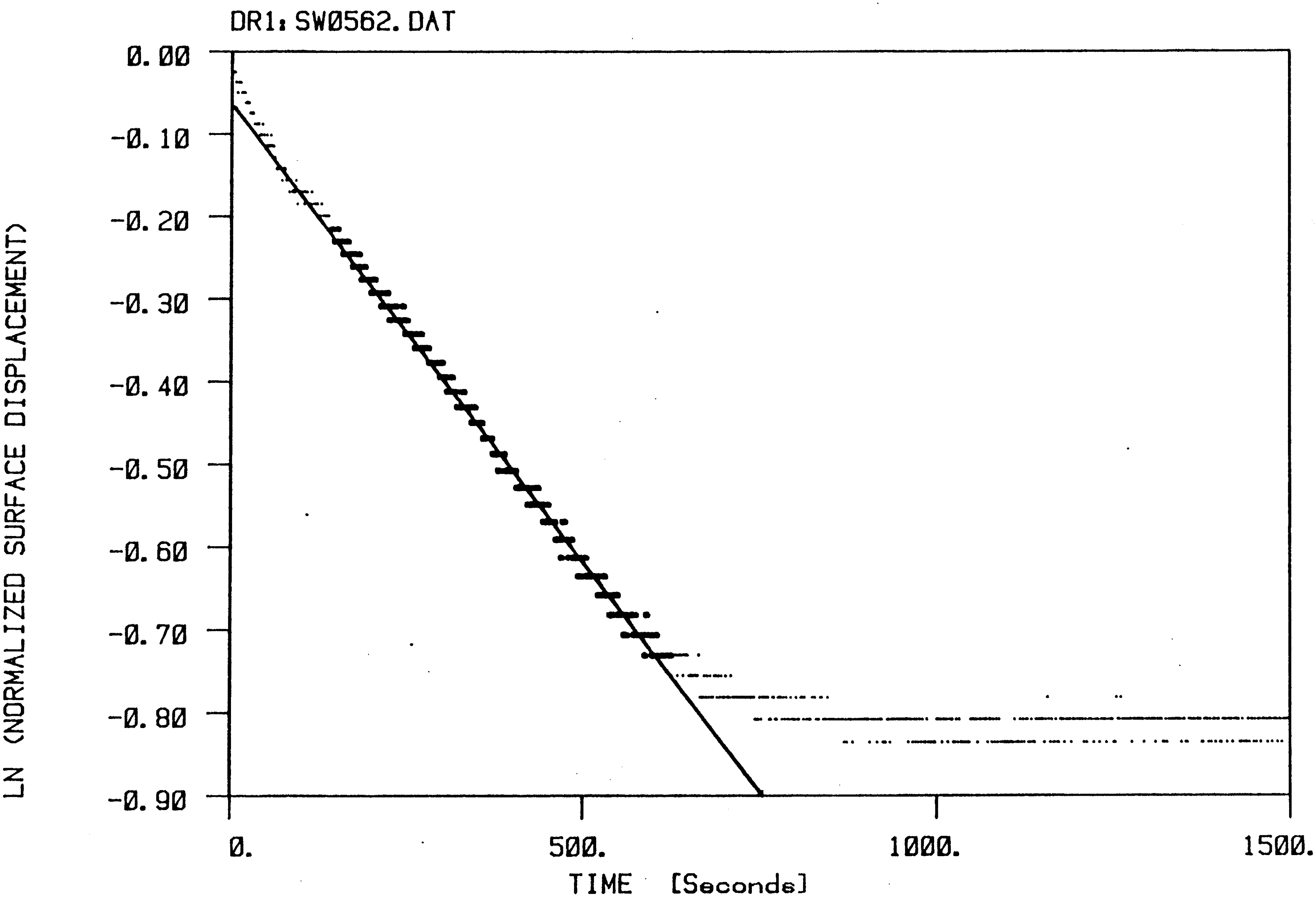

Figure 4-14. Best Linear Fit

was therefore estimated to be 5 X 10 m /Ns.

4.4 PRESSURE DISTRIBUTION

The measurement of the time-history of the total stress on the surface of the cartilage is performed as depicted in Figure 4-15. A static load is applied to the acetabulum using the instrumented prosthesis. At selected time intervals (usually 0,1,2,3,5,10,15,20,25,&30 minutes after the load is applied) the prosthesis is rotated about the load axis in 10 degree increments to generate a complete mapping of the surface stress. The prosthesis can be moved through this sequence by the hip simulator under computer control in about 30 seconds, during which time the pressures vary very little (cartilage layer time constants are on the order of 30 minutes).

Contour plots of the surface stress (Figures 4-16 to 4-18), in a coordinate system fixed relative to the body axes, are generated by fitting the pressure data to two dimensional Fourier series. The average error is less than 0.05 MPa.

4.5 CARTILAGE CONSOLIDATION

The time-history of the consolidation of the cartilage surface is measured as shown in Figure 4-19. By rotating the prosthesis about an axis 15 degrees off the load axis

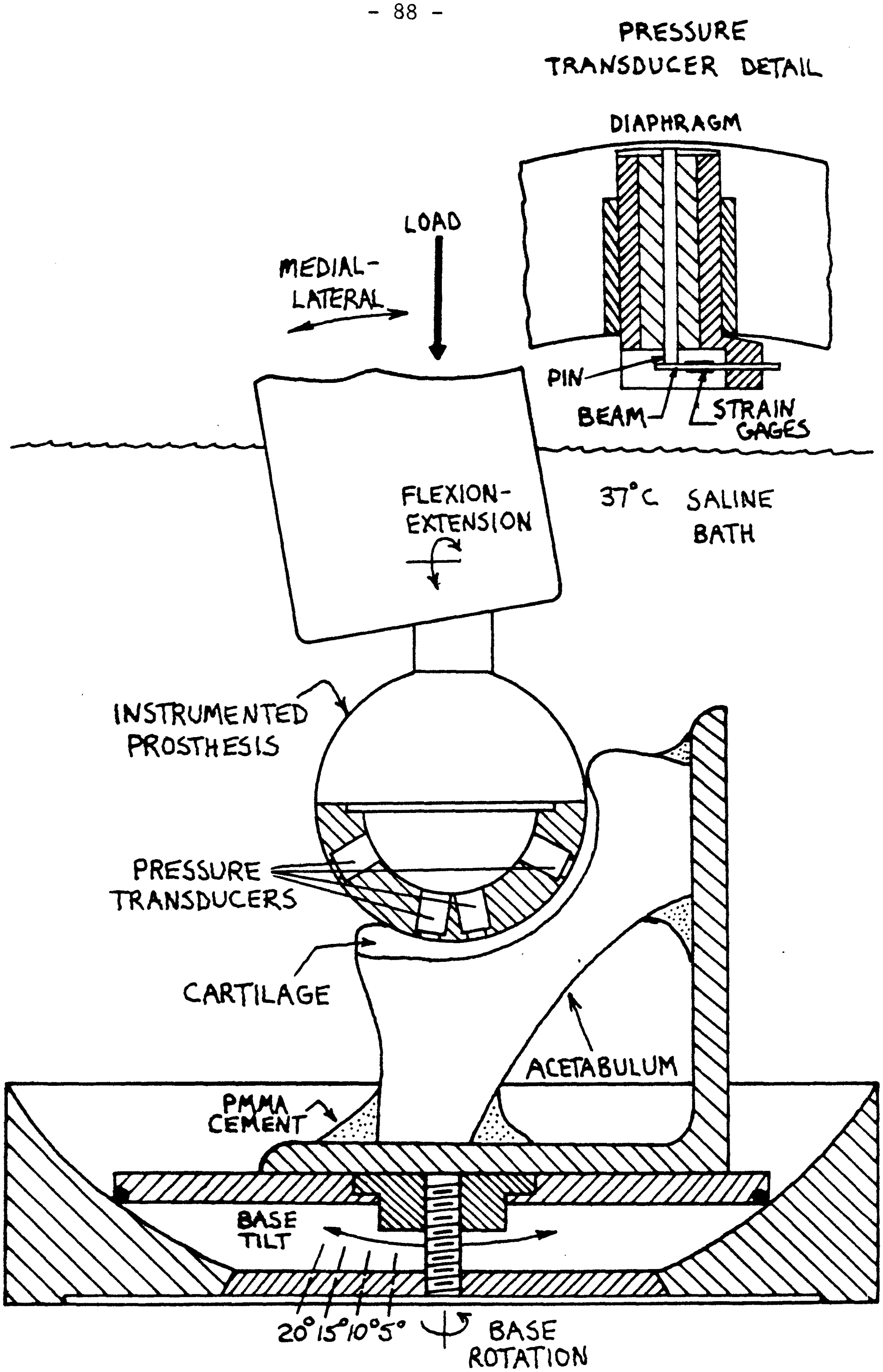

Figure 4-15. Surface Stress Measurement

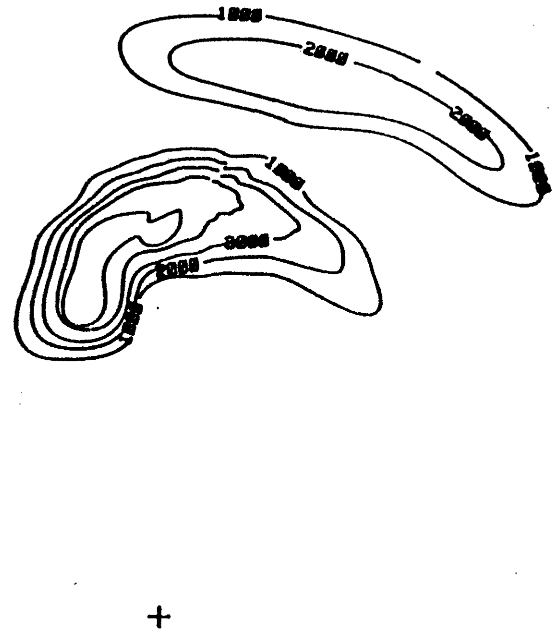

MEASURED
PRESSURE [KPa]
Ø Minutes

Figure 4-16. Surface Stress: 0 Minutes

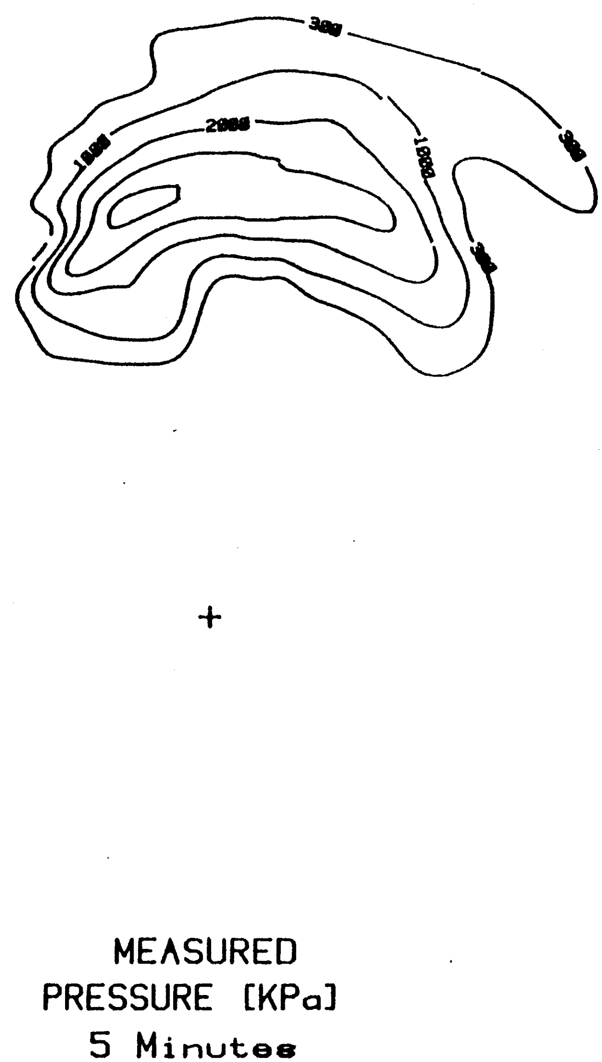

Figure 4-17. Surface Stress: 5 Minutes

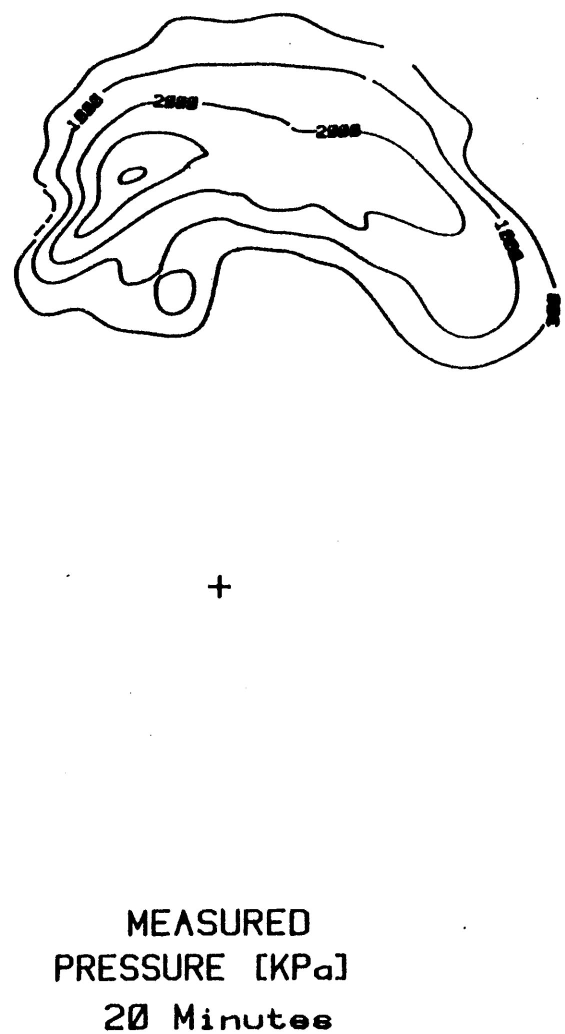

Figure 4-18. Surface Stress: 20 Minutes

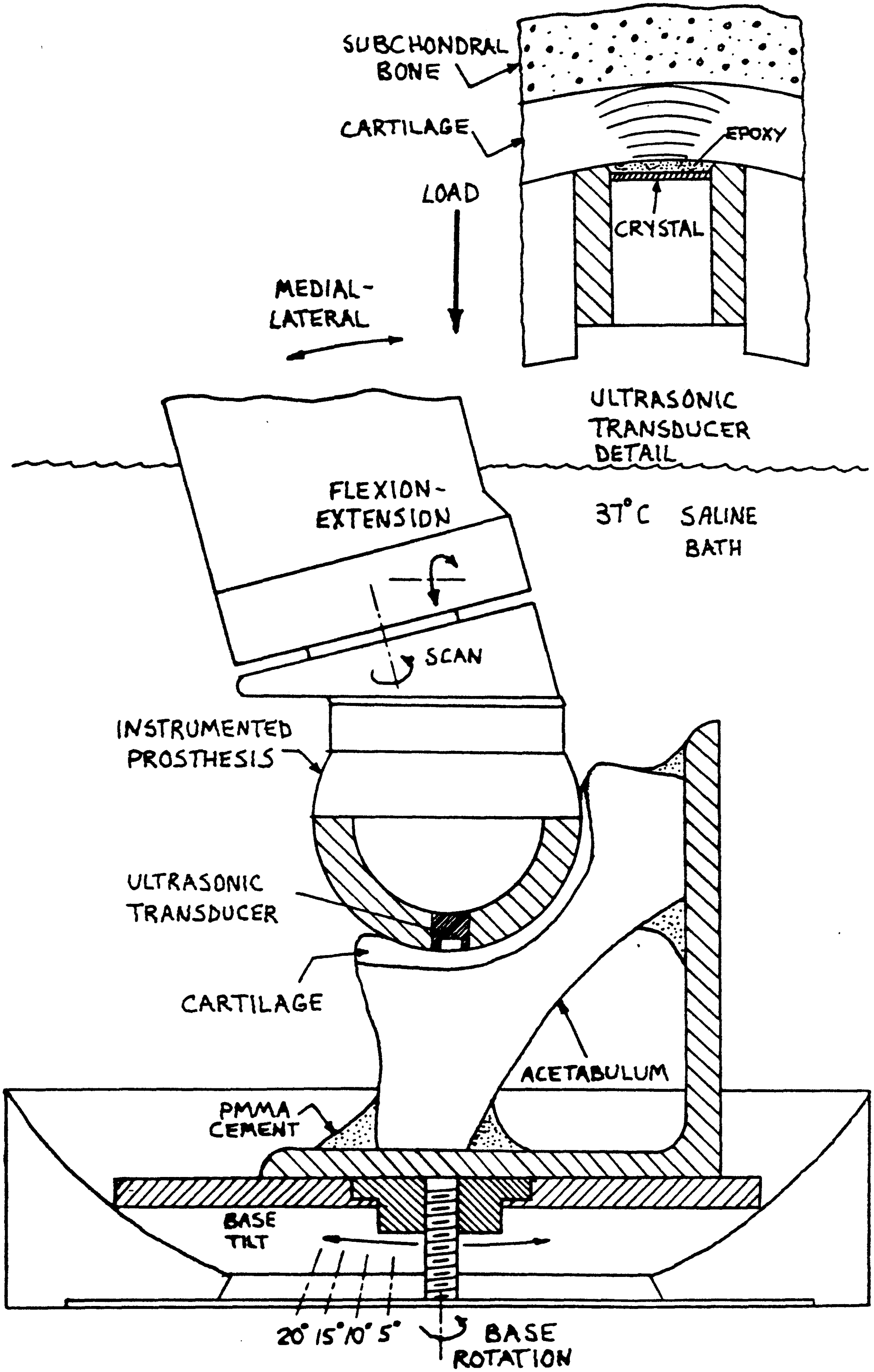

Figure 4-19. Consolidation Measurement

the distance from the prosthesis to the cartilage to calcified-calcified interface is measured at the pole and several locations of 30 degrees latitude. The position of the ball relative to the center of the acetabulum (and therfore the surface displacment of the cartilage in the joint) is calculated (Figure 4-20). The displacement along the load axis is shown in Figure 4-21 for three separate experiments on one acetabulum, with loads of 225, 450, and 900 N. Figure 4-22 shows the data from one test on log-log scale. In all cases the rate of the penetration of the prosthesis into the acetabulum decreases very quickly; a result which was noted by Rushfeldt [121]. The initial rate of penetration is actually <u>less</u> for higher loads; the final rate is proportional to load. The implications of these results in reference to the resistance to interarticular flow are discussed in Chapter 5.

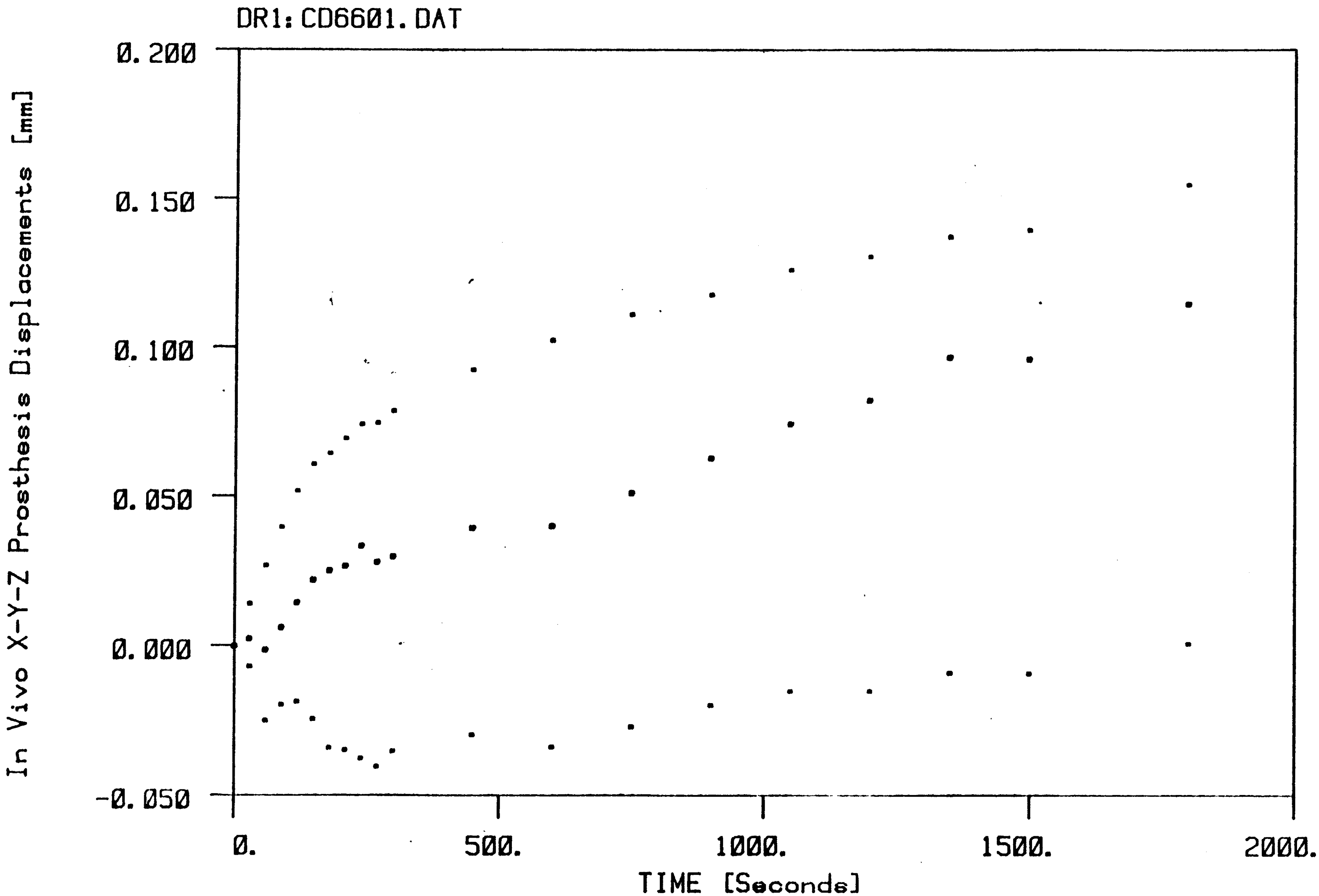

Figure 4-20. Prosthesis Position

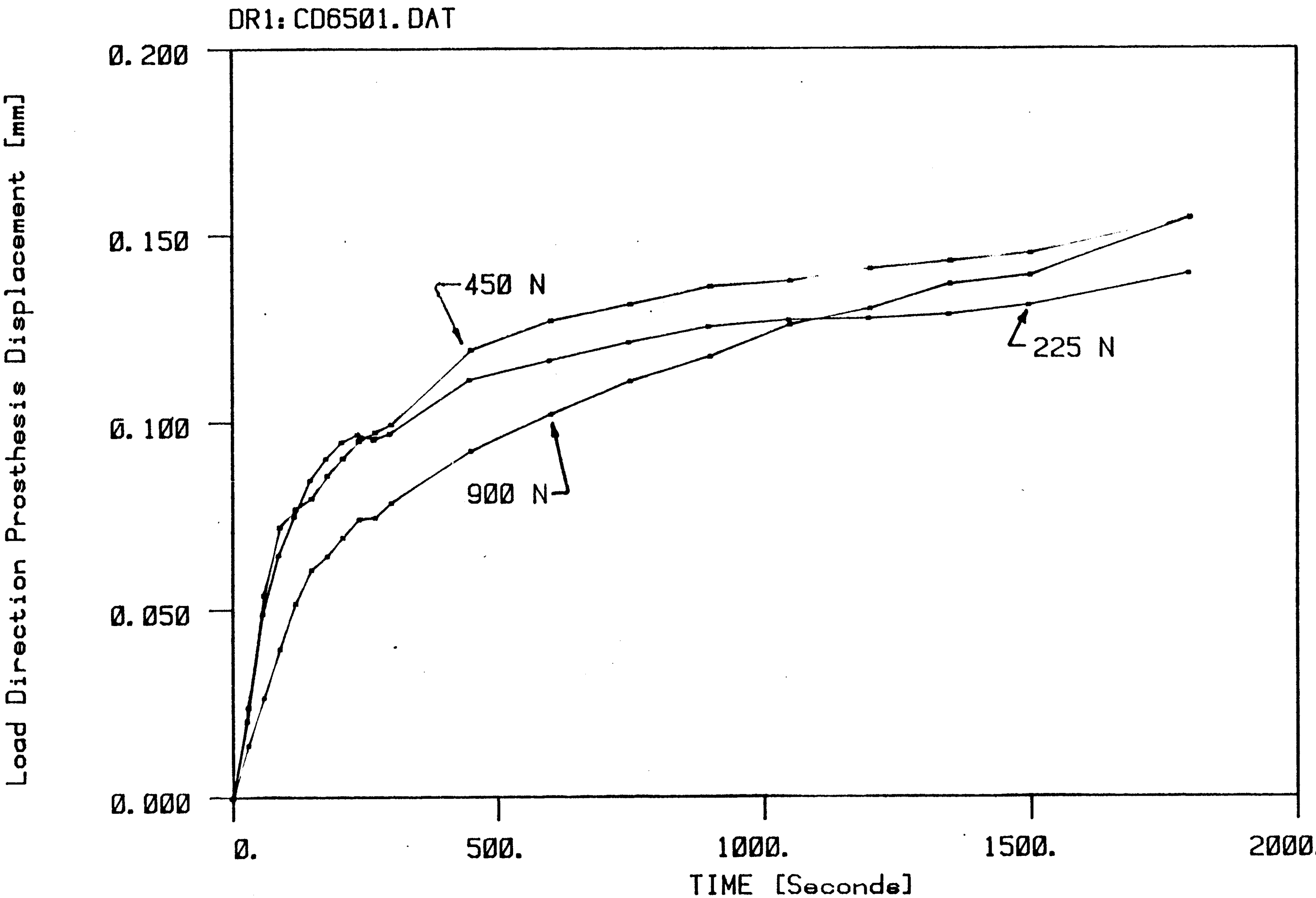

Figure 4-21. Prosthesis Displacement along Load Axis

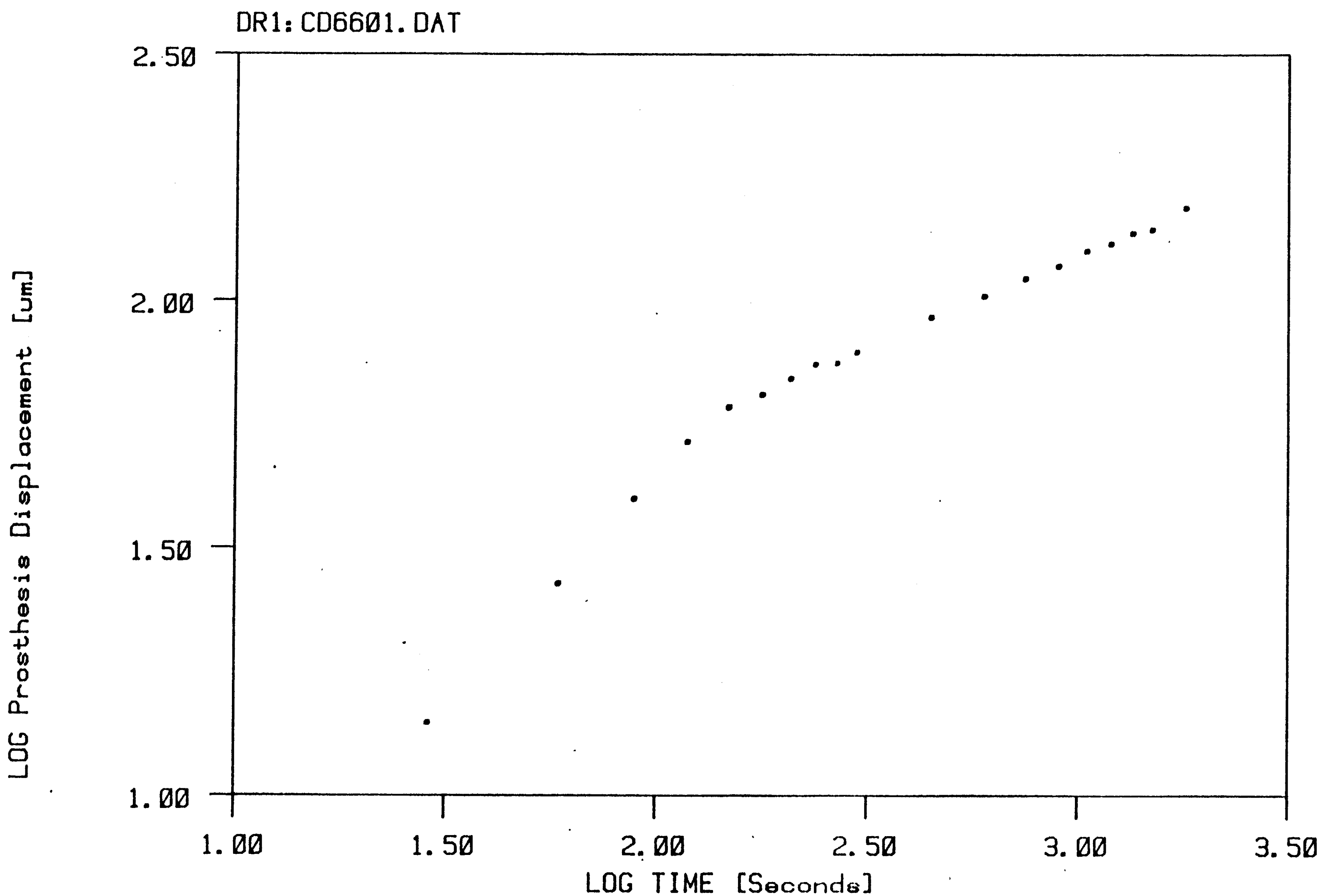

Figure 4-22. Log Prosthesis Displacement

CHAPTER 5

RESPONSE OF THE CARTILAGE LAYER

The development of a model for the articular cartilage layers of the synovial joint which reflects the salient features of the cartilage geometry, dynamic constitutive properties, and boundary conditions is discussed in this chapter. The model incorporates the results of the experiments described in Chapter 4, namely:

1. Geometry of the cartilage layer in the acetabulum, measured with our ultrasonic technique;
2. Permeability and uniaxial strain modulus, estimated from the swelling experiments;
3. Surface stress distribution time-history, measured with the instrumented endoprosthesis;
4. Displacement of the cartilage surface time-history, measured with the ultrasonic prosthesis.

The model will be used to estimate the boundary conditions for fluid flow at the cartilage surface, i.e. the interarticular gap, and describe the response of the solid stress and fluid pressure distributions in the cartilage layer.

5.1 SIMULATION

The goal of the analysis described in this section is the formulation of an idealized model of the cartilage layers which is suitable for numerical solution. A major problem with models used by other investigators has been the assumption that load sharing at the surface is dependent on porosity [102]. The approach taken here is to consider the boundary conditons at the interarticular surface unknown and to use the model results to estimate the actual boundary conditions for fluid flow.

5.1.1 Description

Our capacity to acquire data on the topographical variation of the cartilage geometry and constitutive properties and the stress and displacement at the loaded surface of the cartilage is well suited for the the construction of valid models of the cartilage layer in the acetabulum. In order to fully exploit this capability the finite element method was used to formulate the continuum equations. The simplest constituitive model for the cartilage, consistent with the measurements described in Chapter 4, is that of a porous medium with intrinsically incompressible constituents.

The model, shown schematically in Figure 5-1, assumes the strain in the porous layer is uniaxial, i.e. displacements of the solid matrix are constrained to the vertical (radial) direction (a spherical coordinate system was used due to accurately reflect the joint geometry). Shear and lateral strains in the cartilage are assumed small due to the large width to thickness ratio of the loaded cartilage area and the fixation to bone. No assumptions are made concerning the direction of fluid flow; hence pressures can vary both vertically and laterally in the layer. The supporting bone is assumed rigid so displacements are zero at the cartilage to bone interface, based on the known high stiffness of subchondral and cancellous bone relative to cartilage. The boundary conditions on the loaded surface are the measured total stress and an unknown fluid flow; the surface displacements predicted by the model will be compared with the measurements obtained from the ultrasonic prosthesis to predict the flow at the surface.

A finite element model for the cartilage layer incorporating these assumptions was developed. The cartilage layer in the acetabulum was discretized into three equal layers radially, and every 9 degrees in both orthogonal circumferential directions. Quadratic interpolation was used for the displacements of the solid matrix and linear interpolation for the fluid pressures.

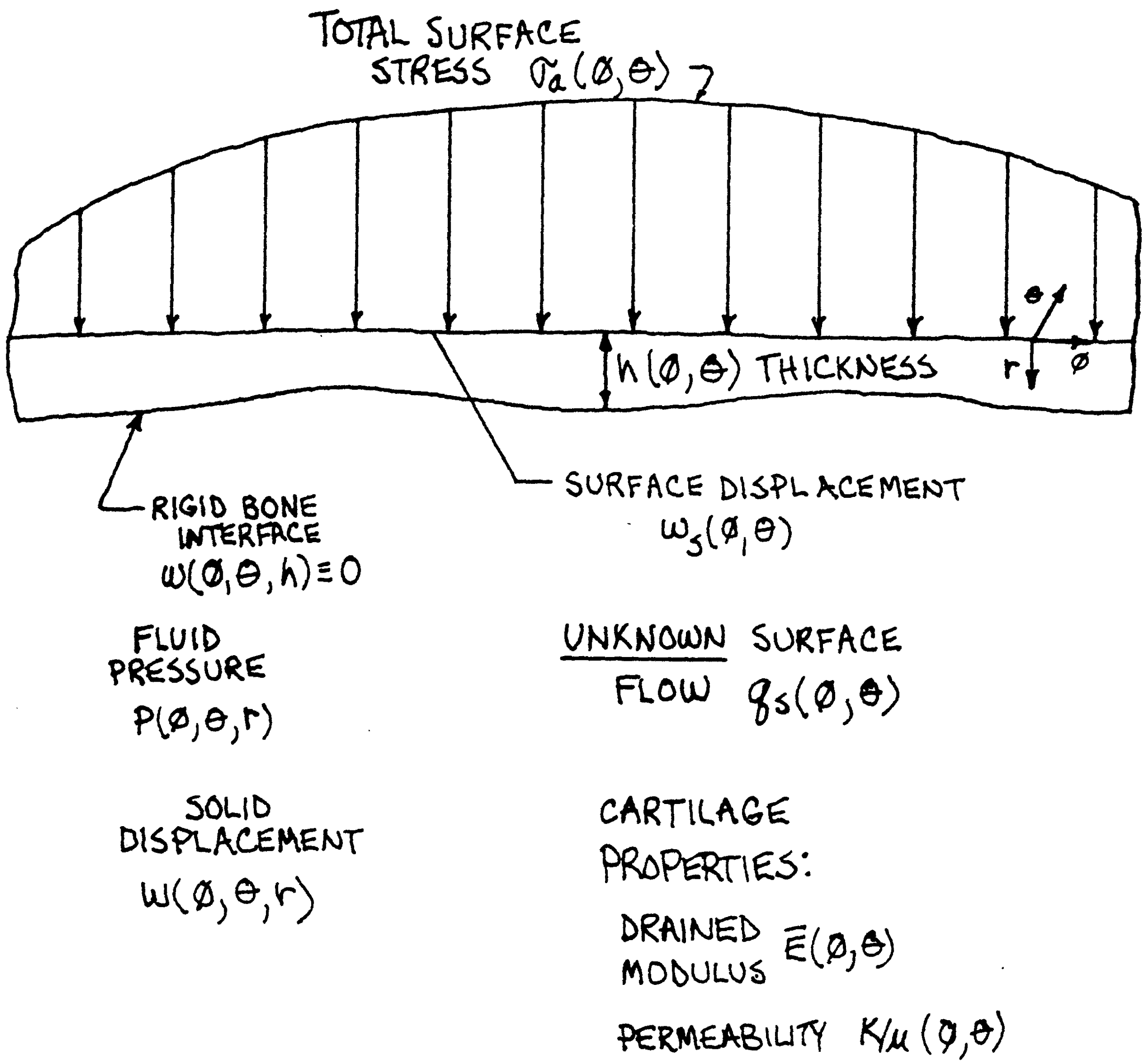

Figure 5-1. Cartilage Layer Model

The model had 1,300 degrees of freedom.

5.1.2 Finite Element Formulation

The finite element equations for equilibrium are derived from the principles of virtual displacements and velocities [9]. These state that for any compatible, small, virtual displacements and velocities imposed on the body, the total internal and external virtual work and energy are equal:

$$\int_V \delta\epsilon^T \tau \, dV \cdot 1 = \int_V \delta u^T f^B dV + \int_S \delta u^T f^S dS \qquad (1)$$

$$\int_V \left[\nabla \delta p^T q + \delta p^T (\nabla \cdot q)\right] dV = \int_S \delta p^T q^S dS \qquad (2)$$

where $\delta\epsilon$ are the virtual strains, δu are the virtual displacements, δp are the virtual pressures, τ are the actual stresses, and q are the actual flows. The field variables in any element are approximated by the interpolation matrices which relate them as a function of the nodal values.

$$u^{(m)} = H^{(m)} \hat{u} \qquad (3)$$

$$p^{(m)} = N^{(m)} \hat{p} \qquad (4)$$

The strains and pressure gradients are obtained by appropriately differentiating the interpolation matrices.

$$\epsilon^{(M)} = B^{(M)}\hat{u} \tag{5}$$

$$\nabla p^{(M)} = G^{(M)}\hat{p} \tag{6}$$

The stresses and flows are related to the displacements and pressures by the material matrices.

$$\tau^{(M)} = C^{(M)}\epsilon^{(M)} + \beta^{(M)}p^{(M)} \tag{7}$$

$$q^{(M)} = K^{F(M)}\nabla p^{(M)} \tag{8}$$

Also conservation of mass is expressed as:

$$\nabla \cdot q = -\frac{\partial \epsilon_{VOL}}{\partial t} = -\beta^T \epsilon \tag{9}$$

Equations 1 and 2 are rewritten as sums of integrations over the volume and areas of the elements:

$$\sum_M \int_{V^{(M)}} \delta\epsilon^{(M)T}\tau^{(M)}dV^{(M)} = \sum_M \int_{V^{(M)}} \delta u^{(M)T} f^{B(M)}dV^{(M)} + \sum_M \int_{S^{(M)}} \delta u^{(M)T} f^{S(M)}dS^{(M)} \tag{10}$$

$$\sum_M \int_{V^{(M)}} \left[\nabla\delta p^{(M)T} q^{(M)} + \delta p^{(M)T}(\nabla \cdot q^{(M)})\right] dV^{(M)} = \sum_M \int_{S^{(M)}} \delta p^{(M)T} q^{S(M)} dS^{(M)} \tag{11}$$

Substituting the expressions for the displacements and pressures, strains and pressure gradients, and stresses and flows we obtain:

$$\delta u^T\left[\left(\int_V B^T C B\, dV\right)\hat{U} + \left(\int_V B^T \beta N\, dV\right)\hat{p} = \int_S B^{S^T} f^S ds\right] \tag{12}$$

$$\delta p^T\left[\left(\int_V -G^T K^F G\, dV\right)\hat{p} + \left(\int_V N^T \beta^T B\, dV\right)\frac{d\hat{u}}{dt} = \int_S N^{S^T} q^S ds\right] \tag{13}$$

Imposing unit virtual displacements and pressures at all the nodes, the equilibrium equations can be written as

$$K_u \hat{u} + L\hat{P} = \hat{R} \tag{14}$$

$$-K_p \hat{P} + \frac{d}{dt} L^T \hat{u} = \hat{Q} \tag{15}$$

where the "stiffness" matrices and "load" vectors are:

$$K_u \equiv \int_V B^T C B \, dV \tag{16}$$

$$L \equiv \int_V B^T \beta N \, dV \tag{17}$$

$$K_p \equiv \int_V G^T K^f G \, dV \tag{18}$$

$$\hat{R} \equiv \int_S B^{S^T} \hat{f}^S \, ds \tag{19}$$

$$\hat{Q} \equiv \int_S N^{S^T} \dot{q}^S \, ds \tag{20}$$

The finite element equations 14 and 15 are solved via a fully implicit time integration scheme. This is unconditionally stable and has the advantage that the system matrix can be assembled once, triangularized, and stored: the solution at each time step simply requires calculation and back substitution of the appropriate load vector, Equations 21 and 22.

$$\begin{bmatrix} K_u & L \end{bmatrix} \begin{bmatrix} \hat{u} \\ \hat{P} \end{bmatrix}^{t+\Delta t} = \begin{bmatrix} 0 & 0 \end{bmatrix} \begin{bmatrix} \hat{u} \\ \hat{P} \end{bmatrix}^{t} + \hat{R}^{t+\Delta t} \tag{21}$$

$$\begin{bmatrix} L^T & -\Delta t K_p \end{bmatrix} \begin{bmatrix} \hat{u} \\ \hat{p} \end{bmatrix}^{t+\Delta t} = \begin{bmatrix} L^T & 0 \end{bmatrix} \begin{bmatrix} \hat{u} \\ \hat{p} \end{bmatrix}^{t} + \Delta t \hat{Q}^{t+\Delta t} \tag{22}$$

These are the same as Equation 12-38 in Desai and Christian [35].

5.1.3 Interarticular Boundary Condition

The general boundary condition for flow into the interarticular space is of the form:

$$p^s = -R_s \frac{\partial p^s}{\partial n} \tag{23}$$

where R_s is the "surface resistance". This can be incorporated as (using the equation for flow):

$$q^s = K^F \frac{dp^s}{\partial n} = -\frac{-K^F}{R_s} p^s \tag{24}$$

If R_s is known then this can be moved to the left hand side of the equation; otherwise we regard the surface flows as unknowns. They can be found by the following sequence (Figure 5-2).

1. Find the solution vectors Um (surface displacements) for a unit flow at the m'th surface node.

2. Assemble and triangularize the matrix Kq where the m'th column in Kq is the vector Um.

   At each time step:

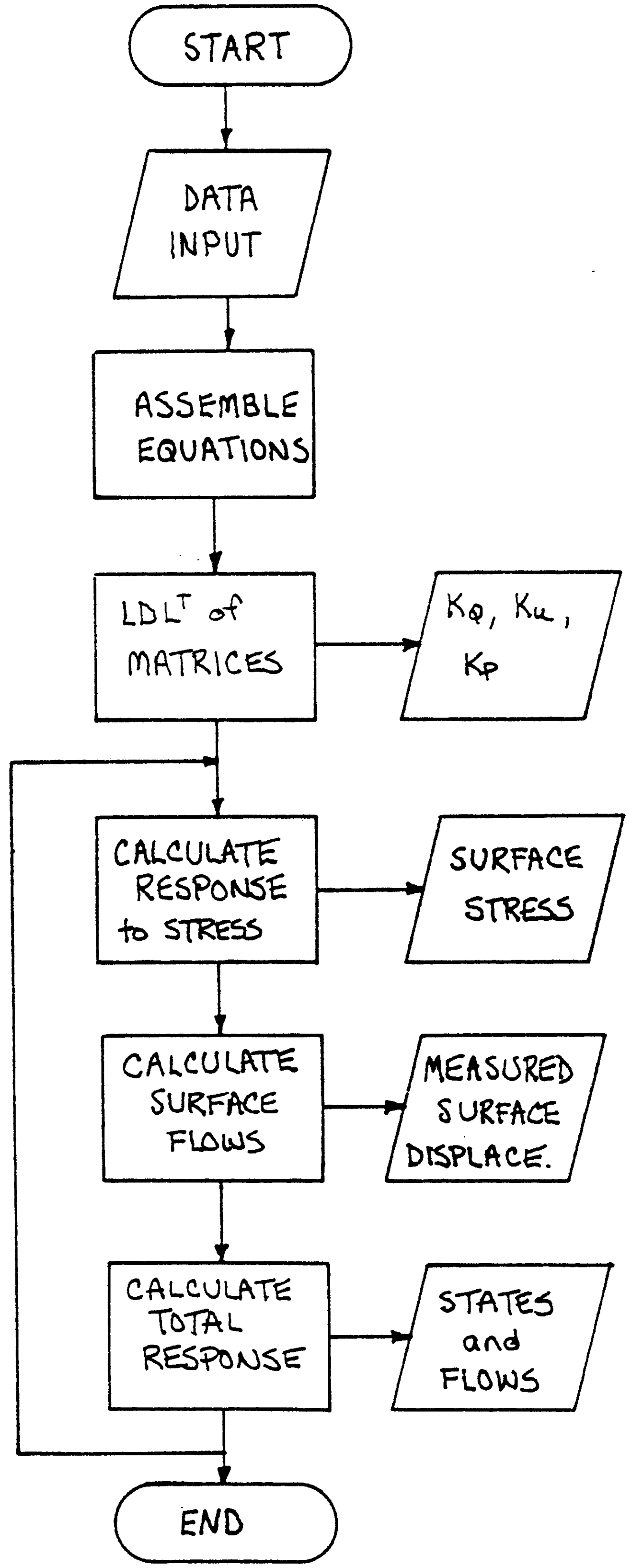

Figure 5-2. Coupled Solid-Fluid Analysis Flowchart

1. Find the solution Ur(t+dt) to Equations 21 and 22 using R(t) for Q(t)=0.

2. Calculate the error in the surface displacements Ue from the desired (measured) surface displacement Us(t+dt) as Ue = Us - Ur.

3. Backsubstitute Ue into Kq to find the flow Qs(t) required for the total displacement at t resulting from the load vector R(t) + Qs(t).

4. Apply the flow Qs(t) and add the resulting Uq(t+dt) to Ur(t+dt). The total displacement will equal Us(t+dt).

5.2 RESULTS

The model was used to calculate the surface flow for two static load cases: 450 N and 900 N. A time step of 30 s was used for the simulation (about 0.01 of the layer time constant). The solution was calculated for 40 time steps; the consolidation rate changes very little after 20 minutes (Figure 4-21).

The calculated flow (Figures 5-3 to 5-5) and surface stress (Figures 5-6 to 5-8) over the cartilage surface is shown for 3 time steps of the 900 N case. The flow decreases dramatically with time. The calculated flows are

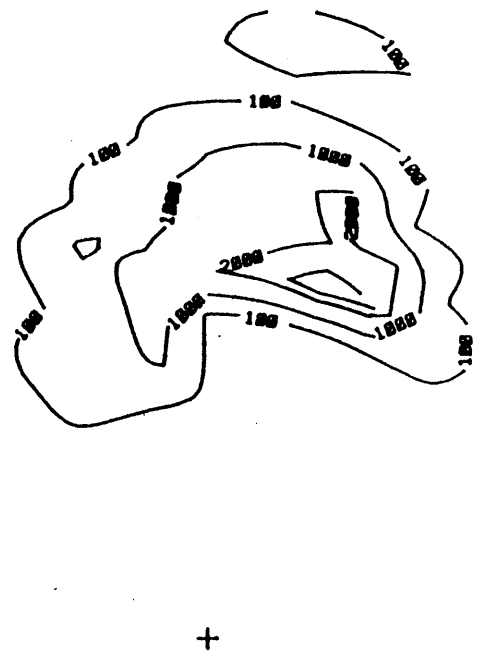

VERTICAL
FLOW [cu. mm/10Ms]
0 Minutes

Figure 5-3. Calculated Surface Flow: 0 Minutes

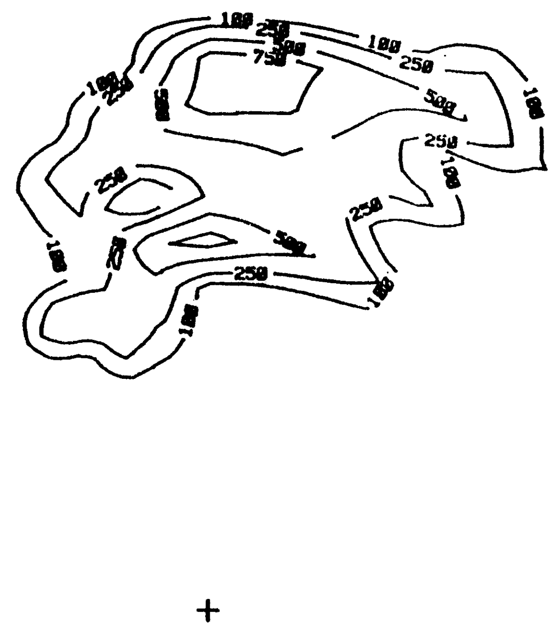

VERTICAL
FLOW [cu. mm/1ØMs]
5 Minutes

Figure 5-4. Calculated Surface Flow: 5 Minutes

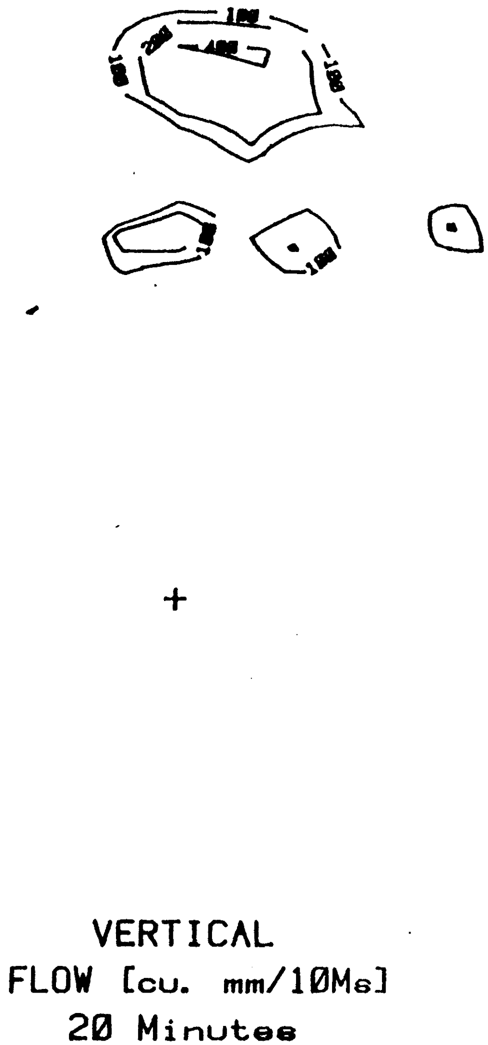

Figure 5-5. Calculated Surface Flow: 20 Minutes

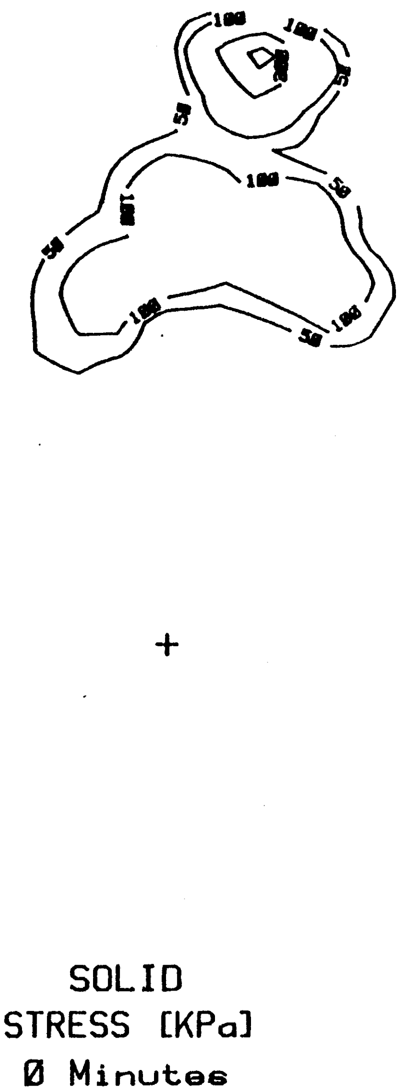

Figure 5-6. Calculated Solid Stress: 0 Minutes

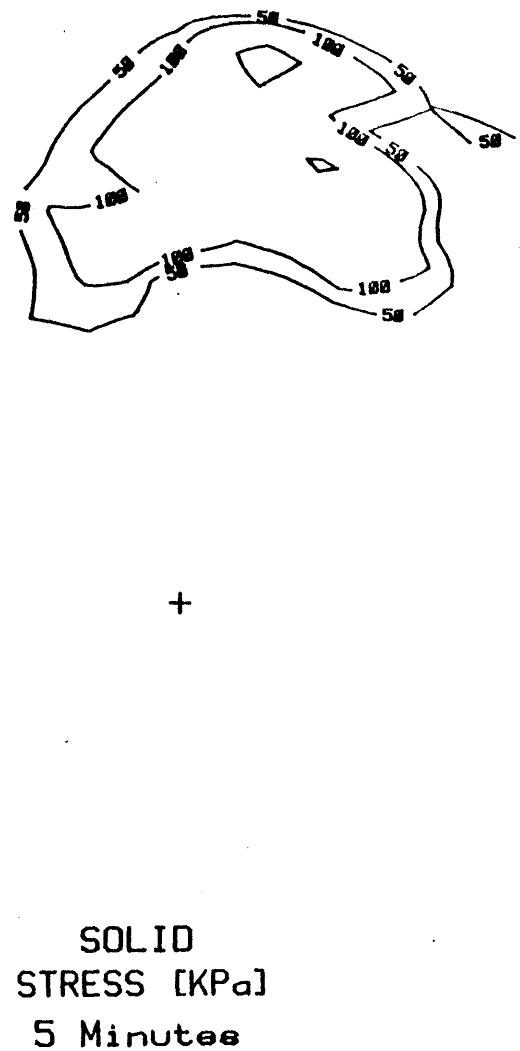

Figure 5-7. Calculated Solid Stress: 5 Minutes

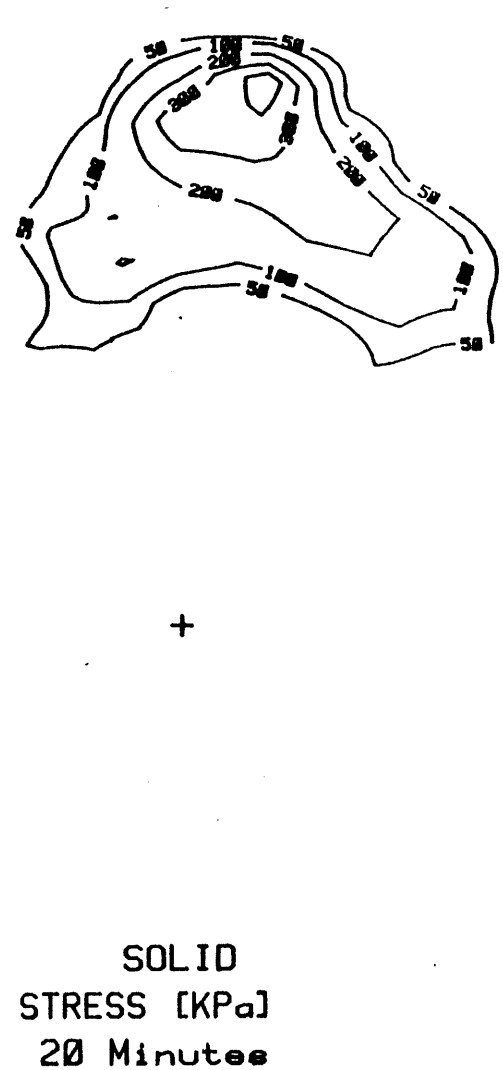

Figure 5-8. Calculated Solid Stress: 20 Minutes

generally highest at the locations where the gradient in surface stress is largest.

An average conductance to flow in the interarticular gap, motivated by the simple model of Section 3.4, is calculated from the ratio of total flow to average fluid pressure. Figures 5-9 and 5-10 show the time-history of the ratio of this average conductance to the conductance of the cartilage layer (permeability times thickness). The initial conductance is higher for the smaller load, consistent with the observation that the consolidation rate is greater. The conductance decreases with time to a minimum value that is nearly the same for both cases.

A measure of the surface conductance to layer conductance in the vertical direction illustrates that vertical equilibrium is dominated by the high surface resistance. By analogy to heat transfer the Biot number (Figure 5-11) is very small. This suggests that a simpler model for the cartilage layer, ignoring the vertical pressure gradient in the cartilage layer, could realistically predict the pressures and displacements in the cartilage. Tepic [139] has used such a model to simulate the dynamics of the cartilage layer during walking. The fluid pressures and flows induced in the cartilage layer, calculated by solving the contact problem using the cartilage geometries, are very similar to the experimental

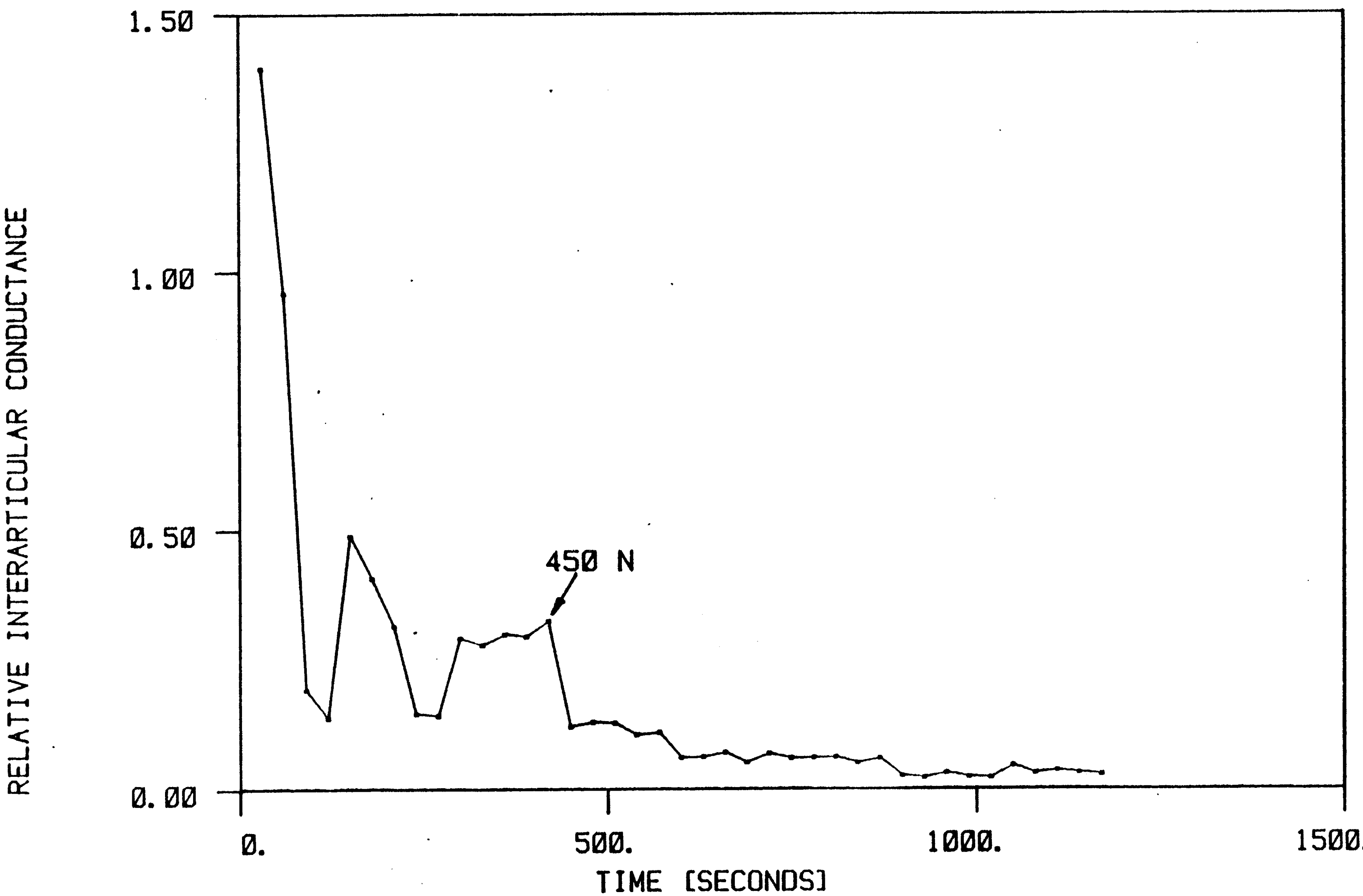

Figure 5-9. Average Gap Conductance: 450 N

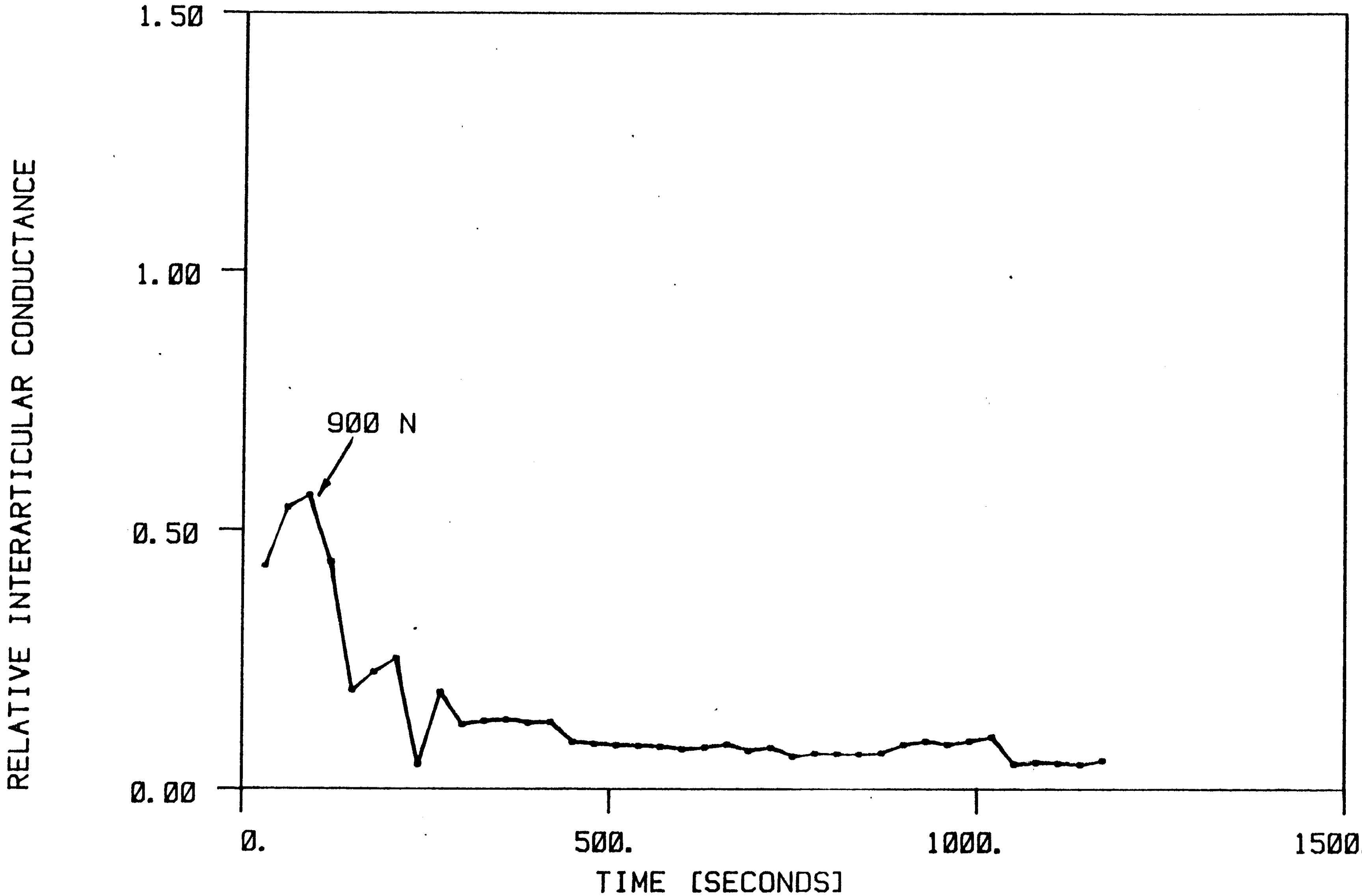

Figure 5-10. Average Gap Conductance: 900 N

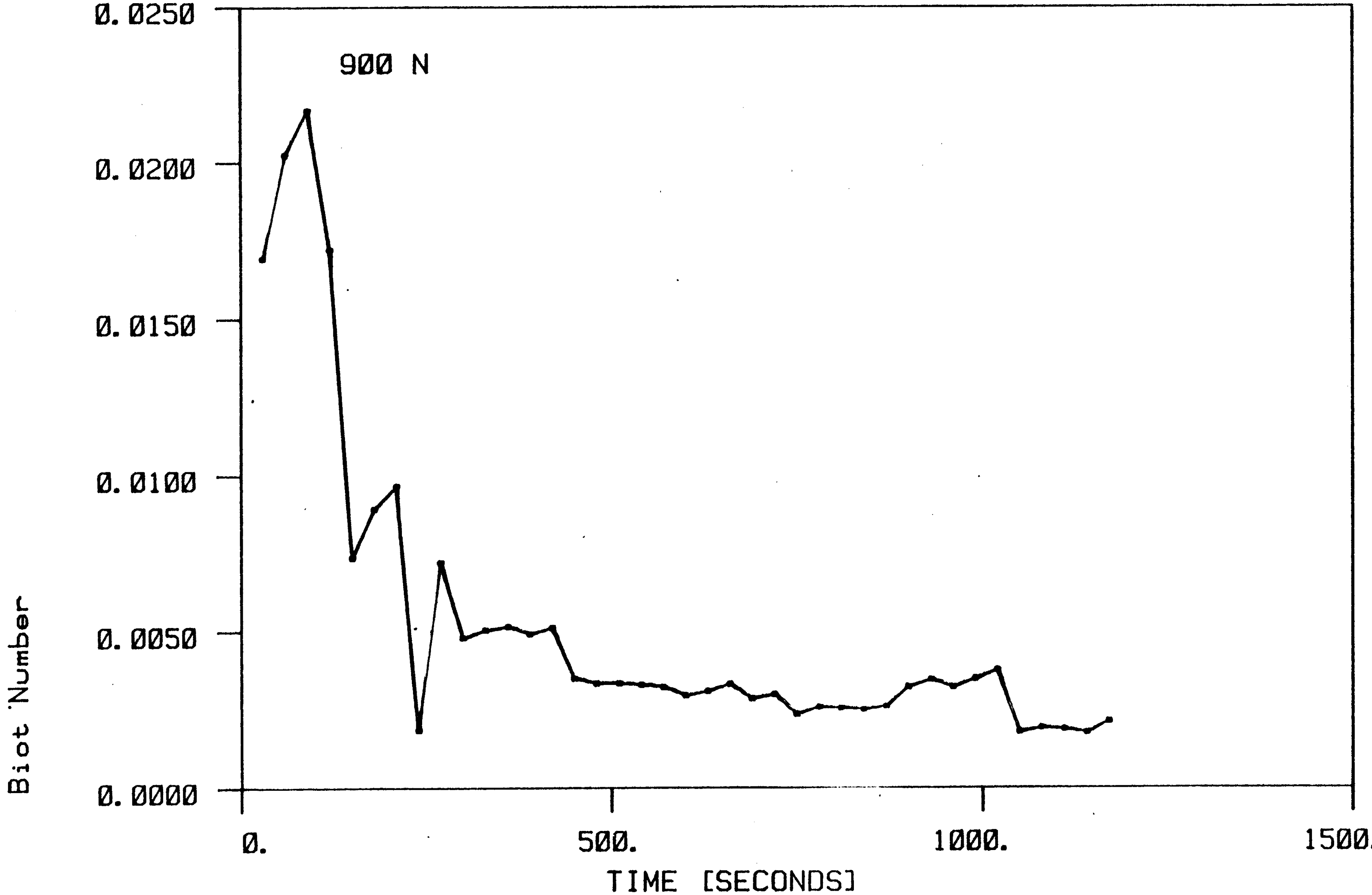

Figure 5-11. Biot Number

and theoretical results decscribe herein.

An overall view of the average stress in the cartilage layer is shown in Figure 5-12. The fluid pressure supports most of the load, even for long times. The difference between the fluid pressure at the bone and the surface, which produces flow in the interarticular gap, decreases with time.

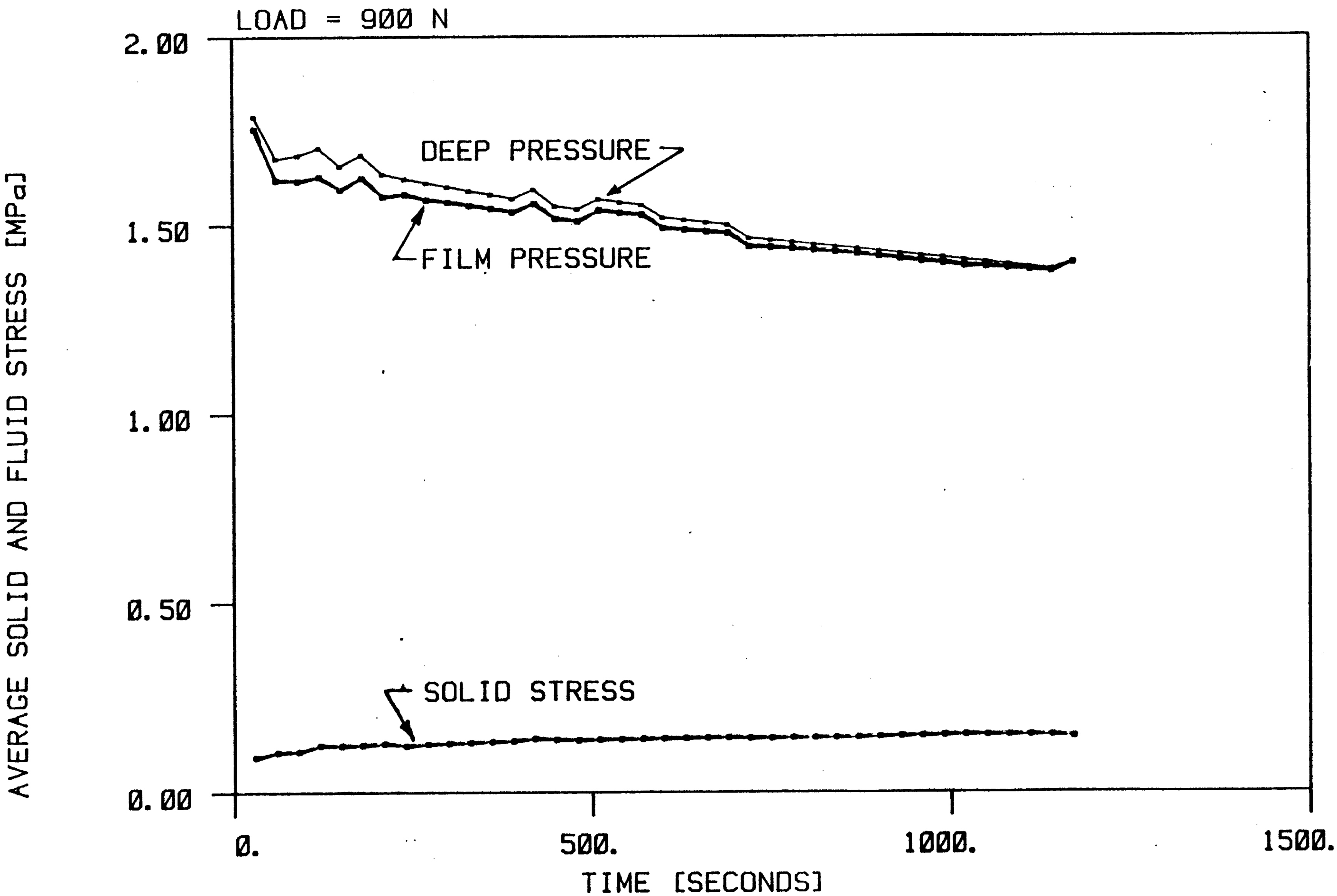

Figure 5-12. Average Stress

CHAPTER 6

CONCLUSIONS

The importance of both global *in situ* measurement of the properties and response of cartilage combined with physically based models is demonstrated. In particular, the nature of the interarticular condition and its implications for the normal (and possibly abnormal) function of the synovial joint is illuminated.

The geometry and the static and dynamic constitutive properties of normal adult articular cartilage *in situ* in the human hip joint have been measured experimentally. This includes the uniaxial strain equilibrium modulus and the hydraulic permeability. The time response of the cartilage in the acetabulum of the human hip joint when loaded by instrumented endoporostheses has been measured. This includes both the surface stress distribution and the surface displacement. Modelling of the synovial joint, in particular the human hip joint, incorporating the measurements described has been used to predict the surface boundary conditions governing interarticular fluid flow. The model is used to estimate the solid stress in the matrix and fluid pressure in the cartilage.

Much of this work depends on refinement and application of experimental techniques and theoretical concepts developed in this laboratory.

6.1 GEOMETRY

Ultrasonic measurment of the geometry of the cartilage layer in the acetabulum of the human hip joint was initiated by Rushfeldt [121]. Tepic [138] extended the technique to the human femoral head, providing conclusive quantitative evidence of the congruency of the natural synovial joint. More recently, using a waveform recorder we have added the capability to sample and record the ultrasonic signal and the reflections from the cartilage layer and the underlying bone. Automated computer control of the data acquisition and off-line processing of the signal have improved the resolution of the distance measurement to less than 2 um. This in turn made the osmotic swelling and cartilage consolidation experiments feasible.

6.2 CONSTITUTIVE PROPERTIES

Osmotic loading of the cartilage layer *in situ*, exploiting the electromechanical properties of articular cartilage, has provided the means to obtain precise, easily interpretable measurements of the constitutive properties of cartilage under simple loading conditions which mimic the *in vivo* environment. An osmotic loading technique has been developed to achieve this. Selective application of solutions of high molecular weight polyethylglycol (PEG) to cartilage through a layer of dialysis membrane lowers the osmotic pressure of the proteoglycan gel and uniformly loads the solid matrix. The return to physiological equilibrium, measured via the same ultrasonic techniques used for the geometry, provided not only an estimate of the dynamic properties of the cartilage but also the nonlinear behavior near equilibrium. This corroborates the static measurements of Maroudas [92].

6.2.1 Ultrastructure

We have also related the ultrastructure of the cartilage to its properties and time response during swelling through the simultaneous measurement of the impedance of the cartilage. We believe these experiments demonstrate that the nonlinearity of the bulk properties and the time response is due to the confinement and restraint of the collagen fiber network and the osmotic or swelling pressure of the proteoglycan gel which keeps the fibers "turgid". This is only possible when the overall volume is near physiological equilibrium (i.e. the fibers are tightly stretched).

We have used the transient response after osmotic loading to estimate the fundamental time constant of the layer by fitting the response to a linear model (as if the proteoglycan gel was approaching its own equilibrium volume). Combined with the static measurement of the equilibrium displacement of the layer under various osmotic pressures and the thickness of the layer, the permeability of the cartilage has been estimated.

The application of Biot's model [11] for porous media to cartilage is predicated on the assumption that the fluid and solid constituents are intrinsically incompressible. We have attempted to verify that the frequency response is consistent with this model; in particular we attempted to find the frequency range over which the phase shift between the surface stress and displacement remains at 45 degrees (Appendix B). Although our experimental technique has eliminated the likely sources of error that have plagued other investigators, the phase shift (Figure B-1) falls below 45 degrees for frequencies above 0.1 Hz or two decades beyond the time constant of the layer. At such high frequencies the total displacement (for this system) is less than 1 um. The roughness of the loader and the assumption of homogeneity (i.e. that the material behaves as a continuum over the relevant time and distance scales) may not be appropriate.

6.3 SURFACE STRESS

The measurements of the surface stress distribution over the cartilage in the human acetabulum using an instrumented endoprosthesis loaded <u>in vitro</u> using our hip simulator were first conducted by Rushfeldt [121]. Additional tests since then and their application as described in this thesis have demonstrated the usefulness of this approach. Recently, other investigators using dissimilar techniques have obtained corroborating results.

Brown [14] mounted 24 0.375 mm thick piezoresistive pressure transducers in recesses machined in the surface of the cartilage layer of the femoral head and loaded the joint in various orientations. The resulting pressure distributions are quantitatively and qualitatively remarkably similar to our results.

6.4 CONSOLIDATION

Armstrong [7] measured the deformation of the cartilage in loaded hip joints via roentgenograms. He claimed a resolution of 1 to 2 percent in the measurement of the cartilage thickness using a magnification of 30 X. Typical deformations were 10 percent after 30 minutes at loads of five times body weight.

The influence of the idiosyncratic character of the cartilage geometry on the pressure distribution is illustrated in the comparisons of the effect of load orientation on the pressure distribution and of load magnitude on the time response of the cartilage deformation.

Small, physiologically relevent, variations in the the direction of the load vector relative to the cartilage in the acetabulum have a dramatic effect on local peaks in the pressure distribution. Interaction with the surrounding areas is mediated by the flow of interarticular fluid and hence the surface resistance.

Furthermore, the short-time response is nearly independent of the applied load. The higher surface stress, while causing more rapid consolidation, also seals the interarticular space more rapidly. In all cases studied an abrupt change in the rate of consolidation occurs at a total consolidation of about 100-150 um, about twice the rms average of the deviations from sphericity at the surface. It appears that for adequate interarticular sealing to occur the interarticular spacing needs to be small (on the order of the the roughness of the cartilage surface) compared to the unloaded shape.

The measurement of the time response of the consolidation has been greatly improved by the high speed automated sampling and analysis of the ultrasonic reflections using the prosthesis with integral ultrasonic transducer. For the first time measurement of the details of the dynamics of the consolidation has been possible. These were used, together with the measurements of the surface stress on the cartilage, in a model to estimate the boundary condition for fluid flow in the interarticular space.

6.5 SURFACE RESISTANCE

The model used to characterize the behavior of the cartilage layer has been motivated by the experiments and analysis of Dent [34] and Kenyon [68], both previously of this project. In particular, they addressed the nature of the fluid flow boundary condition at the surface of the loaded cartilage and its effect on the fluid flow and pressure in the cartilage. The complicated time-varying geometry of the surface of the cartilage layer in the natural synovial joint precludes such simple cases as zero flow or zero pressure. The general boundary condition of a finite resistance to fluid flow (along the interarticular space) will depend on the fluid film thickness, cartilage surface roughess and geometry, and the length and tortuosity of the flow paths [34].

Analytical treatment of the problem of estimating the surface resistance and its effect on load carriage by the cartilage is fraught with difficulty. Kenyon has shown the resistance can be high, greatly affecting the proportioning of stress between the fluid and solid phases. Dent measured the pressure in the fluid film at the loaded surface of compressed cartilage plugs 5 mm in diameter. He found significant load carriage (25 to 75 percent) by the fluid pressure even for long times (20 minutes).

The final part of this thesis incorporates the measurements of the geometry of the cartilage layers, their constitutive properties, and the surface stress and displacement in a model of the cartilage layers in the hip joint. The goal was to estimate the local and global resistance to fluid flow in the interarticular space. Fluid flow toward the space and parallel to it are included. The result is the first experimentally determined estimate of the time dependent resistance to fluid flow in the interarticular space and its effects on the stress in the cartilage.

The relative conductance of the interarticular space to the conductance of the cartilage layer decreases with time from about one to less than 0.05. The relative flow in the interarticular space to that in the layer decreases in about the same proportion. This is because the relative conductance of the path for vertical flow is much greater than for lateral flow; it is likely the fluid pressure, which supports ninety percent of the load, even after twenty minutes, is approximately constant with depth at any location in the joint.

6.6 STRESS IN THE CARTILAGE

Further, the model, incorporating this final boundary condition, is used to predict the stress in the fluid and solid phases of the cartilage. The stress in the solid matrix remains low, never above 0.3 MPa and typically about 0.1 MPa. The severe nonlinearity of the equilibrium modulus at approximately 30 percent compression (0.3 MPa solid stress) suggests that significant irreversible damage may be occurring to the matrix. Cyclic loading could fatigue the fibers via buckling, such as the apparent compaction of the fibers in the STZ, as suggested by Tepic [139].

6.7 IMPLICATIONS

It is clear the cartilage in the joint functions by supporting the load mainly by fluid pressure. Fluid flow both through the cartilage layer and into and through the interarticular space is therefore important. Even under the severe conditions of a static load, the solid stress in the cartilage is minimal. When the joint is unloaded (as during walking) fluid can freely flow into the cartilage, since interarticular resistance is likely very small. Dynamic simulation, such as performed by Tepic [139], incorporating the estimates of interarticular resistance provided by this thesis, are likely to produce very good estimates of the solid stress in the cartilage throughout the walking cycle.

The underlying hypothesis for this work has been that mechanical factors which are important to the cartilage function in a normal synovial joint may play a role in the failure by osteoarthritis. Loss of interarticular sealing will clearly result in increased stress in the cartilage. The range of sealing coefficients and their dependence on cartilage properties and condition need to be established. For example, normal adult cartilage has a larger surface roughness -- does it seal less effectively? Meanwhile experiments on the strength of cartilage, under more physiological conditions such as those described in this thesis, would provide evidence that increased stress through loss of sealing can lead to destruction of the cartilage.

APPENDIX A

Programs

```
C*****************************************************************************
C                                                                            *
C                                  CSFA                                      *
C                                                                            *
C                  COUPLED SOLID-FLUID ANALYSIS PROGRAM                      *
C                                                                            *
C                             TOM MACIROWSKI                                 *
C                                                                            *
C*****************************************************************************
C       Adapted from: STAP in K.J. Bathe, Finite Element Procedures in Engineering
C                     Analysis [9].
        PROGRAM CSFA
        REAL*4 DELTA,RBEST
        COMMON A(175000)
        COMMON /SOL/ NUMNP,NEQ,NWK,NUMEST,MIDEST,MAXEST,MK
        COMMON /DIM/ N1,N2,N3,N4,N5,N6,N7,N8,N9,N10,N11,N12,N13,N14,N15
        COMMON /EL/ IND,NPAR(10),NUMEG,MTOT,NFIRST,NLAST,ITWO
        COMMON /VAR/ NG,MODEX,RBEST,DELTA
        COMMON /TAPES/ IELMNT,ILOAD,IIN,IOUT,IDISP,ISTATE,IKORG,IKTRI
C
        DIMENSION TIM(5),HED(20)
        DIMENSION IA(1)
        EQUIVALENCE (A(1),IA(1))
        BYTE FF,IFILE(15),OFILE(15)
        DATA FF/ 14/
        DATA IFILE/'D','K','1',':','F','E','M','E','6','2',
     *  '.','D','A','T',"0/
        DATA OFILE/'D','K','1',':',6* 0,'.','L','S','T', 0/
C
C       MTOT IS THE MAXIMUM CORE STORAGE AVAILABLE
C
        MTOT=175000
        ITWO=1
C
C       THE FOLLOWING DEVICE NUMBERS ARE USED
C               IELMNT = ELEMENT DATA
C               ILOAD  = LOAD VECTORS
C               IIN    = INPUT DATA
C               IOUT   = OUTPUT LISTING
C               IDISP  = SURFACE DISPLACEMENTS
C               ISTATE = STATE VECTOR
C               IKORG  = ORIGINAL STIFFNESS (K) MATRIX
C               IKTRI  = TRIANGULARIZED K MATRIX
        IELMNT = 11
        ILOAD  = 12
        IIN    = 13
        IOUT   = 14
        IDISP  = 15
        ISTATE = 16
        IKORG  = 17
        IKTRI  = 18
C
        CALL ASSIGN (IELMNT,'DK1:IELMNT.DAT',14)
        CALL ASSIGN (ILOAD,'DK1:ILOAD.DAT',13)
        CALL ASSIGN (IIN,IFILE,14)
        DO 2070 I=5,10
```

```
2070    OFILE(I)=IFILE(I)
        CALL ASSIGN(IOUT,OFILE,14)
        CALL ASSIGN (IDISP,'DK1:IDISP.DAT',13)
        CALL ASSIGN (ISTATE,'DK1:ISTATE.DAT',14)
        CALL ASSIGN (IKORG,'DK1:IKORG.DAT',13)
        CALL ASSIGN (IKTRI,'DK1:IKTRI.DAT',13)
C
200     NUMEST=0
        MAXEST=0
C
C       ***********************************
C
C       * * *  I N P U T   P H A S E  * * *
C
C       ***********************************
C
        CALL SECOND(TIM(1))
C
C
C       R E A D   C O N T R O L   I N F O R M A T I O N
C
C
        READ (IIN,1000) HED,NUMNP,NUMEG,NLCASE,MODEX,RBEST,DELTA
        IF(NUMNP.EQ.0)GO TO 999
        WRITE(IOUT,2000) FF,HED,NUMNP,NUMEG,NLCASE,MODEX,RBEST,DELTA
C
C
C       R E A D   N O D A L   P O I N T   D A T A
C
C
        N1=1
        N2=N1+2*NUMNP
        N3=N2+NUMNP*ITWO
        N4=N3+NUMNP*ITWO
        N5=N4+NUMNP*ITWO
        IF(N5.GT.MTOT) CALL ERROR(N5-MTOT,1)
        IF(N5.GT.MAX)MAX=N5
        TYPE 6000,4*MAX
6000    FORMAT(' Maximum memory used is:',I8,' Bytes ')
C
        CALL INPUT(A(N1),A(N2),A(N3),A(N4),NUMNP,NEQ)
C
        NEQ1=NEQ+1
C
C       C A L C U L A T E   A N D   S T O R E   L O A D   V E C T O R S
C
C
        N6=N5+NEQ*ITWO
        IF(N6.GT.MTOT) CALL ERROR(N6-MTOT,2)
        IF(N6.GT.MAX)MAX=N6
        TYPE 6000,4*MAX
        WRITE(IOUT,2005) FF
C
        REWIND ILOAD
C
        DO 300 L=1,NLCASE
C
        IF(L.GT.1)WRITE(IOUT,2004) FF
```

```
2004    FORMAT(1X,A1)
        READ(IIN,1010)LL,NLOAD,NPRES
        WRITE(IOUT,2010)LL,NLOAD,NPRES
        IF(LL.EQ.L)GOTO 310
        WRITE(IOUT,2020)
        STOP
C
310     CONTINUE
        CALL LOADS(A(N2),A(N3),A(N5),A(N1),NLOAD,NPRES,NEQ,NUMNP)
C
300     CONTINUE
C
C
C       R E A D /  G E N E R A T E /  A N D   S T O R E
C
C                  E L E M E N T   D A T A     .
C
C
C       CLEAR STORAGE
C
        N6=N5+NEQ*ITWO
        DO 10 I=N5,N6
10      A(I)=0
        IND=1
C
        CALL ELCAL
C
        CALL SECOND(TIM(2))
        TYPE 3000,(TIM(2)-TIM(1))
3000    FORMAT(/' DATA INPUT       :',F12.2,' Sec')
C
C       ****************************************
C
C       * * *  S O L U T I O N   P H A S E  * * *
C
C       ****************************************
C
C       A S S E M B L E   S T I F F N E S S   M A T R I X
C
C
        CALL ADDRES(A(N2),A(N5))
C
        MM=NWK/NEQ
        N3=N2+NEQ+1
        N4=N3+NWK*ITWO
        N5=N4+NEQ*ITWO
        N6=N5+MAXEST
        N7=N6+NEQ*ITWO
        IF(N7.GT.MTOT) CALL ERROR(N7-MTOT,4)
        IF(N7.GT.MAX)MAX=N7
        TYPE 6000,4*MAX
C
C       WRITE TOTAL SYSTEM DATA
C
C
        WRITE(IOUT,2025) FF,NEQ,NWK,MK,MM
C
C       IF DATA CHECK SKIP FURTHER CALCULATIONS
```

```
C
      IF(MODEX.GT.0) GO TO 100
      CALL SECOND(TIM(3))
      CALL SECOND(TIM(4))
      CALL SECOND(TIM(5))
      GO TO 120
C
C     CLEAR STORAGE
C
100   NNL=NWK+NEQ
      CALL CLEAR(A(N3),NNL)
C
C
      IND=2
C
      CALL ASSEM(A(N5))
C
      READ(IIN,1005)NSUR
1005  FORMAT(I5)
      NSIZE=NSUR*(NSUR+1)/2
      N8=N7+NSUR
      N9=N8+NSIZE*ITWO
      N10=N9+NSUR+1
      N11=N10+NSUR*ITWO
      IF(N11.GT.MTOT) CALL ERROR(N11-MTOT,5)
      IF(N11.GT.MAX)MAX=N11
      TYPE 6000,4*MAX
      CALL DISPL(A(N7),A(N10),NSUR,NLCASE)
C
      CALL SECOND(TIM(3))
      TYPE 3010,(TIM(3)-TIM(1))
3010  FORMAT(' ASSEMBLE MATRIX  :',F12.2)
C
C     T R I A N G U L A R I Z E   S T I F F N E S S   M A T R I X
C
C
      KTR=1
      WRITE(IKORG) NWK,(A(IQ),IQ=N3,N3-1+NWK*ITWO)
      CALL COLSOL (A(N3),A(N4),A(N2),NEQ,NWK,NEQ1,KTR)
      WRITE(IKTRI) NWK,(A(IQ),IQ=N3,N3-1+NWK*ITWO)
C
35    CALL SECOND(TIM(4))
      TYPE 3020,(TIM(4)-TIM(1))
3020  FORMAT(' TRIANGULARIZATION:',F12.2)
C
      KTR=2
      IND=3
C
      CALL DASSEM (A(N1),A(N7),A(N8),A(N9),A(N4),NSUR,NLCASE)
C
      CALL CLEAR(A(N6),NEQ)              ! U(t0)=0.0
C
      REWIND ILOAD
      REWIND IDISP
      DO 400 L=1,NLCASE
C
C     CALL SAVE(A(N4),A(N6),NEQ)         ! SAVE U(t) in A(N6)
      CALL LOADV(A(N4),NEQ)              ! R(t+dt) in A(N4)
```

```
      CALL DISPV(A(N10),NSUR)          ! Us(t+dt) in A(N10)
      REWIND IKORG
      READ(IKORG) NWK,(A(IQ),IQ=N3,N3-1+NWK*ITWO)
      CALL UPDATE(A(N4),A(N6),A(N1),A(N2),A(N3),NUMNP)! ADD LTxU(t)
      CALL SAVE(A(N4),A(N6),NEQ)       ! SAVE R(t) in A(N6)
C
C
C     C A L C U L A T I O N   O F   D I S P L A C E M E N T S
C
C
      REWIND IKTRI
      READ(IKTRI) NWK,(A(IQ),IQ=N3,N3-1+NWK*ITWO)
      CALL COLSOL(A(N3),A(N4),A(N2),NEQ,NWK,NEQ1,KTR)
C
      CALL FLOW(A(N4),A(N10),A(N1),A(N8),A(N9),A(N7),NSUR,A(N6))
      CALL COLSOL(A(N3),A(N6),A(N2),NEQ,NWK,NEQ1,KTR)
      WRITE (IOUT,2015) FF,L
      CALL WRITE(A(N6),A(N1),NEQ,NUMNP,A(N10),A(N7),NSUR)
C
C
C     C A L C U L A T I O N   O F   S T R E S S E S
C
C
C     CALL STRESS(A(N5))
C
400   CONTINUE
C
      CALL SECOND(TIM(5))
      TYPE 3030,(TIM(5)-TIM(1))
3030  FORMAT(' LOAD SOLUTIONS   :',F12.2)
C
C     PRINT SOLUTION TIMES
C
120   TT=0.
      DO 500 I=1,4
      TIM(I)=TIM(I+1)-TIM(I)
500   TT=TT+TIM(I)
      WRITE(IOUT,2030) FF,HED,(TIM(I),I=1,4),TT,FF
C
C     READ NEXT ANALYSIS CASE
C
      GO TO 200
C
1000  FORMAT(20A4/4I5,2F10.0)
1010  FORMAT(3I5)
C
C
2000  FORMAT(1X,A1,20A4///
     1' C O N T R O L   I N F O R M A T I O N '//5X,
     2' NUMBER OF NODAL POINTS ............. (NUMNP)  =',I5//5X,
     3' NUMBER OF ELEMENT GROUPS ........... (NUMEG)  =',I5//5X,
     4' NUMBER OF LOAD CASES ............... (NLCASE) =',I5//5X,
     5' SOLUTION MODE ...................... (MODEX)  =',I5/5X,
     6'          EQ.0, DATA CHECK'/5X,
     7'          EQ.1, EXECUTION '//5X,
     8' RADIUS ............................. (RREST)  =',F9.3//5X,
     9' TIME STEP .......................... (DELTA)  =',F9.3/)
2005  FORMAT(1X,A1,' L O A D   C A S E   D A T A ')
```

```
2010    FORMAT(////4X,' LOAD CASE NUMBER ................. =',I5//4X,
      1' NUMBER OF CONCENTRATED LOADS ..... =',I5//4X,
      2' NUMBER OF PRESSURE LOADS ......... =',I5/)
2015    FORMAT(1X,A1,' LOAD CASE ',I3)
2020    FORMAT(' *** ERROR  LOAD CASES ARE NOT IN ORDER *** ')
2025    FORMAT(1X,A1,
      1' TOTAL SYSTEM DATA '///5X,
      2' NUMBER OF EQUATIONS .................. (NEQ)  =',I8//5X,
      3' NUMBER OF MATRIX ELEMENTS ............ (NWK)  =',I8//5X,
      4' MAXIMUM HALF BANDWIDTH ............... (MK)   =',I8//5X,
      5' MEAN HALF BANDWIDTH .................. (MM)   =',I8)
2030    FORMAT(1X,A1,' S O L U T I O N   T I M E   L O G   I N
      *  SECONDS'//
      112X,'FOR PROBLEM'//1X,20A4 ////5X,
      2' TIME FOR INPUT PHASE .......................  =',F12.2//5X,
      3' TIME FOR CALCULATION OF STIFFNESS MATRIX ...  =',F12.2//5X,
      4' TRIANGULARIZATION OF STIFFNESS MATRIX ......  =',F12.2//5X,
      5' TIME FOR LOAD CASE SOLUTIONS ...............  =',F12.2//5X,
      6' T O T A L   S O L U T I O N   T I M E ....  =',F12.2/1X,A1)
C
999     CALL CLOSE(IELMNT)
        CALL CLOSE(ILOAD)
        CALL CLOSE(IIN)
        CALL CLOSE(IOUT)
        CALL CLOSE(IDISP)
        CALL CLOSE(ISTATE)
        CALL CLOSE(IKORG)
        CALL CLOSE(IKTRI)
        END
```

```
C***********************************************************************
C                                                                      *
C       INPUT -- READ AND PRINT NODAL POINT INPUT DATA                 *
C             -- CALCULATE AND STORE EQUATION NUMBERS                  *
C                                                                      *
C***********************************************************************
C
        SUBROUTINE INPUT(ID,P,T,R,NUMNP,NEQ)
C       IMPLICIT REAL*8 (A-H,O-Z)
        COMMON /TAPES/ IELMNT,ILOAD,IIN,IOUT,IDISP,ISTATE,IKORG,IKTRI
        COMMON /ONED/NUMET,DELTA
        DIMENSION P(1),T(1),R(1),ID(2,NUMNP)
        BYTE FF
        DATA FF/"14/
C
C       READ NODAL POINT DATA
C
        DO 10 IQ=1,NUMNP
        READ(IIN,1000)N,ID(1,N),ID(2,N),P(N),T(N),R(N)
1000    FORMAT(3I5,3E15.5)
10      CONTINUE
C
C
C       WRITE(IOUT,2000) FF
C       WRITE(IOUT,2015)
C       WRITE(IOUT,2020)
C       DO 200 N=1,NUMNP
C200    WRITE(IOUT,2030) N,(ID(I,N),I=1,2),P(N),T(N),R(N)
C
C       NUMBER UNKNOWNS
C
        NEQ=0
        DO 100 N=1,NUMNP
        DO 100 I=1,2
        IF(ID(I,N)) 110,120,110
120     NEQ=NEQ+1
        ID(I,N)=NEQ
        GO TO 100
110     ID(I,N)=0
100     CONTINUE
C
C       WRITE EQUATION NUMBERS
C
C       WRITE(IOUT,2040) FF,(N,(ID(I,N),I=1,2),N=1,NUMNP)
        RETURN
C
2000    FORMAT(1X,A1,'N O D A L   P O I N T   D A T A '//)
2015    FORMAT(' GENERATED NODAL DATA'//)
2020    FORMAT('  NODE ',9X,'BOUNDARY',24X,'NODAL POINT',17X,
     1  /' NUMBER',5X,'CONDITION CODES',21X,'COORDINATES'
     2  //15X,'X    P',30X,' PHI',8X,'THETA',8X,'RADIUS')
2030    FORMAT(I5,6X,2I5,22X,3F13.3)
2040    FORMAT(1X,A1' EQUATION NUMBERS'//,4X,'NODE',9X,
     1  'DEGREE OF FREEDOM'/3X,'NUMBER'//,
     2  '     N',13X,'X    P'/(1X,I5,9X,2I5))
C
        END
```

```
C*************************************************************************
C                                                                        *
C       LOADS -- READ NODAL POINT DATA                                   *
C             -- CALCULATE LOAD VECTOR R FOR EACH LOAD CASE AND          *
C                WRITE TC DISC FILE ILOAD                                *
C                                                                        *
C*************************************************************************
C
        SUBROUTINE LCADS (PH,TH,R,ID,NLCAD,NPRES,NEQ,NUMNP)
        COMMON /VAR/ NG,MODEX,RBEST,DELTA
        COMMON /TAPES/ IEIMNT,ILOAD,IIN,IOUT,IDISP,ISTATE,IKORG,IKTRI
        DIMENSION PH(NUMNP),TF(NUMNP),R(NEQ)
        DIMENSION ID(2,NUMNP),NODPR(4),PRESS(4),PP(4),TP(4),RP(4)
C
        DO 21Ø I=1,NEQ
21Ø     R(I)=Ø.
        IF(NLCAD.EQ.Ø)GO TO 1ØØ
        WRITE(IOUT,2ØØØ)
C       IF(MODEX.EQ.Ø)RETURN
C
C
        IF(NLOAD.EQ.Ø)GO TO 1ØØ
C
        DO 22Ø L=1,NLOAD
        READ(IIN,1ØØØ) NOD,IDIRN,FLOAD
        WRITE(IOUT,2Ø1Ø) NOD,IDIRN,FLOAD
        LN=NOD
        LI=IDIRN
        II=ID(LI,LN)
        IF(II) 22Ø,22Ø,24Ø
24Ø     R(II)=R(II)+FLOAD
C
22Ø     CONTINUE
C
C       PRESSURE LOADS
C
1ØØ     IF(NPRES.EQ.Ø)GO TO 3ØØ
C
        RADIAN=57.29577951
C       WRITE(IOUT,2Ø2Ø)
        DO 25Ø L=1,NPRES
        READ(IIN,1Ø1Ø) IEL,(NODPR(I),I=1,4),(PRESS(I),I=1,4)
        DO 26Ø K=1,4
        PP(K)=PH(NODPR(K))/RADIAN
26Ø     TP(K)=TH(NODPR(K))/RADIAN
C
        CALL PLOAD(PP,TP,PRESS,RP)
C
C       WRITE(IOUT,2Ø4Ø)
        DO 27Ø K=1,4
        LI=1
        LN=NODPR(K)
C
C       WRITE(IOUT,2Ø3Ø) NODPR(K),LI,RP(K),PRESS(K)
C
        II=ID(LI,LN)
        IF(II.GT.Ø) R(II)=R(II)+RP(K)
```

```
270     CONTINUE
250     CONTINUE
C
300     WRITE(ILOAD)R
C
200     CONTINUE
C
1000    FORMAT(2I5,F10.0)
1010    FORMAT(5I5,4F10.1)
2000    FORMAT(////'    NODE       DIRECTION          LOAD'/
     1'   NUMBER',19X,' MAGNITUDE')
2010    FORMAT(1X,I6,9X,I4,7X,E12.5)
2020    FORMAT(////'    NODE       DIRECTION          LOAD
     1           PRESSURE               '/
     2'   NUMBER',19X,' MAGNITUDE            MAGNITUDE ')
2030    FORMAT(1X,I6,9X,I4,2E19.5)
2040    FORMAT(/)
        RETURN
        END
```

```
C***********************************************************************
C                                                                      *
C       ELEMNT -- CALL THE APPROPRIATE ELEMENT SUBROUTINE              *
C                                                                      *
C***********************************************************************
C
        SUBROUTINE ELEMNT
        COMMON A(1)
        COMMON /EL/ IND.NPAR(1Ø),NUMEG.MTOT,NFIRST,NLAST,ITWO
C
        NPAR1=NPAR(1)
C
        GO TO (1,2,3,4,5),NPAR1
C
1       RETURN
C
2       RETURN
3       CALL THREED
        RETURN
4       RETURN
5       RETURN
C
        END
```

```
C*************************************************************************
C                                                                        *
C       PLOAD -- CALCULATE CONSISTENT PRESSURE LOADING                  *
C                                                                        *
C*************************************************************************
C
        SUBROUTINE PLOAD (PHI,THETA,PRESS,RP)
        COMMON /SOL/ NUMNP,NEQ,NWK,NUMEST,MIDEST,MAXEST,MK
        COMMON /VAR/ NG,MODEX,RBEST,DELTA
        COMMON /DIM/ N1,N2,N3,N4,N5,N6,N7,N8,N9,N10,N11,N12,N13,N14,N15
        COMMON /EL/ IND,NPAR(10),NUMEG,MTOT,NFIRST,NLAST,ITWO
        COMMON /TAPES/ IELMNT,ILOAD,IIN,IOUT,IDISP,ISTATE,IKORG,IKTRI
        DIMENSION PHI(1),THETA(1),PRESS(1),RP(1),H(4)
        DIMENSION XX(2,4),XG(4,4),WGT(4,4)
C
C
        DO 600 J=1,4
        XX(2,J)=PHI(J)
        XX(1,J)=THETA(J)
600     CONTINUE
C
        NINT=2
C
C       XG STORES G-L SAMPLING POINTS
C
        DATA XG /    0.,                0.,                0.,                0.,
     1  -.5773502691896, .5773502691896,                 0.,                0.,
     2  -.7745966692415,                .,  .7745966692415,                0.,
     3  -.8611363115941,-.3399810435849, .3399810435849, .8611363115941/
C
C       WGT STORES G-L WEIGHTING FACTORS
C
        DATA WGT / 2.00,               0.,                0.,                0.,
     1  1.0000000000000,1.0000000000000,                 0.,                0.,
     2   .5555555555556, .8888888888889, .5555555555556,                 0.,
     3   .3478548451375, .6521451548625, .6521451548625, .3478548451375/
C
C
        DO 30 J=1,4
30      RP(J)=0.0
C
        DO 80 LX=1,NINT
        RI=XG(LX,NINT)
        DO 80 LY=1,NINT
        SI=XG(LY,NINT)
C
C       EVALUATE DERIVATIVE H AND JACOBIAN DET
C
        CALL DM(XX,H,DET,RI,SI)
C
        WT=WGT(LX,NINT)*WGT(LY,NINT)*DET
        DO 40 K=1,4
        DO 40 L=1,4
40      RP(K)=RP(K)+H(K)*H(L)*PRESS(L)*WT
80      CONTINUE
        RETURN
        END
```

```
C*************************************************************************
C                                                                        *
C       DM -- EVALUATE THE MATRIX H                                      *
C             AT POINT (R,S) FOR A QUAD ELEMENT                          *
C                                                                        *
C*************************************************************************
C
        SUBROUTINE DM(XX,H,DET,R,S)
        COMMON /VAR/ NG,MODEX,RBEST,DELTA
        COMMON /TAPES/ IELMNT,ILOAD,IIN,IOUT,IDISP,ISTATE,IKORG,IKTRI
        DIMENSION XX(2,1),H(4),P(2,4),XJ(2,2),XJI(2,2)
C
        RP = 1. + R
        SP = 1. + S
        RM = 1. - R
        SM = 1. - S
C
C       INTERPOLATION FUNCTIONS
C
        H(1)=0.25*RP*SP
        H(2)=0.25*RM*SP
        H(3)=0.25*RM*SM
        H(4)=0.25*RP*SM
C
C       NATURAL COORDINATE DERIVATIVES W.R.T. INTERPOLATION FUNCTIONS
C
C               1. W.R.T  R
C
        P(1,1)=0.25*SP
        P(1,2)=-P(1,1)
        P(1,3)=-0.25*SM
        P(1,4)=-P(1,3)
C
C               2. W.R.T  S
C
        P(2,1)=0.25*RP
        P(2,2)=0.25*RM
        P(2,3)=-P(2,2)
        P(2,4)=-P(2,1)
C
C       EVALUATE JACOBIAN MATRIX AT (R,S)
C
10      DO 30 I=1,2
        DO 30 J=1,2
        DUM=0.0
        DO 20 K=1,4
20      DUM=DUM+P(I,K)*XX(J,K)
30      XJ(I,J)=DUM
C
C       COMPUTE DETERMINATE OF JACOBIAN MATRIX AT (R,S)
C
        DET=XJ(1,1)*XJ(2,2)-XJ(2,1)*XJ(1,2)
        IF(DET.GT.0.00000001) GO TO 40
        WRITE(IOUT,2000)
        STOP
C
C       COMPUTE INVERSE OF JACOBIAN MATRIX
```

```
C
40      DUM=1./DET
        XJI(1,1)=XJ(2,2)*DUM
        XJI(1,2)=-XJ(1,2)*DUM
        XJI(2,1)=-XJ(2,1)*DUM
        XJI(2,2)=XJ(1,1)*DUM
C
        THETA=0.0
        DO 50 IQ=1,4
50      THETA=THETA+H(IQ)*XX(1,IQ)
        DET=DET*RBEST*RBEST*SIN(THETA)
2000    FORMAT(' NEGATIVE OR ZERO JACOBIAN IN PRESSURE LOADING ')
        RETURN
        END
```

```
C*********************************************************************
C                                                                    *
C       ELCAL -- LOOP OVER ELEMENT GRCUPS FOR READING,               *
C                GENERATING, AND STORING THE ELEMENT DATA            *
C                                                                    *
C*********************************************************************
C
        SUBROUTINE ELCAL
        COMMON /SOL/ NUMNP,NEQ,NWK,NUMEST,MIDEST,MAXEST,MK
        COMMON /EL/ IND,NPAR(10),NUMEG,MTOT,NFIRST,NLAST,ITWO
        COMMON /TAPES/ IELMNT,ILOAD,IIN,IOUT,IDISP,ISTATE,IKORG,IKTRI
        COMMON A(1)
        BYTE FF
        DATA FF/ 14/
C
C
        REWIND IELMNT
        WRITE(IOUT,2000) FF
C
C       LOOP OVER ALL ELEMENTS
C
        DO 100 N=1,NUMEG
C
        READ(IIN,1000)NPAR
C
        CALL ELEMNT
C
        IF(MIDEST.GT.MAXEST)MAXEST=MIDEST
C
        WRITE (IELMNT)MIDEST,NPAR,(A(I),I=NFIRST,NLAST-1)
C
C
100     CONTINUE
C
        RETURN
C
1000    FORMAT(10I5)
2000    FORMAT(1X,A1,' E L E M E N T   G R O U P   D A T A '///)
2010    FORMAT(1X,A1)
C
        END
```

```
C***********************************************************************
C                                                                      *
C       THREED -- SET UP STORAGE FOR PCROUS SUBRCUTINE                 *
C                                                                      *
C***********************************************************************
C
        SUBROUTINE THREED
        COMMON /SOL/ NUMNP,NEQ,NWK,NUMEST,MIDEST,MAXEST,MK
        COMMON /DIM/ N1,N2,N3,N4,N5,N6,N7,N8,N9,N10,N11,N12,N13,N14,N15
        COMMON /EL/ IND,NPAR(10),NUMEG,MTOT,NFIRST,NLAST,ITWO
        COMMON /TAPES/ IEIMNT,ILOAD,IIN,ICUT,IDISP,ISTATE,IKCRG,IKTRI
        COMMON A(1)
        DIMENSION IA(1)
C
        EQUIVALENCE (NPAR(2),NUME),(NPAR(3),NUMMAT)
        EQUIVALENCE (A(1),IA(1))
C
        NFIRST=N6
        IF(IND.GT.1)NFIRST=N5
        N101=NFIRST
        N102=N101+NUMMAT*ITWO
        N103=N102+NUMMAT*ITWO
        N104=N103+20*NUME
        N105=N104+36*NUME*ITWO
        N106=N105+NUME
        NLAST=N106
C
        IF(IND.GT.1)GO TO 100
        IF(NLAST.GT.MTOT) CALL ERROR(NLAST-MTOT,3)
        GO TO 200
100     IF(NLAST.GT.MTOT) CALL ERROR(NLAST-MTOT,4)
C
200     MIDEST=NLAST-NFIRST
C
        CALL POROUS(A(N1),A(N2),A(N3),A(N4),A(N4),A(N5),
     *  A(N101),A(N102),A(N103),A(N104),A(N105))
C
        RETURN
C
        END
```

```
C*********************************************************************
C                                                                    *
C       POROUS -- POROUS ELEMENT SUBRCUTINE                          *
C                                                                    *
C*********************************************************************
C
        SUBROUTINE POROUS (ID,P,T,R,U,MHT,E,PERM,LM,XYZ,MATP)
C       IMPLICIT REAL*8 (A-H,O-Z)
        COMMON /SOL/ NUMNP,NEQ,NWK,NUMEST,MIDEST,MAXEST,MK
        COMMON /DIM/ N1,N2,N3,N4,N5,N6,N7,N8,N9,N10,N11,N12,N13,N14,N15
        COMMON /EL/ IND,NPAR(10),NUMEG,MTOT,NFIRST,NLAST,ITWO
        COMMON /VAR/ NG,MODEX,RBEST,DELTA
        COMMON /TAPES/ IELMNT,ILOAD,IIN,IOUT,IDISP,ISTATE,IKORG,IKTRI
        COMMON A(1)
        REAL*4 A
C
        DIMENSION P(1),T(1),R(1),ID(2,1),E(1),PERM(1),LM(20,1)
        DIMENSION XYZ(36,1),U(1),MHT(1),MATP(1)
        DIMENSION SU(210),NOD(12),SUPL(304)
        DIMENSION XX(3,12),B(12),HP(8),G(3,8),XG(4,4),WGT(4,4)
        REAL*4 KU(12,12),KP(8,8),KL(12,8)
C
        EQUIVALENCE (NPAR(1),NPAR1),(NPAR(2),NUME),(NPAR(3),NUMMAT)
        EQUIVALENCE (KU(1,1),SUPL(1)),(KP(1,1),SUPL(145))
        EQUIVALENCE (KL(1,1),SUPL(209))
C
        BYTE FF
        DATA FF/"14/
C
C
C       XG STORES G-I SAMPLING POINTS
C
        DATA XG /    0.,                0.,                0.,               0.,
     1  -.5773502691896, .5773502691896,                0.,               0.,
     2  -.7745966692415,                0., .7745966692415,               0.,
     3  -.8611363115941,-.3399810435849, .3399810435849, .8611363115941/
C
C       WGT STORES G-L WEIGHTING FACTORS
C
        DATA WGT / 2.00,                0.,                0.,               0.,
     1  1.0000000000000,1.0000000000000,                0.,               0.,
     2   .5555555555556, .8888888888889, .5555555555556,               0.,
     3   .3478548451375, .6521451548625, .6521451548625, .3478548451375/
C
C
        ND=20
        RADIAN=57.29577951
        NINTX=3
        NINTY=3
        NINTZ=3
C
        GO TO (300,610,900),IND
C
C
C       G E N E R A T E   E L E M E N T   I N F O R M A T I O N
C
C
```

```
C       MATERIAL INFO
C
300     WRITE(IOUT,2000)NPAR1,NUME
        IF(NUMMAT.EQ.0)NUMMAT=1
        WRITE(IOUT,2010)NUMMAT
C
        WRITE (IOUT,2020)
        DO 10 I=1,NUMMAT
        READ(IIN,1000)N,E(N),PERM(N)
10      WRITE (IOUT,2030)N,E(N),PERM(N)
C
C       READ ELEMENT INFO
C
        WRITE (IOUT,2040) FF
C
        DO 30 NEL=1,NUME
        READ(IIN,1030)M,MTYPE,(NOD(IQ),IQ=1,12)
1030    FORMAT(14I5)
        MATP(NEL)=MTYPE
        WRITE (IOUT,2050)M,(NOD(IQ),IQ=1,12),MTYPE
C
        DO 150 I=3,36,3
        XYZ(I-2,NEL)=T(NOD(I/3))/RADIAN
        XYZ(I-1,NEL)=P(NOD(I/3))/RADIAN
150     XYZ(I-0,NEL)=R(NOD(I/3))
C
        DO 380 L=1,12
380     LM(L,NEL)=ID(1,NOD(L))
        DO 390 I=13,20
390     LM(L,NEL)=ID(2,NOD(I-12))
C
C       UPDATE COLUMN HEIGHTS AND BANDWIDTH
C
        CALL COLHT(MHT,ND,LM(1,NEL))
C
C
30      CONTINUE
        RETURN
C
C
C
C       A S S E M B L E    S T I F F N E S S    M A T R I X
C
C
C
610     DO 500 NEL=1,NUME
        MTYPE=MATP(NEL)
        YM=E(MTYPE)
        PF=PERM(MTYPE)
C
        DO 505 IQ=1,210
505     SU(IQ)=0.0
C
        DO 600 J=1,12
        DO 600 I=1,3
        INDEX=3*(J-1)+I
600     XX(I,J)=XYZ(INDEX,NEL)
C
```

```
        DO 6Ø1 IQ=1,3Ø4
6Ø1     SUPI(IQ)=Ø.Ø
C
        DO 8Ø LX=1,NINTX
        RI=XG(LX,NINTX)
        DO 8Ø LY=1,NINTY
        SI=XG(LY,NINTY)
        DO 8Ø LZ=1,NINTZ
        TI=XG(LZ,NINTZ)
C
        CALL STDPM (XX,B,HP,G,DET,RI,SI,TI,NEL)
C
        WT=WGT(LX,NINTX)*WGT(LY,NINTY)*WGT(LZ,NINTZ)*DET
C
        DO 4Ø IR=1,12
        DO 4Ø JC=1,12
4Ø      KU(IR,JC)=KU(IR,JC)+WT*YM*B(IR)*B(JC)
        DO 45 IR=1,8
        DO 45 JC=1,8
        SUM=Ø.Ø
        DO 46 IK=1,3
46      SUM=SUM-G(IK,IR)*G(IK,JC)*PF*DELTA
45      KP(IR,JC)=KP(IR,JC)+WT*SUM
        DO 5Ø IR=1,12
        DO 5Ø JC=1,8
5Ø      KL(IR,JC)=KL(IR,JC)+WT*B(IR)*HP(JC)
8Ø      CONTINUE
C
        INDEX=1
        DO 6Ø IR=1,12
        DO 65 JC=IR,12
        SU(INDEX)=KU(IR,JC)
        INDEX=INDEX+1
65      CONTINUE
        DO 7Ø JC=1,8
        SU(INDEX)=KL(IR,JC)
        INDEX=INDEX+1
7Ø      CONTINUE
6Ø      CONTINUE
        DO 75 IR=1,8
        DO 75 JC=IR,8
        SU(INDEX)=KP(IR,JC)
        INDEX=INDEX+1
75      CONTINUE
C
        IF(NEL.NE.1) GOTO 4ØØØ
C
        WRITE(IOUT,3ØØØ) "14
3ØØØ    FORMAT(1X,A1,///' KU MATRIX '/)
        DO 3Ø2Ø I=1,12
        WRITE(IOUT,3Ø1Ø) (KU(I,J),J=1,12)
3Ø1Ø    FORMAT(1X,12F1Ø.5)
3Ø2Ø    CONTINUE
        WRITE(IOUT,3Ø25)
3Ø25    FORMAT(//' KI MATRIX '/)
        DO 3Ø3Ø I=1,12
        WRITE(IOUT,3Ø4Ø) (KL(I,J),J=1,8)
3Ø4Ø    FORMAT(1X,8F1Ø.5)
```

```
3030      CONTINUE
          WRITE(IOUT,3050)
3050      FORMAT(//' KP MATRIX '/)
          DO 3060 I=1,8
          WRITE(IOUT,3070) (KP(I,J),J=1,8)
3070      FORMAT(1X,8F10.5)
3060      CONTINUE
C         WRITE(IOUT,3080)
C3080     FORMAT(//' SU MATRIX '/)
C         DO 3090 IQ=1,INDEX-1
C         WRITE(IOUT,3100)IQ,SU(IQ)
C3100     FORMAT(I10,F10.5)
C3090     CONTINUE
C
4000      CALL ADDBAN(A(N3),A(N2),SU,LM(1,NEL),ND)
C
C
500       CONTINUE
          RETURN
C
C
C         S T R E S S     C A L C U L A T I O N S
C
C
900       IPRINT=0
          DO 830 N=1,NUME
          IPRINT=IPRINT+1
          IF(IPRINT.GT.50)IPRINT=1
          IF(IPRINT.EQ.1)
     *    WRITE(IOUT,2060)NG
          MTYPE=MATP(N)
          STR=0.
          I=LM(L,N)
          WRITE(IOUT,2070)N,P,STR
830       CONTINUE
C
          RETURN
C
1000      FORMAT(I5,2F10.0)
1010      FORMAT(2F10.0)
1020      FORMAT(5I5)
2000      FORMAT(' E L E M E N T     D E F I N I T I O N '///,
     1' ELEMENT TYPE ',13(' .'),'( NPAR(1) ) . . =',I5/,
     2'      EQ.1, ONE-D ELEMENTS'/,
     3'      EQ.2, TWO-D ELEMENTS'/,
     *'      GE.3, ELEMENTS CURRENTLY NOT AVAILABLE'/,
     4' NUMBER OF ELEMENTS.',10(' .'),'( NPAR(2) ) . . =',I5//)
2010      FORMAT(' M A T E R IA L     D E F I N I T I O N '///,
     1' NUMBER OF DIFFERENT SETS OF MATERIAL CONSTANTS'/,
     3 4(' .'),'( NPAR(3) ) . . =',I5//)
2020      FORMAT(///'  SET      UNIAXIAL      PERMEABILITY'/
     1' NUMBER      MODULUS',/
     2'                E              Kf ')
2030      FORMAT(/I5,4X,E12.5,3X,E12.5)
2040      FORMAT(1X,A1,' E L E M E N T    I N F O R M A T I O N '///,
     1' ELEMENT      NODE    NODE    NODE    NODE    NODE    NODE    NODE
     *  NODE    NODE    NODE    NODE    NODE       MATERIAL'/,
     2' NUMBER-N       1       2       3       4       5       6       7
```

```
     *     8      9       10      11      12       SET NUMBER'/)
2050    FORMAT(I5,8X,12(I5,2X),5X,I5)
2060    FORMAT(////' S T R E S S   C A L C U L A T I O N S   F O R ',
     1' E L E M E N T   G R O U P',I4//,2X,
     2' ELEMENT           FORCE               STRESS '/,3X,'NUMBER'/)
2070    FORMAT(1X,I5,11X,E13.6,4X,E13.6)
C
        END
```

```
C***********************************************************************
C                                                                      *
C       STDPM -- EVALUATE THE STRAIN-DISPLACEMENT-PRESSURE             *
C                MATRICES B,N,G AT POINT (R,S,T) FOR A                 *
C                POROUS ELEMENT                                        *
C                                                                      *
C***********************************************************************
C
        SUBROUTINE STDPM(XX,B,HP,G,DET,R,S,T,NEL)
C       IMPLICIT REAL*8 (A-H,O-Z)
        COMMON /TAPES/ IELMNT,ILOAD,IIN,IOUT,IDISP,ISTATE,IKORG,IKTRI
        DIMENSION XX(3,1),B(1),HP(1),G(3,1),H(12),P(3,12),PP(3,8)
        DIMENSION XJ(3,3),XJI(3,3),AA(3,3)
C
        RP = 1. + R
        SP = 1. + S
        TP = 1. + T
        RM = 1. - R
        SM = 1. - S
        TM = 1. - T
C
        RR = 1. - R * R
        SS = 1. - S * S
        TT = 1. - T * T
C
C       INTERPOLATION FUNCTIONS
C
        H(1)=0.125*RP*SP*TP
        H(2)=0.125*RM*SP*TP
        H(3)=0.125*RM*SM*TP
        H(4)=0.125*RP*SM*TP
C
        H(5)=0.125*RP*SP*TM
        H(6)=0.125*RM*SP*TM
        H(7)=0.125*RM*SM*TM
        H(8)=0.125*RP*SM*TM
C
        H(9)=0.25*RP*SP*TT
        H(10)=0.25*RM*SP*TT
        H(11)=0.25*RM*SM*TT
        H(12)=0.25*RP*SM*TT
C
C
C       NATURAL COORDINATE DERIVATIVES W.R.T. INTERPOLATION FUNCTIONS
C
C               1. W.R.T  R
C
        P(1,1)=0.125*SP*TP
        P(1,2)=-P(1,1)
        P(1,3)=-0.125*SM*TP
        P(1,4)=-P(1,3)
C
        P(1,5)=0.125*SP*TM
        P(1,6)=-P(1,5)
        P(1,7)=-0.125*SM*TM
        P(1,8)=-P(1,7)
C
```

```
      P(1,9)=0.25*SP*TT
      P(1,10)=-P(1,9)
      P(1,11)=-0.25*SM*TT
      P(1,12)=-P(1,11)
C
C               2. W.R.T  S
C
      P(2,1)=0.125*RP*TP
      P(2,2)=0.125*RM*TP
      P(2,3)=-P(2,2)
      P(2,4)=-P(2,1)
C
      P(2,5)=0.125*RP*TM
      P(2,6)=0.125*RM*TM
      P(2,7)=-P(2,6)
      P(2,8)=-P(2,5)
C
      P(2,9)=0.25*RP*TT
      P(2,10)=0.25*RM*TT
      P(2,11)=-P(2,10)
      P(2,12)=-P(2,9)
C
C               3. W.R.T  T
C
      P(3,1)=0.125*RP*SP
      P(3,2)=0.125*RM*SP
      P(3,3)=0.125*RM*SM
      P(3,4)=0.125*RP*SM
C
      P(3,5)=-0.125*RP*SP
      P(3,6)=-0.125*RM*SP
      P(3,7)=-0.125*RM*SM
      P(3,8)=-0.125*RP*SM
C
      P(3,9)=-0.5*RP*SP*T
      P(3,10)=-0.5*RM*SP*T
      P(3,11)=-0.5*RM*SM*T
      P(3,12)=-0.5*RP*SM*T
C
C~~~~~~~~~~~~~~~~~~~~~~~~~~~~~~~~~~~~~~~~~~~~~~~~~~~~~~~~~~~~~~~~~~~~~
C
      DO 100 IQ=1,8
      HP(IQ)=H(IQ)
      DO 100 IP=1,3
      PP(IP,IQ)=P(IP,IQ)
100   CONTINUE
C
      DO 110 IQ=1,4
      H(IQ)=H(IQ)-H(IQ+8)/2.
      H(IQ+4)=H(IQ+4)-H(IQ+8)/2.
      DO 110 IP=1,3
      P(IP,IQ)=P(IP,IQ)-P(IP,IQ+8)/2.
      P(IP,IQ+4)=P(IP,IQ+4)-P(IP,IQ+8)/2.
110   CONTINUE
C~~~~~~~~~~~~~~~~~~~~~~~~~~~~~~~~~~~~~~~~~~~~~~~~~~~~~~~~~~~~~~~~~~~~~
C
C
C     EVALUATE JACOBIAN MATRIX AT (R,S,T)
```

```
C
10      DO 30 I=1,3
        DO 30 J=1,3
        DUM=0.0
        DO 20 K=1,12
20      DUM=DUM+P(I,K)*XX(J,K)
        XJ(I,J)=DUM
30      CONTINUE
C
C       COMPUTE DETERMINATE OF JACOBIAN MATRIX AT (R,S,T)
C
        AA(1,1)=+(XJ(2,2)*XJ(3,3)-XJ(3,2)*XJ(2,3))
        AA(1,2)=-(XJ(2,1)*XJ(3,3)-XJ(3,1)*XJ(2,3))
        AA(1,3)=+(XJ(2,1)*XJ(3,2)-XJ(3,1)*XJ(2,2))
        DET=0.
        DO 25 I=1,3
25      DET=DET+XJ(1,I)*AA(1,I)
        IF(DET.GT.0.0000001) GO TO 40
        WRITE(IOUT,2000) NEL
        STOP
C
40      AA(2,1)=-(XJ(1,2)*XJ(3,3)-XJ(3,2)*XJ(1,3))
        AA(2,2)=+(XJ(1,1)*XJ(3,3)-XJ(3,1)*XJ(1,3))
        AA(2,3)=-(XJ(1,1)*XJ(3,2)-XJ(3,1)*XJ(1,2))
        AA(3,1)=+(XJ(1,2)*XJ(2,3)-XJ(2,2)*XJ(1,3))
        AA(3,2)=-(XJ(1,1)*XJ(2,3)-XJ(2,1)*XJ(1,3))
        AA(3,3)=+(XJ(1,1)*XJ(2,2)-XJ(2,1)*XJ(1,2))
C
C
C       COMPUTE INVERSE OF JACOBIAN MATRIX
C
        DUM=1./DET
        DO 35 IROW=1,3
        DO 35 JCOL=1,3
35      XJI(IROW,JCOL)=AA(JCOL,IROW)*DUM
C
C       EVALUATE GLOBAL DERIVATIVE OPERATOR B
C
        DO 50 K=1,12
        B(K)=0.
        DO 50 I=1,3
50      B(K)=B(K)+XJI(3,I)*P(I,K)
C
        DO 60 K=1,8
        DO 60 J=1,3
        G(J,K)=0.0
        DO 60 I=1,3
60      G(J,K)=G(J,K)+XJI(J,I)*PP(I,K)
C
        THETA=0.0
        RAD=0.0
        DO 75 IQ=1,12
        THETA=THETA+H(IQ)*XX(1,IQ)
75      RAD=RAD+H(IQ)*XX(3,IQ)
        ST=SIN(THETA)
        DET=DET*RAD*RAD*ST
C
        D1=1./RAD
```

```
      D2=D1/ST
      DO 8Ø K=1,8
      G(1,K)=G(1,K)*D1
      G(2,K)=G(2,K)*D2
8Ø    CONTINUE
C
      RETURN
C
2ØØØ  FORMAT(///' *** ERROR , ZERO OR NEGATIVE JACOBIAN FOR
     1ELEMENT (',I4,') *** '//)
C
      END
```

```
C***********************************************************************
C                                                                      *
C       CCLHT -- CALCULATE COLUMN HEIGHTS                              *
C                                                                      *
C***********************************************************************
C
        SUBROUTINE CCLHT(MHT,ND,LM)
        COMMON /SOL/ NUMNP,NEQ,NWK,NUMEST,MIDEST,MAXEST,MK
        DIMENSION LM(1),MHT(1)
C
        LS=10000
        DO 100 I=1,ND
        IF(LM(I))110,100,110
110     IF(LM(I)-LS)120,100,100
120     LS=LM(I)
100     CONTINUE
C
        DO 200 I=1,ND
        II=LM(I)
        IF(II.EQ.0)GO TO 200
        ME=II-LS
        IF(ME.GT.MHT(II))MHT(II)=ME
200     CONTINUE
C
        RETURN
        END
```

```
C***********************************************************************
C                                                                      *
C       ADDRES -- CALCULATE ADDRESSES OF DIAGONAL ELEMENTS IN          *
C                 BANDED MATRIX WHOSE COLUMN HEIGHTS ARE KNOWN         *
C                                                                      *
C               MHT = ACTIVE COLUMN HEIGHTS                            *
C               MAXA = ADDRESSES OF DIAGONAL ELEMENTS                  *
C                                                                      *
C***********************************************************************
C
        SUBROUTINE ADDRES(MAXA,MHT)
        COMMON /SOL/ NUMNP,NEQ,NWK,NUMEST,MIDEST,MAXEST,MK
        DIMENSION MAXA(1),MHT(1)
C
C       CLEAR ARRAY AREA
C
        NN=NEQ+1
        DO 20 I=1,NN
20      MAXA(I)=0.0
C
        MAXA(1)=1
        MAXA(2)=2
        MK=0
        IF(NEQ.EQ.1)GO TO 100
        DO 10 I=2,NEQ
        IF(MHT(I).GT.MK)MK=MHT(I)
10      MAXA(I+1)=MAXA(I)+MHT(I)+1
100     MK=MK+1
        NWK=MAXA(NEQ+1)-MAXA(1)
C
        RETURN
        END
```

```
C***********************************************************************
C                                                                      *
C       CLEAR -- CLEAR ARRAY A                                         *
C                                                                      *
C***********************************************************************
C
        SUBROUTINE CLEAR(A,N)
C       IMPLICIT REAL*8 (A-H,O-Z)
        DIMENSION A(1)
        DO 10 I=1,N
10      A(I)=0.
        RETURN
        END
```

```
C***********************************************************************
C                                                                      *
C       ASSEM -- CALL ELEMENT SUBROUTINE FOR ASSEMBLAGE OF THE         *
C                STRUCTURE STIFFNES MATRIX                             *
C                                                                      *
C***********************************************************************
C
        SUBROUTINE ASSEM(AA)
        COMMON /EL/ IND,NPAR(10),NUMEG,MTOT,NFIRST,NLAST,ITWO
        COMMON /TAPES/ IELMNT,ILOAD,IIN,IOUT,IDISP,ISTATE,IKORG,IKTRI
        DIMENSION AA(1)
C
        REWIND IELMNT
C
        DO 200 N=1,NUMEG
        READ(IELMNT)NUMEST,NPAR,(AA(I),I=1,NUMEST)
C
        CALL ELEMNT
C
200     CONTINUE
        RETURN
C
C
        END
```

```
C*************************************************************************
C                                                                        *
C       ADDBAN -- ASSEMBLE UPPER TRIANGULAR ELEMENT STIFFNESS            *
C                 INTO COMPACTED GLOBAL STIFFNESS                        *
C                                                                        *
C               A = GLOBAL STIFFNESS                                     *
C               S = ELEMENT STIFFNESS                                    *
C               ND = DEGREES OF FREEDOM IN ELEMENT  TIFFNESS             *
C                                                                        *
C                    S(1)          S(2)          S(3)          +++       *
C               S =                S(ND+1)       S(ND+2)       +++       *
C                                                S(2*ND)       +++       *
C                                                              +++       *
C                                                                        *
C                                                                        *
C               .    A(1)          A(3)          A(6)          +++       *
C               A =                A(2)          A(5)          +++       *
C                                                A(4)          +++       *
C                                                              +++       *
C                                                                        *
C*************************************************************************
C
      SUBROUTINE ADDBAN(A,MAXA,S,LM,ND)
C     IMPLICIT REAL*8 (A-H,O-Z)
      DIMENSION A(1),MAXA(1),S(1),LM(1)
C
      NDI=0
      DO 200 I=1,ND
      II=LM(I)
      IF(II)200,200,100
100   MI=MAXA(II)
      KS=I
      DO 220 J=1,ND
      JJ=LM(J)
      IF(JJ)220,220,110
110   IJ=II-JJ
      IF(IJ)220,210,210
210   KK=MI+IJ
      KSS=KS
      IF(J.GE.I)KSS=J+NDI
      A(KK)=A(KK)+S(KSS)
220   KS=KS+ND-J
200   NDI=NDI+ND-I
C
      RETURN
      END
```

```
C***********************************************************************
C                                                                      *
C       SECOND -- OBTAIN SYSTEM TIME                                   *
C                                                                      *
C***********************************************************************
C
        SUBROUTINE SECOND(TIM)
        TIM=SECNDS(0.)
        RETURN
        END
```

```
C***********************************************************************
C                                                                      *
C       COLSOL -- SOLVE FINITE ELEMENT STATIC EQUILIBRIUM EQUATIONS    *
C                 IN CORE, USING COMPACTED STORAGE AND COLUMN          *
C                 REDUCTION SCHEME                                     *
C                                                                      *
C       -- INPUT VARIABLES --                                          *
C       A(NWK)    = STIFFNESS MATRIX STORED IN COMPACTED FORM          *
C       V(NN)     = RIGHT-HAND-SIDE LOAD VECTOR                        *
C       MAXA(NNM) = VECTOR CONTAINING THE ADDRESSES OF DIAGONAL        *
C                   ELEMENTS OF STIFFNESS MATRIX IN A                  *
C       NN        = NUMBER OF EQUATIONS                                *
C       NWK       = NUMBER OF ELEMENTS BELOW SKYLINE OF MATRIX         *
C       NNM       = NN + 1                                             *
C       KKK       = INPUT FLAG                                         *
C            EQ.1 TRIANGULARIZATION OF STIFFNESS MATRIX                *
C            EQ.2 REDUCTION AND BACK-SUBSTITUTION OF LOAD VECTOR       *
C       IOUT      = LOGICAL UNIT FOR OUTPUT DEVICE                     *
C                                                                      *
C                                                                      *
C       -- OUTPUT --                                                   *
C       A(NWK)    = D AND L FACTORS OF STIFFNESS MATRIX                *
C       V(NN)     = DISPLACEMENT VECTOR                                *
C                                                                      *
C***********************************************************************
C
        SUBROUTINE COLSOL(A,V,MAXA,NN,NWK,NNM,KKK)
C       IMPLICIT REAL*8 (A-H,O-Z)
        COMMON /TAPES/ IELMNT,ILOAD,IIN,IOUT,IDISP,ISTATE,IKORG,IKTRI
        DIMENSION A(NWK),V(NN),MAXA(NNM)
C
C       PERFORM L*D*LT FACTORIZATION OF STIFFNESS MATRIX
C
        IF(KKK-2)40,150,150
40      DO 140 N=1,NN
        KN=MAXA(N)
        KL=KN+1
        KU=MAXA(N+1)-1
        KH=KU-KL
        IF(KH)110,90,50
50      K=N-KH
        IC=0
        KLT=KU
        DO 80 J=1,KH
        IC=IC+1
        KLT=KLT-1
        KI=MAXA(K)
        ND=MAXA(K+1)-KI-1
        IF(ND)80,80,60
60      KK=MIN0(IC,ND)
        C=0.
        DO 70 L=1,KK
70      C=C+A(KI+L)*A(KLT+L)
        A(KLT)=A(KLT)-C
80      K=K+1
90      K=N
        B=0.
```

```
      DO 100 KK=KL,KU
      K=K-1
      KI=MAXA(K)
      C=A(KK)/A(KI)
      B=B+C A(KK)
100   A(KK)=C
      A(KN)=A(KN)-B
110   IF(A(KN))140,120,140     ! IGNORE NEGATIVE
120   WRITE(IOUT,2000)N,A(KN)
      STOP
140   CONTINUE
      RETURN
C
C     REIUCE RIGHT-HAND-SIDE LOAD VECTOR
C
150   DO 180 N=1,NN
      KL=MAXA(N)+1
      KU=MAXA(N+1)-1
      IF(KU-KL)180,160,160
160   K=N
      C=0.
      DO 170 KK=KL,KU
      K=K-1
170   C=C+A(KK)*V(K)
      V(N)=V(N)-C
180   CONTINUE
C
C     BACK-SUBSTITUTE
C
      DO 200 N=1,NN
      K=MAXA(N)
200   V(N)=V(N)/A(K)
      IF(NN.EQ.1)RETURN
      N=NN
      DO 230 L=2,NN
      KL=MAXA(N)+1
      KU=MAXA(N+1)-1
      IF(KU-KL)230,210,210
210   K=N
      DO 220 KK=KL,KU
      K=K-1
220   V(K)=V(K)-A(KK)*V(N)
230   N=N-1
      RETURN
2000  FORMAT(//' STOP - STIFFNESS MATRIX NOT PCSITIVE DEFINITE '//
     1' NONPOSITIVE PIVOT FOR EQUATION ',I4,//
     2' PIVOT = ',E20.12)
      END
```

```
C*************************************************************************
C                                                                        *
C       LOADV -- OBTAIN THE LOAD VECTOR                                  *
C                                                                        *
C*************************************************************************
C
        SUBROUTINE LOADV(R,NEQ)
C       IMPLICIT REAL*8 (A-H,O-Z)
        COMMON /TAPES/ IELMNT,ILOAD,IIN,IOUT,IDISP,ISTATE,IKORG,IKTRI
        DIMENSION R(NEQ)
C
        READ (ILOAD)R
        RETURN
        END
```

```
C***********************************************************************
C                                                                      *
C       DISPV -- OBTAIN THE DISPLACEMENT VECTOR                        *
C                                                                      *
C***********************************************************************
C
      SUBROUTINE DISPV(U,NSUR)
C     IMPLICIT REAL*8 (A-H,O-Z)
      COMMON /TAPES/ IELMNT,ILOAD,IIN,IOUT,IDISP,ISTATE,IKORG,IKTRI
      DIMENSION U(NSUR)
C
      READ (IDISP)U
      RETURN
      END
```

```
C*************************************************************************
C                                                                        *
C       WRITE -- PRINT DISPLACEMENTS AND FLOWS                           *
C                                                                        *
C*************************************************************************
C
        SUBROUTINE WRITE(DISP,ID,NEQ,NUMNP,FLOW,NSNOD,NSUR)
C       IMPLICIT REAL*8 (A-H,O-Z)
        COMMON /TAPES/ IELMNT,ILOAD,IIN,IOUT,IDISP,ISTATE,IKORG,IKTRI
        DIMENSION DISP(NEQ),ID(2,NUMNP),D(3),FLOW(NSUR),NSNOD(NSUR)
        BYTE FF
        DATA FF/"14/
C
C       PRINT DISPLACEMENTS
C
        WRITE (IOUT,2000)
        IC=4
C
        DO 100 II=1,NUMNP
        IC=IC+1
        IF(IC.LT.54)GO TO 105
C       WRITE (IOUT,2020) FF
        IC=0
105     DO 110 I=1,3
110     D(I)=0.
C
        DO 120 I=1,2
        KK=ID(I,II)
        IL=I
120     IF(KK.NE.0)D(IL)=DISP(KK)
C
        DO 130 IQ=1,NSUR
        KK=NSNOD(IQ)
130     IF(KK.EQ.II)D(3)=FLOW(IQ)
        IF(D(3).EQ.0.0)GOTO 100
C
        WRITE(IOUT,2010)II,D
100     CONTINUE
C
C       WRITE DISPLACEMENTS AND FLOWS TO FILE
C
        WRITE(ISTATE) (DISP(I),I=1,NEQ)
        WRITE(ISTATE) (FLOW(I),I=1,NSUR)
C
        RETURN
2000    FORMAT(////' D I S P L A C E M E N T S ,  P R E S S U R E S ,
     *  & S U R F A C E   F L O W S '///' NODE ',
     18X,' DISPLACEMENT          PRESSURE              FLOW '/)
2010    FORMAT(1X,I3,8X,3E18.6)
2020    FORMAT(1X,A1' D I S P L A C E M E N T S ,  P R E S S U R E S ,
     *  & S U R F A C E   F L O W S '///' NODE ',
     18X,' DISPLACEMENT          PRESSURE              FLOW '/)
C
        END
```

```
C***********************************************************************
C                                                                      *
C       STRESS -- CALL THE ELEMENT SUBROUTINE TO CALCULATE STRESSES    *
C                                                                      *
C***********************************************************************
C
        SUBROUTINE STRESS(AA)
        COMMON /VAR/ NG,MODEX,RBEST,DELTA
        COMMON /EL/ IND,NPAR(10),NUMEG,MTOT,NFIRST,NLAST,ITWO
        COMMON /TAPES/ IELMNT,ILOAD,IIN,IOUT,IDISP,ISTATE,IKORG,IKTRI
        DIMENSION AA(1)
C
C       LOOP OVER ALL ELEMENT GROUPS
C
C
        REWIND IELMNT
C
        DO 100 N=1,NUMEG
        NG=N
C
        READ (IELMNT) NUMEST,NPAR,(AA(I),I=1,NUMEST)
C
        CALL ELEMNT
C
100     CONTINUE
        RETURN
        END
```

```
C***********************************************************************
C                                                                      *
C       ERROR -- PRINT ERROR MESSAGES WHEN STORAGE IS EXCEEDED         *
C                                                                      *
C***********************************************************************
C
        SUBROUTINE ERROR(N,I)
        COMMON /TAPES/ IELMNT,ILOAD,IIN,IOUT,IDISP
C
        GO TO (1,2,3,4,5),I
C
1       WRITE(IOUT,2000)
        GO TO 6
2       WRITE(IOUT,2010)
        GO TO 6
3       WRITE(IOUT,2020)
        GO TO 6
4       WRITE(IOUT,2030)
        GO TO 6
5       WRITE(IOUT,2040)
C
6       WRITE(IOUT,2050) N
        STOP
2000    FORMAT(//' NOT ENOUGH STORAGE FOR READ-IN OF ID ARRAY AND'
     1/' NODAL POINT COORDINATES ')
2010    FORMAT(//' NOT ENOUGH STORAGE FOR DEFINITION OF LOAD VECTORS ')
2020    FORMAT(//' NOT ENOUGH STORAGE FOR ELEMENT DATA INPUT ')
2030    FORMAT(//' NOT ENOUGH STORAGE FOR ASSEMBLAGE OF STRUCTURE'
     2/' STIFFNESS, AND DISPLACEMENT AND STRESS SOLUTION PHASE ')
2040    FORMAT(//' NOT ENOUGH STORAGE FOR SURFACE DISPLACEMENT INPUT ')
2050    FORMAT(//' *** ERROR    STORAGE EXCEEDED BY ',I9,' LONGWORDS ')
        END
```

```
C***********************************************************************
C                                                                      *
C       SAVE -- SAVE THE DISPLACEMENT VECTOR                           *
C                                                                      *
C***********************************************************************
C
        SUBROUTINE SAVE(U,UOLD,NEQ)
C       IMPLICIT REAL*8 (A-H,O-Z)
        DIMENSION U(NEQ),UOLD(NEQ)
C
        DO 10 IQ=1,NEQ
10      UOLD(IQ)=U(IQ)
        RETURN
        END
```

```
C***********************************************************************
C                                                                      *
C       UPDATE -- UPDATE THE RHS USING PREVIOUS DISPLACEMENTS          *
C                                                                      *
C***********************************************************************
C
        SUBROUTINE UPDATE(R,UOLD,ID,MAXA,A,NUMNP)
C       IMPLICIT REAL*8 (A-H,O-Z)
        COMMON /TAPES/ IELMNT,ILOAD,IIN,IOUT,IDISP,ISTATE,IKORG,IKTRI
        DIMENSION A(1),R(1),UOLD(1),MAXA(1),ID(2,1)
C
C
        DO 200 IP=1,NUMNP                          ! PRESSURE COLUMNS
        II=ID(2,IP)
        IF(II.EQ.0)GOTO 200
        IHT=MAXA(II+1)-MAXA(II)-1
        SUM=0.
        DO 250 IU=1,NUMNP                          ! DISPLACEMENT ROWS
        JJ=ID(1,IU)
        IF(JJ.EQ.0)GOTO 250
        ICOL=II-JJ
        IF(ICOL.LE.0)GOTO 250
        IF(ICOL.GT.IHT)GOTO 250
        INDEX=MAXA(II)+ICOL
        SUM=SUM+UOLD(JJ)*A(INDEX)
250     CONTINUE
        R(II)=R(II)+SUM
200     CONTINUE
C
        DO 300 IU=1,NUMNP                          ! DISPLACEMENTS COLUMNS
        II=ID(1,IU)
        IF(II.EQ.0)GOTO 300
        IHT=MAXA(II+1)-MAXA(II)-1
        DO 350 IP=1,NUMNP                          ! PRESSURE ROWS
        JJ=ID(2,IP)
        IF(JJ.EQ.0)GOTO 350
        ICOL=II-JJ
        IF(ICOL.LE.0)GOTO 350
        IF(ICOL.GT.IHT)GOTO 350
        INDEX=MAXA(II)+ICOL
        R(JJ)=R(JJ)+UOLD(II)*A(INDEX)
350     CONTINUE
300     CONTINUE
C
        RETURN
        END
```

```
C***********************************************************************
C                                                                      *
C       OUT -- CONVERT TO REAL*4 FOR OUTPUT                            *
C                                                                      *
C***********************************************************************
C
        SUBROUTINE OUT(D,R)
        REAL*8 D
        REAL*4 R
        R=D
        RETURN
        END
```

```
C*****************************************************************************
C                                                                            *
C       DISPL -- READ SURFACE DISPLACEMENT DATA                              *
C                WRITE TO DISC FILE IDISP                                    *
C                                                                            *
C*****************************************************************************
C
        SUBROUTINE DISPL (NSNOD,SDISP,NSUR,NLCASE)
        COMMON /VAR/ NG,MODEX
        COMMON /TAPES/ IELMNT,ILOAD,IIN,IOUT,IDISP,ISTATE,IKORG,IKTRI
        DIMENSION NSNOD(NSUR),SDISP(NSUR)
        BYTE FF
        DATA FF/"14/
C
        DO 200 I=1,NSUR
        READ(IIN,1005) NSNOD(I)
1005    FORMAT(I5)
200     CONTINUE
C
        DO 230 LL=1,NLCASE
C       WRITE(IOUT,2000) FF,LL
        DO 240 I=1,NSUR
240     SDISP(I)=0.
        DO 250 N=1,NSUR
        READ(IIN,1000) NOD,DISP
        IF(NSNOD(N).NE.NOD)GOTO 250
        SDISP(N)=DISP
C       WRITE(IOUT,2010) N,NOD,SDISP(N)
250     CONTINUE
        WRITE(IDISP)SDISP
230     CONTINUE
C
1000    FORMAT(I5,F10.0)
2000    FORMAT(1X,A1,1X,' L O A D   C A S E   #',I3////
     1'            NODE   DISPLACEMENT '/
     1'           NUMBER')
2010    FORMAT(1X,I5,5X,I5,F12.3)
        RETURN
        END
```

```
C***********************************************************************
C                                                                      *
C       DASSEM -- ASSEMBLE SURFACE FLOW MATRIX                         *
C                                                                      *
C***********************************************************************
C
      SUBROUTINE DASSEM (ID,NSNOD,AKQ,MAXB,DISP,NSUR,NLCASE)
      COMMON /VAR/ NG,MODEX,RBEST,DELTA
      COMMON /SOL/ NUMNP,NEQ,NWK,NUMEST,MIDEST,MAXEST,MK
      COMMON /DIM/ N1,N2,N3,N4,N5,N6,N7,N8,N9,N10,N11,N12,N13,N14,N15
      COMMON /TAPES/ IELMNT,ILOAD,IIN,IOUT,IDISP,ISTATE,IKORG,IKTRI
      DIMENSION ID(2,1),NSNOD(NSUR),AKQ(1),MAXB(1),DISP(1)
      COMMON A(1)
      BYTE FF
      DATA FF/"14/
C
      INDEX=1
      NEQ1=NEQ+1
      DO 200 I=1,NSUR
      MAXB(I)=INDEX
      DO 210 IQ=1,NEQ
210   DISP(IQ)=0.0
      IF=ID(2,NSNOD(I))
      DISP(IF)=DELTA
      CALL COLSOL(A(N3),DISP,A(N2),NEQ,NWK,NEQ1,2)
      DO 230 N=I,1,-1
      NUM=ID(1,NSNOD(N))
      AKQ(INDEX)=DISP(NUM)
      INDEX=INDEX+1
230   CONTINUE
200   CONTINUE
C
      NSUR1=NSUR+1
      MAXB(NSUR1)=INDEX
      NSIZE=NSUR*NSUR1/2
      CALL COLSOL(AKQ,DISP,MAXB,NSUR,NSIZE,NSUR1,1)
C
      RETURN
      END
```

```
C***********************************************************************
C                                                                      *
C       FLOW -- FIND THE SURFACE FLOWS                                 *
C                                                                      *
C***********************************************************************
C
        SUBROUTINE FLOW(UR,US,ID,AKQ,MAXB,NSNOD,NSUR,R)
C       IMPLICIT REAL*8 (A-H,O-Z)
        COMMON /VAR/ NG,MODEX,RBEST,DELTA
        COMMON /TAPES/ IELMNT,ILOAD,IIN,IOUT,IDISP,ISTATE,IKORG,IKTRI
        DIMENSION AKQ(1),UR(1),US(1),MAXB(1),ID(2,1),R(1),NSNOD(1)
C
C
        DO 200 IP=1,NSUR
        NUM=ID(1,NSNOD(IP))
200     US(IP)=US(IP)-UR(NUM)
C
        NSUR1=NSUR+1
        NSIZE=NSUR*NSUR1/2
        KTR=2
        CALL COLSOL(AKQ,US,MAXB,NSUR,NSIZE,NSUR1,KTR)
C
C       CORRECT LOAD VECTOR
C
        DO 300 IQ=1,NSUR
        NUM=ID(2,NSNOD(IQ))
300     R(NUM)=R(NUM)+US(IQ)*DELTA
        RETURN
        END
```

APPENDIX B

FREQUENCY RESPONSE

As shown in Chapter 3, the frequency response of the cartilage layer, modelled as an elastic network submerged in an incompressible fluid, exhibits a characteristic 45-degree phase shift between the surface stress and displacement (displacement lags). The shift will decrease as effects of the compressibility of the fluid and/or the network become significant. The bulk modulus of water is 2.24 GPa; of the solid constituents of cartilage it is likely even higher (it would otherwise be difficult to account for the high speed of wave propagation we measured in cartilage). Therefore, we should not expect significant effects of bulk compressibility until the uniaxial strain stiffness of the layer is say 0.2 GPa (stiffness is the ratio of the surface stress to the <u>average</u> strain).

Figure B-1 shows our design for the confinement chamber. (See Tepic [139] for a detailed discussion of the advantages of this experimental technique). A plug of cartilage is positioned on top of a 20 MHz ultrasonic tranducer which faces the plug and the loader on top of it. Thickness of the plug is measured by timing the reflections of ultrasonic pulses emitted from and received by the transducer. The displacement is thus measured <u>across the specimen</u> alone. The resolution of the measurement is better than a micron, which at high frequencies is insufficient for a very precise estimate of the stiffness, but, as long as there are at least two levels of the surface position

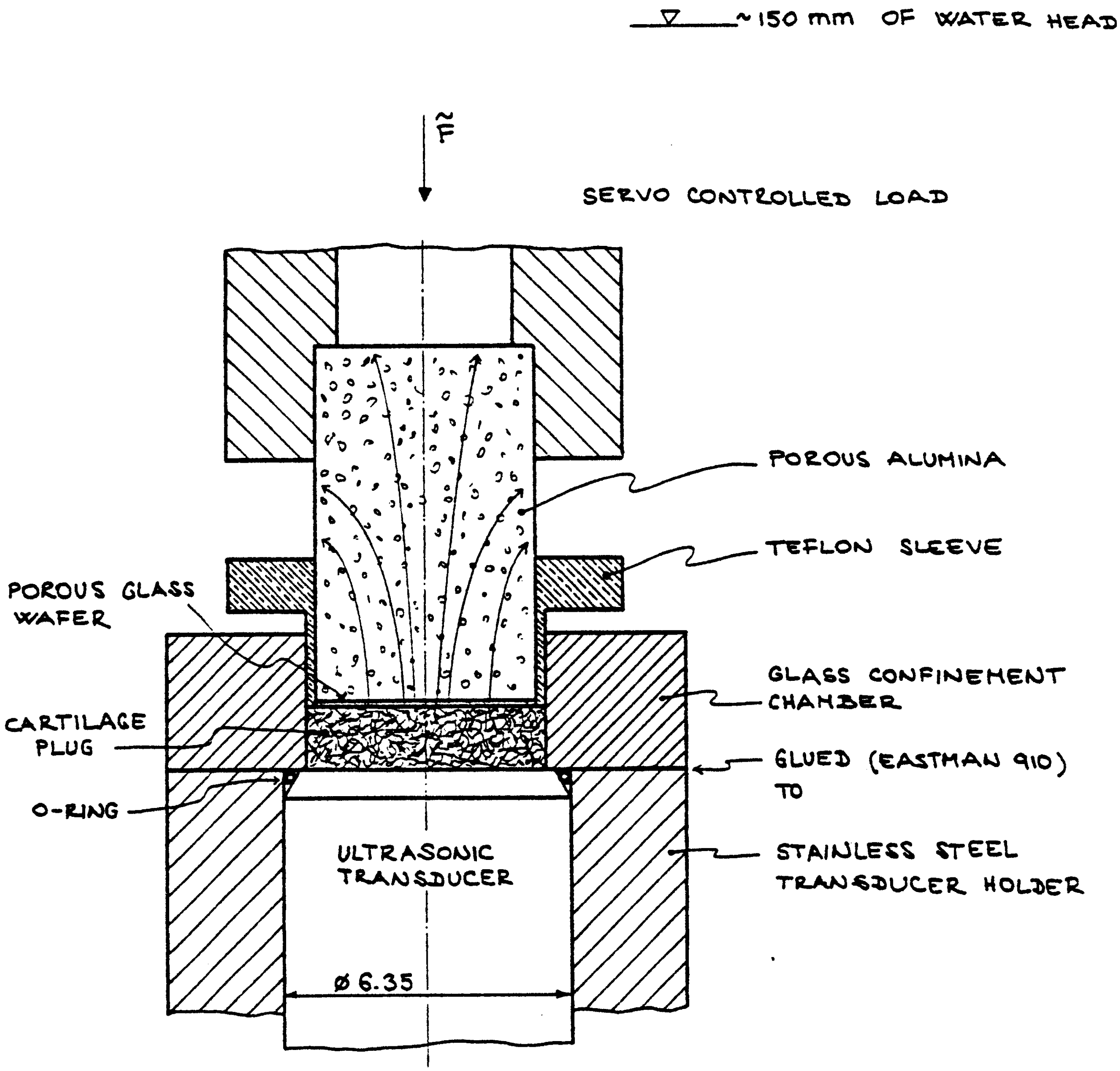

Figure B-1. Cartilage Plug Confinement for the Frequency Response Measurements recorded, is sufficient to determine the phase shift. The thick-walled confinement chamber was made from a glass (pyrex) rod which was bored and then polished. The loader consists of a porous alumina rod and a thin, very fine porous pyrex glass wafer, ground by hand to final thickness of only 0.125 mm. The result was a low permeability loader (the fluid resistance was measured to be 1.5 x 10 Ns/m) with a smooth loading surface (the surface roughness should be measured in the future). To prevent scratching against the glass the loader is lined by a thin teflon sleeve.

The load was applied by our servo-controlled Hip Simulator which for this purpose served as any load-controlled testing machine.

The ultrasonic signals were processed as described in Sections 4.1. The load signals from the simulator and a square-wave output from the function generator, used only to determine the frequency, were sampled through LPS analog-to-digital converter. Five to twenty full cycles were recorded and the phase shift was determined by simply computing the corresponding coefficients of the Fourier series of the load signal and of the reconstructed displacement measurements.

The results of the phase shift measurements are shown on Figure B-2. Curve 1 shows an average of many trials on different plugs with the alumina loader without the glass wafer; the data on Curve 2 was obtained with the glass wafer. Curve 1 is shifted by about a decade with respect to Lee's [72] data (Curve 3); Curve 2 by an additional decade. At lower frequencies we have consistently measured shifts of 45 to 50 degrees, as expected, but the fall off above 0.1 Hz persisted.

Even if we had a "perfect" loader, the surface effects can never be completely eliminated, because the cartilage material is not homogenous and even if microtomed (as in some of our tests) will retain some surface roughness.

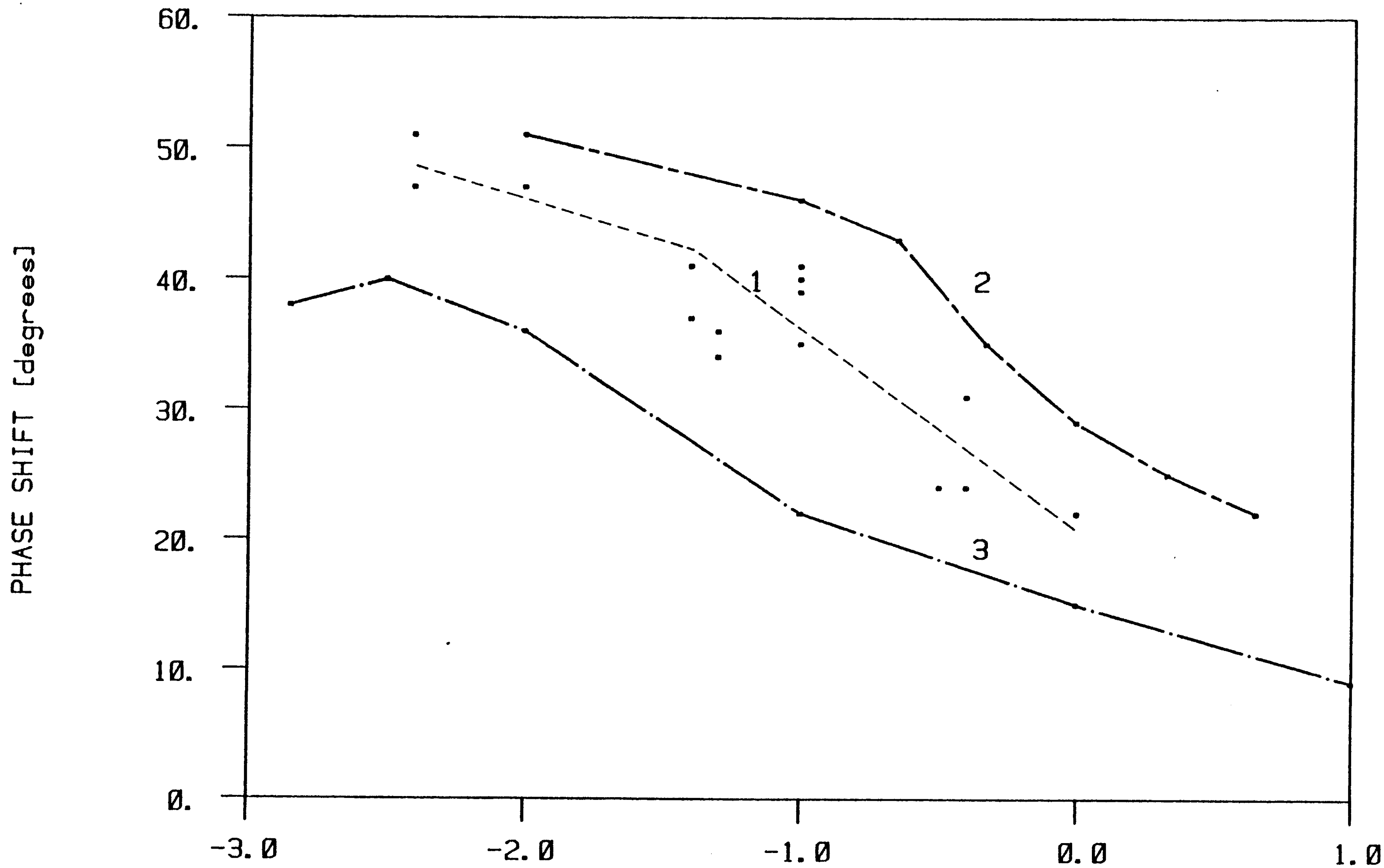

Figure B-2. **Phase Shift Between Surface Displacement and Load**

References

1. Acheson, R. M., and A. B. Collart: New Haven survey of joint disease. XVII. Relationship between some systemic characteristics and osteoarthrosis in a general population, <u>Ann. Rheum. Dis.</u>, 34(5): 379-87,1975.

2. Ahmed, A.M., D.L. Burke, A. Tencer, and Stachiewicz, J.W.: A method for the in vitro measurement of pressure distribution at articular interfaces of synovial joints, Trans. 23rd Orthopaedic Research Society (Las Vegas), 178, 1977.

3. Antonsson, E. K.: A Three-dimensional Kinematic Acquisition and Intersegmental Dynamic Analysis System for Human Motion, Ph.D. Thesis, Department of Mechanical Engineering, M.I.T., 1982.

4. Armstrong, C. G., Bahrani, A. S., and Gardner, D. L.: Changes in the deformational behavior of human hip cartilage with age, <u>Journal of Biomechanical Engineering</u>, 102: 214-220, 1980.

5. Armstrong, C. G., Bahrani, A. S., and Gardner, D. L.: In vitro measurement of articular cartilage deformations in the intact human hip joint under load, <u>Journal of Bone and Joint Surgery</u>, 61A(5): 744-55, 1979.

6. Armstrong, C. G., Bahrani, A. S., and Gardner, D. L.: Alteration with age in compliance of human femoral-head cartilage, <u>Lancet</u>, 1103-1104, 1977.

7. Armstrong, C. G.: Ageing human articular cartilage: a biomechanical study of the human hip joint, Ph.D. Thesis, Queens University of Belfast, 1977.

8. Askew, M. J., and Mow, V. C.: The biomechanical function of the collagen fibril ultrastructure of articular cartilage, <u>Journal of Biomechanical Engineering</u>, 100: 105-115, 1978.

9. Bathe, K. J.: Finite element procedures in engineering analysis. Prentice-Hall, 1982.

10. Benninghoff, A.: Form und Bau der Gelenkknorpel in ihren Bezeihungen zur Funktion. I. Der modellierenden und formerhaltenden Faktoren des Knorpelreliefs, Z. Gesamte Anat., 76, 43-63, 1925.

11. Biot, M. A.: General solutions of the equations of elasticity and consolidation for a porous material, Journal of Applied Mechanics, 91-96, 1956.

12. Bollet, A.J., and Nance, J.L.: Biochemical findings in normal and osteoarthritic articular cartilage. II. Chondroitin sulfate concentration and chain length, water, and ash content, Journal of Clincal Investigation 45(7): 1170-1177, 1966.

13. Bollet, A.J.: An essay on the biology of osteoarthritis, Arthitis and Rheumatism, 12(2): 152-163, 1969.

14. Brown, T. D., and Shaw, D. T.: A technique for measuring instantaneous in vitro contact stress distibutions in articular joints, Journal of Biomechanics, 15: 329-333, 1982.

15. Bullough, P., Goodfellow, J., Greenwald, A. S., and O'Connor, J.: Incongruent surfaces in the human hip joint, Nature, 217: 1290, 1968.

16. Bullough, P., Goodfellow, J., and O'Connor, J.: The relationship between degenerative changes and load bearing in the human hip, Journal of Bone and Joint Surgery, 55B(4): 746, 1973.

17. Byers, P.D., F.T. Hoaglund, G.S. Purewal, and Yau, A.C.M.C.: Articular cartilage changes in Caucasian and Asian hip joints, Annals Rheumatic Diseases, 33(2): 157-61, 1974.

18. Carlson, C. E.: An instrumented prosthesis for measuring the cartilage surface pressure distribution in the human hip, Sc.D. Thesis, Department of Mechanical Engineering, M.I.T., 1972.

19. Carlson, C. E., and Mann, R. W.: A look at the prosthesis- cartilage interface: design of a hip prosthesis containing pressure transducers, Journal of Biomedical Materials Research, Symposium, No. 5, 1974.

20. Carlson, C. E., Mann, R. W., and Harris, W. H.: A radio telemetry device for monitoring cartilage surface pressures in the human hip, IEEE Transactions in Biomedical Engineering, BME-21(4): 257, 1974.

21. Carslaw, H. S., and Jaeger, J. C.: Conduction of Heat in Solids. second edition, Oxford University Press, 1959.

22. Cathcart, R. F.: The shape of the femoral head and preliminary results of clinical use of a non-spherical hip prosthesis, Journal of Bone and Joint Surgery, 53A(2): 397, 1971.

23. Cathcart, R. F.: The shape of the normal femoral head and results from clinical use of more normally shaped non-spherical hip-replacement prosthesis, Journal of Bone and Joint Surgery, 54A(7): 1559, 1972.

24. Charnley, J.: The lubrication of animal joints, in Symposium on Biomechanics, Institution of Mechanical Engineers, London. 12-22, 1959.

25. Christel, P., P. Derethe, and Sedel, L.: Mesure par simulation de l'amortissement d'une hanche normale et prothesee, Acta Orthop. Belg., 42(Suppl. 1): 183-193, 1976.

26. Clarke, I. C.: Human articular surface contours and related surface depression frequency studies, Annals of Rheum. Dis., 30(1): 15-23, 1971.

27. Clarke, I. C.: Surface characteristics of human articular cartilage: a scanning electron microscope study, Journal of Anatomy, 108(1): 23-30, 1971.

28. Clarke, I. C.: The microevaluation of articular surface contours, Annals of Biomedical Engineering, 1: 31-43, 1972.

29. Clarke, I. C., and Amstutz, H. C.: Human hip joint geometry and hemiarthroplasty selection. in The Hip: Proceedings of the Third Annual Open Scientific Meeting of the Hip Society (San Francisco), C. V. Mosby, St. Louis, 63-89, 1975.

30. Collins, D.H.: The Pathology of Articular and Spinal Diseases, Edward Arnold, London, 1949.

31. Crandall, S. H., Karnopp, D. C., Kurtz, E. F. Jr., Pridmore-Brown, D. C.: Dynamics of mechanical and electromechanical systems. McGraw-Hill, 1968.

32. Crowninshield, R. D., Johnston, R. C., Andrews, J. G., and Brand, R. A.: A biomechanical investigation of the human hip, Journal of Biomechanics, 11: 75-85, 1978.

33. Day, W. H., Swanson, S. A. V., and Freeman, M. A. R.: Contact pressures in the loaded human cadaver hip, Journal of Bone and Joint Surgery, 57B(3): 302-13, 1975.

34. Dent, J. R.: Compression of articular cartilage, Ph.D. Thesis, Deptment of Mechanical Engineering, M.I.T., 1979.

35. Desai, C., and Christian, J.: Numerical methods in geotechnical engineering, McGraw-Hill, 1977.

36. Dintenfass, L.: Lubrication in synovial joints: a theoretical analysis. A Rheological approach to the problems of joint movements and joint lubrication, Journal of Bone and Joint Surgery, 45A(6): 1241-1256, 1963.

37. Editorial: Pathogenesis of osteoarthrosis, The Lancet, 2: 1131-1133, 1973.

38. Edwards, J.: Physical characteristics of articular cartilage, Proceeding of the Institute of Mechanical Engineering, 181: 16-24, 1967.

39. Elson, R.A., and Charnley, J.: The direction and the resultant force in total prosthetic replacement of the hip joint, Medical and Biological Engineering, 6: 19-27, 1968.

40. English, T. A., and Klivington, M.: In vivo records of hip loads using a femoral implant with telemetric output (a preliminary report), Journal of Biomechanical Engineering, 1(2): 111-5, 1979.

41. Eyre, D.R.: Collagen: molecular diversity in the body's protein scaffold, Science, 207: 1315-1322, 1980.

42. Freeman, M.A.R.: The fatique of cartilage in the pathogenesis of osteoarthritis, Acta Orthop. Scand., 46: 323-328, 1975.

43. Freeman, M. A. R. (ed.): Adult articular cartilage. 2nd ed. Pitman Medical Publishing Co., Kent, England, 1979.

44. Freeman, M. A. R., Kempson, G. E., and Swanson, S. A. V.: Variations in the physico-chemical and mechanical properties of human articular cartilage, in perspectives in biomedical engineering, Kenedi, R. M., ed., Macmillan, London, 157-161, 1973.

45. Freeman, M. A. R., and Meachim, G.: Ageing and degeneration in adult articular cartilage, Freeman, ed., 487-543, 1979.

46. Fry, F. J. (ed): Ultrasound: its applications in medicine and biology, Part I. Elsevier North-Holland, 1978

47. Fry, F. J. (ed): Ultrasound: its applications in medicine and biology, Part II. Elsevier North-Holland, 1978

48. Goss, S. A., and Dunn, F.: Ultrasonic propagation properties of collagen, Phys. Med. Biol., 25: 827-837, 1980.

49. Gray, H.: Anatomy, descriptive and surgical. 15th ed. Amer. rev., The classic Collector's Edition, Bounty Books, New York, 1977. also, Gray, H.: Anatomy of the Human Body. 29th ed., C.M. Goss (ed.), Lea and Febiger, Philadelphia, 1973.

50. Greenwald, A. S., and O'Connor, J. J.: The transmission of load through the human hip joint, Journal of Biomechanics, 4(6): 507-28, 1971.

51. Greenwald, A. S., and Haynes, D. W.: Weight-bearing areas in the human hip joint, Journal of Bone and Joint Surgery, 54B(1): 157-63, 1972.

52. Greenwald, A. S.: Joint congruence - a dynamic concept, in The Hip: Proceedings of the Second Open Scientific Meeting of the Hip Society (Dallas). C.V. Mosby, St. Louis. 3-21, 1974.

53. Grodzinsky, A. J., Roth, V., Myers, E., Grossman, W. D., and Mow, V. C.: The significance of the electromechanical and osmotic forces in the nonequilibrium swelling behavior of articular cartilage in tension, Journal of Biomechanical Engineering, 103: 221-231, 1981.

54. Hammond, B. T., and Charnley, J.: The sphericity of the femoral head, Med. and Biol. Engr. 5: 445-53, 1967.

55. Harris, W.H.: Role of intertrochanteric osteotomy in the treatment of arthritis of the hip, Surg. Clin. N. Amer., 49(4): 775-778, 1969.

56. Harris, W. H., Rushfeldt, P. D., Carlson, C. E., Scholler, J. M., and and Mann, R. W.: Pressure distribution in the hip and selection of hemiarthroplasty, in The Hip: Proceedings of the Third Annual Open Scientific Meeting of the Hip Society (San Francisco). C.V. Mosby, St. Louis. 93-8, 1975.

57. Harrison, M.H.M., F. Schajowicz, and Trueta J.: Osteoarthritis of the hip: a study of the nature and evolution of the disease, Journal of Bone and Joint Surgery, 35B(4): 598-625, 1953.

58. Hayes, W. C., Keer, L. M., Herrmann, G., and Mocros, L. F.: A mathematical analysis for indentation tests of articular cartilage, Journal of Biomechanics, 5: 541-551, 1972.

59. Hayes, W. C.: Mechanics of human articular cartilage, Ph.D. Thesis, Northwestern University, 1970.

60. Heglund, N. C., Taylor, C. R., and McMahon, T. A.: Scaling Stride Frequency to Animal Size: Mice to Horses, Science, 186: 1112, 1974.

61. Higginson, G. R., and Snaith, J. E.: The mechanical stiffness of articular cartilage in confined oscillating compression, Engineering in Medicine, 8: 11-14, 1979.

62. Inman, V.T.: Functional aspects of the abductor muscles of the hip, Journal of Bone and Joint Surgery, 29A(3): 607-619, 1947.

63. Karnopp, D., and Rosenberg, R.: System dynamics: A unified approach. Willey-Interscience, 1975.

64. Kempson, G.E., H. Muir, S.A.V. Swanson, and Freeman, M.A.R.: Correlations between stiffness and the chemical constituents of human articular cartilage on the human femoral head, Biochim. Biophys. Acta, 215: 70-77, 1970.

65. Kempson, G. E., Freeman, M. A. R., and Swanson, S. A. V.: The determination of a creep modulus for articular cartilage from indentation tests on the human femoral head, Journal of Biomechanics, 4(4): 239-50, 1971.

66. Kempson, G. E., Muir, H., Pollard, C., and Tuke, M.: The tensile properties of the cartilage of human femoral condyles related to the content of collagen and glycosaminoglycans, Biochim. Biophys. Acta, 297: 456, 1972.

67. Kempson, G. E.: Mechanical properties of articular cartilage. in Adult Articular Cartilage, M. A. R. Freeman (ed.) 333-414, 1979.

68. Kenyon, D. E.: A model for surface flow in cartilage, Journal of Biomechanics, 13(2): 129-34, 1980.

69. Kilvington, M., and Goodman, R. M. F.: In vivo hip joint forces recorded on a strain gauged 'English' prosthesis using an implanted transmitter, Engineering in Medicine, 10: 175-187, 1981.

70. Lane, J, M., and Weiss, C.: Review of articular cartilage research, Arthritis and Rheumatism, 18:(6): 553-562, 1975.
Lanyon, L. E., and Goodship, A. E., Pye, C. J., and MacFie, J. H.: Mechanically adaptive bone remodelling, Journal of Biomechanics, 15: 141-154, 1982.

71. Lanyon, L. E., and Baggot, D.G.: Mechanical function as an influence on the structure and form of bone, Journal of Bone and Joint Surgery, 58B, 436-443, 1976.

72. Lee, R. C., Frank, E. H., Grodzinsky, A. J., and Roylance, D. K.: Oscillatory compressional behavior of articular cartilage and its associated electromechanical properties, Journal of Biomechanical Engineering, 103: 280-292, 1981.

73. Lee, R. C.: Cartilage electromechanics: The relationship of physicochemical to mechanical properties, Sc.D. Thesis, M.I.T., 1979.

74. Lewis, P. R. and McCutchen, C. W.: Evidence for weeping lubrication in mammalian joints, Nature, 184: 1285, 1959.

75. Linn, F.C., and Sokoloff, L.: Movement and composition of interstitial fluid of cartilage, Arthritis and Rheumatism, 8(4): 481-494, 1965.

76. Linn, F.C., and Radin, E.L.: Lubrication of animal joints. III. The effect of certain chemical alterations of the cartilage and lubricant, Arthritis and Rheumatism, 11(5): 674-682, 1968.

77. Linn, F. C.: Lubrication of animal joints, Journal of Lubrication Technology, 329-341, 1969.

78. Little, T., Freeman, M. A. R., and Swanson, S. A. V.: Experiments on friction in the human hip joint, in Lubrication and wear in joints, Wright, V., ed., 110, 1969.

79. MacConaill, M. A.: Lubrication of mammalian joints, Nature, 185: 920, 1960.

80. Macirowski, T. J., Mann, R. W., and Harris, W. H.: The role of the resultant load on pressure distribution in the human acetabulum, Transections of the 27th Ann. Orthopaedic Research Society Mtg., Las Vegas, 1981.

81. Madreperla, S.: S. M. Thesis, Department of Mechanical Engineering, M.I.T., in progress, 1983.

82. Mankin, H. J.: Current concepts review: The response of articular cartilage to mechanical injury, Journal of Bone and Joint Surgery, 64-A, 460-466, 1982.

83. Mankin, H. J.: Alterations in the structure and metabolism of the matrix of articular cartilage in osteoarthritis of the human hip, Tenth Open Scientific Meeting of the Hip Society, New Orleans, 1982.

84. Mankin, H. J., and Lippiello, L.: Biochemical and metabolic abnormalities in articular cartilage from osteo-arthritic human hips I, Journal of Bone and Joint Surgery, 52A(3): 424-434, 1970.

85. Mankin, H. J., Dorfman, H., Lippiello, L., and Zarins, A.: Biochemical and metabolic abnormalities in articular cartilage from osteo-arthritic human hips , II. Correlation of morphology with biochemical and metabolic Data, Journal of Bone and Joint Surgery, 53A(3): 523-537, 1971.

86. Mankin, H. J., Johnson, M. S., and Lippiello, L.: Biochemical and metabolic abnormalities in articular cartilage from osteo-arthritic human hips , III. Distribution and metabolism of amino sugar-containing macromolecules, Journal of Bone and Joint Surgery, 63A(1): 131-139, 1981.

87. Mankin, H.J., and Lippiello, L.: The turnover of adult rabbit articular cartilage, Journal of Bone and Joint Surgery, 51A(8): 1591-1600, 1969.

88. Mann, R. W., Rushfeldt, P. D., Tepic, S., Macirowski, T., and Harris, W. H.: Synovial joint mechanics via a model incorporating precise global cartilage thickness distributions, 8th International. Congress on Biomechanics, Nagoya, Japan, 1981.

89. Mann, R. W., Tepic, S., Rushfeldt, P. D., and Harris, W. H.: Quantative synovial joint geometry, congruency and load distribution, 1980 Advances in Bioengineering, New York: ASME, 81, 1980.

90. Maroudas, A.: Balance between swelling pressure and collagen tension in normal and degerate cartilage, Nature, 260: 808-809, 1976.

91. Maroudas, A.: Physicochemical properties of articular cartilage, in Adult Articular Cartilage, M.A.R. Freeman (ed.), 1979.

92. Maroudas, A. and Bannon, C.: Measurement of the swelling pressure in cartilage and comparison with the osmotic pressure of constiuent proteoglycans, Biorheolgy, 18: 619-632, 1981.

93. McCutchen, C. W.: Mechanisms of animal joints: sponge-hydrostatic and weeping bearings, Nature, 184: 1284-5, 1959.

94. McCutchen, C. W.: The frictional properties of animal joints, Wear, 5: 1-17, 1962.

95. McCutchen, C.W.: A note upon tensile stresses in the collagen fibers of articular cartilage, Med. Electron. Biol. Engr., 3: 447-450, 1965.

96. McCutchen, C. W.: A note on weeping lubrication, in Perspectives in Biomedical Engineering, R. M. Kenedi, ed., MacMillan, 1973.

97. McCutchen, C. W.: An approximate equation for weeping lubrication, solved with an electrical analogue, Annals of Rheumatic Diseases, 34: 85-90, 1975.

98. McCutchen, C. W.: Lubrication of joints, in The joints and synovial fluid, Sokoloff, L., ed., 437-483, 1978.

99. McCutchen, C. W.: Cartilage is poroelastic, not viscoelastic (Including an exact theorem about strain energy and viscous loss, and an order of magnitude relation for equilibration time), Journal of Biomechanics, 15: 325-327, 1982.

100. Meachim, G.: Light microscopy of indian ink preparations of fibrillated cartilage, Annals of Rheumatic Diseases, 31: 457, 1972.

101. Meachim, G., and Stockwell, R. A.: The matrix, in Adult articular cartilage, Freeman, ed., 1-67, 1979.

102. Mow, V. C., and Mansour, J. M.:The non-linear interaction between cartilage deformation and interstitial fluid flow, Journal of Biomechanics, 10(1): 31-9, 1977.

103. Mow, V. C., Kuei, S. C., Lai, W. M., and Armstrong, C. G.: Biphasic creep and stress relaxation of articular cartilage in compression: Theory and experiments, Journal of Biomechanical Engineering, 102: 73-84, 1980.

104. Muir, I. H. M.: Biochemistry. in Adult Articular Cartilage, M .A. R. Freeman (ed.) 145-214, 1979.

105. Murray, R.O.: The aetiology of primary osteoarthritis of the hip, British Journal of Radiology, 38(445): 810-824, 1965.

106. Nuki, G. (ed.).: The Aetiopathogenesis of Osteoarthrosis. Pitman Medical Publ. Co., Kent, England, 1980.

107. Numata, T.: Effect of hydrostatic pressure on proteoglycan synthesis by calf articular cartilage, M.D. Thesis, Harvard-M.I.T. Division of Health Sciences and Technology, 1979.

108. O'Connor, P., Bland, C., and Gardner, D. L.: Fine structure of artificial splits in femoral condylar cartilage of the rat: A scanning electron microscopic study, Journal of Pathology, 132: 169-179, 1980.

109. Paul, J. P.: Forces transmitted by joints in the human body, Proc. Instn. Mech. Engrs., 181(pt.3J): 8-15, 1967.

110. Pauwels, F.: Biomechanics of the Normal and Diseased Hip. Springer-Verlag, Berlin, 1976.

111. Piotrowski, G.: Non-newtonian lubrication of synovial joints, Ph.D. Thesis, Department of Biomedical Engineering, Case Western Reserve University, 1975.

112. Radin, E. L., Paul, I. L., and Rose, R. M.: Role of mechanical factors in the pathogenesis of primary osteoarthritis, Lancet, 1: 519-21, 1972.

113. Radin, E. L., and Paul, I. L.: Response of joints to impact loading. I. In vitro wear, Arthritis and Rheumatism, 14(3): 356-62, 1971.

114. Radin, E. L., Parker, H. G., Pugh, J. W., Steinberg, R. S., Paul, I. L., and Rose, R. M.: Response of joints to impact loading - III, Journal of Biomechanics, 6: 51-57, 1973.

115. Redler, I., Mow, V. C., Zimny, M. L., and Mansell, J.: The ultrastructure and biomechanical significance of the tidemark of articular cartilage, Clinical Orthopaedics and Related Research, 112: 357-362, 1975.

116. Rice, J. R., and Cleary, M. P.: Some basic stress diffusion solutions for fluid-saturated elastic porous media with compressible constituents, Rev. Geophysics and Space Physics, 14: 227, 1976.

117. Rubin, C., and Lanyon, L. E.: Peak functional strain and fatigue life in bone, Proc. of 28th Annual Orthop. Res. Soc. Mtg., New Orleans, 1982.

118. Rushfeldt, P. D., Mann, R. W., and Harris, W. H.: Improved techniques for measuring in vitro the geometry and pressure distribution in the human acetabulum, Part 1: Ultrasonic measurement of acetabular surfaces, sphericity and cartilage thickness, Journal of Biomechanics, 14: 253-260, 1981.

119. Rushfeldt, P. D., Mann, R. W., and Harris, W. H.: Improved techniques for measuring in vitro the geometry and pressure distribution in the human acetabulum, Part 2: Instrumented endoprosthesis measurement of articular surface pressure distribution, Journal of Biomechanics, 14: 315-323, 1981.

120. Rushfeldt, P. D., Mann, R. W., and Harris, W. H.: Influence of cartilage geometry on the pressure distribution in the human hip joint, Science, 204: 413-5, 1979.

121. Rushfeldt, P. D.: Human hip joint geometry and the resulting pressure distributions, Sc.D. Thesis, Deptartment of Mechanical Engineering, M.I.T., 1978.

122. Rushfeldt, P. D., Palmer, D. W., Mann, R. W., and Harris, W. H.: In vitro hip joint pressure distribution testing facility. Proc. of AAMI 13th Annual Meeting, Washington, 1978.

123. Rushfeldt, P. D., Carlson, C. E., Mann, R. W., and Harris, W. H.: Load distribution across human acetabular cartilage: in vitro studies using an insrtumented femoral head prosthesis, Journal of Bone and Joint Surgery, 57A(4): 565, 1975.

124. Rushfeldt, P. D., Mann, R. W., and Harris, W. H.: Effect of incongruity in hemiarthroplasty on pressures and torques in the hip joint. Proc. 28th Ann. Conference on Engineering in Medicine and Biology (New Orleans), 145, 1975.

125. Rydell, N. W.: Forces acting on the femoral head prosthesis. Acta Ortho. Scand. Supp. 88(37): 9-125, 1966.

126. Sayles, R. S, Thomas, T. R., et al.: Measurement of the surface microgeometry of articular cartilage. Journal of Biomechanics, 12: 257-267, 1979.

127. Simon, S. R., Radin, E. L., Paul, I. L., and Rose, R. M.: The response of joints to impact loading. II. In vivo behavior of subchondral bone. Journal of Biomechanics, 5(3): 267-72, 1972.

128. Simon, W.: Scale effects in animal joints. I. Articular cartilage thickness and compressive stress. Arthritis and Rheumatism 13(3): 244-56, 1970.

129. Sokoloff, L.: The Biology of Degenerative Joint Disease, University of Chicago Press, Chicago, 1969.

130. Sokoloff, L. (ed.): The Joints and Synovial Fluid, Vol. 1. Acdemic Press, New York, 1978.

131. Sokoloff, L. (ed.): The Joints and Synovial Fluid, Vol. 2. Acdemic Press, New York, 1978.

132. Stearns, S. D.: Digital signal analysis. Hayden Book Co., 1975.

133. Stulberg, S.D., and Harris, W.H.: Acetabular dysplasia and development of osteoarthritis of hip. in The Hip: Proceedings of the Second Open Scientific Meeting of the Hip Society (Dallas), C.V. Mosby, St. Louis, 82-92, 1974.

134. Stulberg, S. D., Cordell, L. D., Harris, W. H., Ramsey, P .L., and MacEwen, G. D.: Unrecognized childhood hip disease: a major cause of idiopathic osteoarthritis of the hip. in The Hip: Proceedings of the Third Open Scientific Meeting of the Hip Society (San Francisco). C.V. Mosby, St. Louis, 212-28, 1975.

135. Swanson, S. A. V.: Friction, wear and lubrication, in Adult articular cartilage, Freeman, ed., 415-460, 1979.

136. Tanaka, T., and Fillmore, D. J.: Kinetics of swelling of gels, Journal of Chemical Physics, 70: 1214, 1979.

137. Tanaka, T., Hocker, L. O., and Benedek, G. B.: Spectrum of light scattered from a viscoelastic gel, Journal of Chemical Physics, 59: 5151, 1973.

138. Tepic, S.: Congruency of the human hip joint, S.M. Thesis, Deptartment of Mechanical Engineering, M.I.T., 1980.

139. Tepic, S.:Dynamics of and entropy production in the cartilage layers of the synovial joint, Sc.D. Thesis, M.I.T., Department of Mechanical Engineering, May, 1982.

140. Tepic, S., Macirowski, T. J., Mann, R. W., and Harris, W. H.: Entropy production in the cartilage layers of the human hip joint, Proc. of 28th Annual Orthop. Res. Soc. Mtg., New Orleans, 1982.

141. Tepic, S., Macirowski, T. J., Mann, R. W., and Harris, W. H.: Behavior of cartilage layers subjected to periodic dynamic regimes, Proc. of Fifth Ann. Conf. of American Soc. of Biomechanics, Cleveland, 1981.

142. Tepic, S., Mann, R. W., and Harris, W. H.: Analytical approach to interarticular congruency of the human hip joint, Proc. of 27th Annual Orthop. Res. Soc. Mtg., Las Vegas, 1981.

143. Tepic, S., Mann, R. W., and Harris, W. H.: Analytical macrogeometry representation and congruency of the human hip joint, Proc. of Fourth Ann. Conf. of American Soc. of Biomechanics, Burlington, 1980.

144. Tepic, S., Mann, R. W., and Harris, W. H.: Geometry and congruency of the human hip joint, 33rd Annual Conf. on Eng in Medicine and Biology, Washington D. C., 1980.

145. Tepic, S., Mann, R. W., and Harris, W. H.: Geometry of the human hip joint, Proc. of the Eighth Ann. Bioengineering Conf., M.I.T., Cambridge, 1980.

146. Tepic, S., Mann, R. W., and Harris, W. H.: Ultrasonic measurement of the femoral head geometry, Trans. 26th Orthop. Res. Soc., Atlanta, 189, 1980.

147. Thomas, T. R., Sayles, R. S., and Haslock, I.: Human joint performance and the roughness of articular cartilage, Journal of Biomechanical Engineering, 102: 50-56, 1980.

148. Urban, J. P. G., Maroudas, A., Bayliss, M. T., and Dillon, J.: Swelling pressures of proteoglycans at the concentrations found in cartilaginous tissues, Biorheolgy, 16: 447-464, 1979.

149. Unsworth, A., Dowson, D., and Wright, V.: Some new evidence on human joint lubrication, Annals of Rheumatic Diseases, 34: 277, 1975.

150. Walker, P. S., Dowson, D., Longfield, M. D., and Wright, V.: Boosted lubrication in synovial joints by fluid entrapment and enrichment, Annals of Rheumatic Diseases, 27: 512. 1968.

151. Walmsley, T.: The articular mechanism of the diarthroses, Journal of Bone and Joint Surgery, 10(1): 40-5, 1928.

152. Weightman, B. O., Freeman, M. A. R., and Swanson, S. A. V.: Fatique of articular cartilage, Nature, 224(5414): 303-4, 1973.

153. Weightman, B.: Tensile Fatique of Human Articular Cartilage, Journal of Biomechanics, 9(4): 193-200, 1976.

154. Weightman, B., and Kempson, G. E.: Load Carriage. in Adult Articular Cartilage, M.A.R. Freeman (ed.) 291-331, 1979.

155. Wells, P. N. T.: Biomedical ultrasonics. Academic Press, 1977.

156. Wijesinghe, A. M., and Kingsbury, H. B.: On the dynamic behavior of poroelastic materials, Journal of Acoustical Society of America, 65: 90-95, 1979.

157. Zarek, J.M., and Edwards, J.: The stress-structure relationship in articular cartilage, _Med. Electron. Biol. Engr._, 1: 497-507, 1963.